

Phase-dependent closed-loop modulation of beta-frequency network oscillations in parkinsonian rats

Doctor of Philosophy (D.Phil.) Thesis

November, 2020

Max Rothwell

St. John's College

MRC Brain Network Dynamics Unit

Nuffield Department of Clinical Neurosciences

University of Oxford

Oxford, UK

Abstract

Normal brain function is associated with an assortment of oscillations of various frequencies, each reflecting the timing of separate computational processes and levels of synchronization within and between brain areas. Stimulation accurately delivered on a specified phase of a given oscillation provides the opportunity to target individual aspects of brain function. To achieve this, we have developed a highly responsive system to produce a continuous online phase-estimate. In addition to stable oscillations, the system accurately tracks the early cycles of short, transient oscillations and can operate across the frequency range of most established neuronal oscillations (4 to 250 Hz).

Here we demonstrate bidirectional modulation of the pathologically elevated parkinsonian beta-band oscillation (around 35 Hz) in 6-OHDA hemi-lesioned rats. Beta phase, monitored using a single channel electrocorticogram above secondary motor cortex, was used to drive electrical stimulation of the globus pallidus or subthalamic nucleus on one of eight phases spanning the oscillation cycle. Stimulation of the early ascending phase suppressed the oscillation whereas stimulation of the early descending phase was amplifying. By implementing a rule that prevented stimulation when the phase estimate was unstable, we achieved a system that could adapt stimulation rate and pattern to respond to the changes produced in the target oscillation. This allowed the electronic system to create and maintain a state of equilibrium with the biological system resulting in continuous stable modulation of the target oscillation over time.

Elevated beta-band activity correlates with motor impairment in humans, primates, and rodents. In an attempt to establish a causal relationship, we used phase-locked stimulation to modulate ongoing cortical beta activity during concurrent assessment of spontaneous forelimb use or goal-directed walking. Despite large deficits in paw use on the injured side during the cylinder task, phase-locked stimulation was unable to modulate forelimb asymmetry. In contrast, consistent reductions in average speed were produced when amplifying beta activity that were driven by a change in running style preference that favoured smaller and slower steps. Altered stand time variance was also observed during individual runs, suggesting that beta-band amplification impaired interlimb coordination. Locomotor deficits were phase-dependent and only present when targeting amplifying phases, thus supporting the functional role of beta-band oscillations in parkinsonian motor impairment.

The results in this study demonstrate the feasibility of phase locked stimulation as a more refined strategy for remediation of pathological beta oscillations in the treatment of the motor symptoms of Parkinson’s disease. Furthermore, they establish the utility of our algorithm and allow for the potential to assess the contribution of rhythmic activity in neuronal computation across a number of brain systems.

Acknowledgements

It is with great pride that I submit my thesis and want to take this opportunity to thank those who made it possible. First and foremost, I must thank my supervisors Dr. Andrew Sharott and Dr. Colin McNamara for their incredible levels of support, guidance, and commitment to my development as a scientist. I could not have asked for two better mentors. I would also like to thank all BNDU members past and present for their friendship, in particular those who helped me experimentally: Jane Westcott for expert animal care, Grace Tennant and Andreia Madalena for behavioural analysis, and Lauren Waite for histology. I leave my final acknowledgement to my family who, without their unconditional support, I would not have achieved this work. It is to them I dedicate my report.

Contents

Abstract i

Acknowledgements iii

Tables and figures vii

Abbreviations viii

1 Introduction 1

1.1 Parkinson's disease and the basal ganglia: then and now 1

1.1.1 Brief overview of Parkinson's disease 1

1.1.2 Initial discoveries 1

1.1.3 The Albin/DeLong hypothesis 2

1.1.4 The proposed role of dopamine 5

1.1.5 The impact of MPTP primate models 6

1.1.6 The introduction of deep brain stimulation 8

1.1.7 Limitations of the Albin/DeLong hypothesis 9

1.1.8 Optogenetic insights into basal ganglia function 12

1.1.9 Rodent models of dopamine depletion 14

1.2 Beta oscillations: timing is everything 16

1.2.1 A brief introduction to oscillations 16

1.2.2 History of beta oscillations in Parkinson's disease 17

1.2.3 History of beta oscillations in animal models of Parkinson's disease 19

1.2.4 The role of beta oscillations in network stabilisation 21

1.2.5 The transient nature of beta activity 23

1.2.6 Where is pathological beta activity generated? 24

1.2.7 The role of cortical beta-band oscillations 29

1.3 Closed-loop phase-locked stimulation: a future therapy? 32

1.3.1 Introduction to closed-loop approaches for Parkinson's disease 32

1.3.2 Beta as a biomarker 34

1.3.3 Rationale for phase-locked stimulation 36

1.3.4 Examples of phase-locked stimulation 38

1.3.5 The effect of phase-locked stimulation on neural dynamics 41

1.4 Aims 43

2 Materials and methods 45
2.1 Surgical procedures 45
2.2 Closed-loop phase-locked stimulation 46
2.2.1 Real-time phase tracking and closed-loop trigger algorithm 46
2.2.2 Data acquisition and electrical stimulation 48
2.3 Open field recording protocol 49
2.4 Stimulation parameter selection 50
2.5 Electrophysiological analysis 51
2.6 Behaviour 52
2.6.1 Cylinder assessment 52
2.6.2 Gait assessment 52
2.7 Tissue analysis 56
3 Physiological response to phase-dependent stimulation 59
3.1 Introduction 59
3.2 Results 63
3.2.1 Histological verification of dopamine lesion and electrode placement 64
3.2.2 Phase-tracking accuracy in freely moving parkinsonian rats 67
3.2.3 Example traces of phase-locked stimulation 70
3.2.4 Modulation of cortical beta power by pallidal phase-locked stimulation 72
3.3 Discussion 74
4 Closed-loop properties of the system 78
4.1 Introduction 78
4.2 Results 81
4.2.1 Effect of target phase on the accuracy and rate of stimulation 82
4.2.2 Effect of target phase on future stimulation 84
4.2.3 Triggering open-loop stimulation using closed-loop patterns 86
4.3 Discussion 89
5 Assessment of motor function during closed-loop stimulation 93
5.1 Introduction 93
5.2 Results 97
5.2.1 Effect of stimulation on paw use during the cylinder task 99
5.2.2 Effect of stimulation on cortical beta power on the CatWalk 101
5.2.3 Effect of stimulation on average speed 104

5.2.4 Effect of stimulation on running style 107
5.2.5 Effect of stimulation on gait asymmetry 112
5.2.6 Effect of stimulation on within-run variance..... 114
5.3 Discussion 116

6 General discussion 126

6.1 Implications for academic research..... 128
6.2 Implications for Parkinson's disease 130
6.3 Future directions 134
6.4 Concluding remarks 136

7 References.....138

Tables and figures

Figure 1-1: Schematic of the basal ganglia (DeLong, 1990) 4
Table 2-1: Subjects list and electrode placement data 58
Figure 3-1: Histological verification of dopamine lesion and electrode placement ... 66
Figure 3-2: Increased cortical beta power is present on the lesioned side 68
Figure 3-3: Phase-tracking accuracy in freely moving parkinsonian rats..... 69
Figure 3-4: Example traces of phase-locked stimulation 71
Figure 3-5: Modulation of cortical beta power by pallidal phase-locked stimulation . 73
Figure 4-1: Effect of target phase on the accuracy and rate of stimulation..... 83
Figure 4-2: Effect of target phase on future stimulation 85
Figure 4-3: Triggering open-loop stimulation using closed-loop activity patterns 87
Figure 4-4: Quantification of closed- and open-loop beta-band modulation 88
Figure 5-1: Effect of stimulation on paw use during the cylinder task..... 100
Figure 5-2: Effect of phase-locked stimulation on cortical power on the CatWalk .. 102
Figure 5-3: Effect of 130 Hz stimulation on cortical power on the CatWalk 103
Figure 5-4: Effect of stimulation on average speed 105
Figure 5-5: Effect of stimulation on average speed relative to no stimulation..... 106
Figure 5-6: Effect of stimulation on running style 109
Figure 5-7: Effect of running style on average speed 110
Figure 5-8: Relationship between average speed and bounding 111
Figure 5-9: Effect of stimulation on gait asymmetry 113
Figure 5-10: Effect of stimulation on within-run variance..... 115

Abbreviations

#

6-OHDA	six-hydroxydopamine

A

AP	anterior-posterior axis

B

BG	basal ganglia
BUA	background unit activity

C

CEP	cortically evoked potential
CPU	caudate putamen unit
CA3	cornu ammonis 3

D

DBS	deep brain stimulation
dMSN	direct medium spiny neurone
DV	dorsal-ventral axis

E

ECoG	electrocorticogram
EEG	electroencephalography
EC	entorhinal cortex

F

FoxP2	forkhead box protein P2

G

GABA	gamma-aminobutyric Acid
GFP	green fluorescent protein
GPe	external globus pallidus
GPi	internal globus pallidus

I

IC	internal capsule
iMSN	indirect medium spiny neurone

L

LF	left front
LFP	local field potential
LTP	long term potentiation
LTD	long term depression
LH	left hind

M

M1	primary motor cortex
MFB	medial forebrain bundle
ML	medial-lateral axis
MPTP	1-Methyl-4-Phenyl1,2,3,6-Tetrahydropyridine

N

NHP	non-human primate

P

PCR	polymerase chain reaction
PD	parkinson’s disease
PSD	power spectral density
PV	parvalbumin

R

RF	right front
RH	right hind

S

SD	standard deviation
SEM	standard error of the mean
SNc	substantia nigra pars compacta
SNr	substantia nigra pars reticulata
STN	subthalamic nucleus
SUA	single unit activity

T

TACS	transcranial alternating current stimulation
TH	tyrosine hydroxylase

U

UPDRS	unified parkinson’s disease rating scale

V

VTA	ventral tegmental area

1 Introduction

1.1 Parkinson's disease and the basal ganglia: then and now

1.1.1 Brief overview of Parkinson's disease

Parkinson's disease (PD) is a neurodegenerative disorder that affects 6.1 million people worldwide. The number diagnosed with the disorder has more than doubled since 1990 due to an ageing global population and, at a cost of between £3500 and £10000 per patient per year, PD represents a significant societal and economic burden (Dorsey et al., 2018). It manifests as an array of cognitive, motor, psychiatric, and autonomic dysfunction, but is predominantly characterised as a motor disorder as impaired movement is the presenting symptom that has the biggest impact upon daily life. Rigidity, slowness of movement (bradykinesia), tremor, and postural disturbances are the four cardinal motor symptoms, which worsen over time due to the progressive nature of PD.

1.1.2 Initial discoveries

James Parkinson first described PD in *An Essay on Shaking Palsy* in 1817 where he referred to patients with lessened muscular power, a stooped posture, and that shook at rest (Parkinson, 1817). It was not until the mid-20th century that dopamine loss was identified in the pathogenesis of the disorder (Bertler & Rosengren, 1959). Before then, with little-to-no options or rationale for treatment, surgeons persisted with lesioning areas throughout the brain that were largely inaccurate and ineffective. It was noted that the pallidum was the most effective site however, and

lesions located more posterior-ventrally were particularly consistent (Svennilson et al., 1960). Surgeries were abandoned after 1961 due to the development of dopamine replacement therapy to treat the motor symptoms of PD. Levodopa is a precursor to dopamine that can pass through the blood brain barrier; where it is then broken down to replace dopamine no longer being produced by dopaminergic cells in the midbrain. While levodopa is highly effective in the initial stages of PD, it became apparent that the responsiveness of drug therapy fluctuates as the disease progresses, and involuntary movements, termed dyskinesias, develop over time (Schrag & Quinn, 2000). It was for these reasons that surgeries once again became an option, and the benefit of pallidotomies was shown to be reproducible (Laitinen et al., 1992).

1.1.3 The Albin/DeLong hypothesis

This time, surgeons could leverage a wealth of new evidence regarding the role of the basal ganglia (BG) in movement gathered largely from non-human primates (NHPs). The BG is made up of multiple interconnected subcortical nuclei that includes the striatum (caudate nucleus and putamen), the external and internal globus pallidus (GPe, GPi), the subthalamic nucleus (STN), and the substantia nigra pars reticulata and pars compacta (SNr, SNc). DeLong (1971) first described rate changes in the pallidum of primates in response to movement, which provided an initial basis as to why pallidotomies were particularly successful in treating motor symptoms in PD. The subsequent discovery of anatomically and functionally segregated sub-regions that connect to different thalamic and cortical areas, divided the BG into three parallel loops responsible for motor, associative, and limbic function (Alexander et al., 1986); providing further evidence as to why pallidal lesions restricted to the posterior segment provided superior treatment benefit.

Building upon such work, the BG motor loop was first described by Albin et al., (1989) and DeLong (1990) using NHPs. It was noted that the striatum received excitatory input from across the cortex, as well as midbrain dopaminergic innervation, thus was perfectly placed to integrate a variety of incoming sensory information. Prior retrograde tracing studies in both cats and monkeys had shown two efferent striatal pathways projecting to both the substantia nigra (Bunney & Aghajanian, 1976) and pallidum (DiFiglia et al., 1976), which DeLong (1990) termed the “direct” and “indirect” pathway respectively. Under this framework, the striatum has bidirectional control of the SNr and GPi (i.e. BG-output), either by direct pathway inhibition, or via indirect pathway GPe innervation that excites output nuclei through STN disinhibition (Figure 1-1). The STN is therefore the output of the indirect pathway and provides glutamatergic input to the GPi and SNr, meaning that both pathways converge onto the same output nuclei with inverse polarity. In essence, the two pathways are thought to be in balance, such that direct pathway activation reduces BG output, while the indirect pathway increases it. BG-output then influences motor circuits through two major output pathways – a direct projection to brainstem nuclei or through tonic inhibition of motor thalamus which then projects back to the cortex.

The Albin/DeLong hypotheses became the prevailing theory of BG function based mainly on this simplified anatomical structure, stating that both pathways have opposing effects on motor function, with the balance of activity between pathways critical for determining the speed and size of movements (Albin et al., 1989; DeLong, 1990). Under this framework, the opposing actions of each pathway on GPi activity act to scale intended movements in a push-pull manner. This hypothesis was particularly well received as it could account for symptomatic observations recorded across an array of kinetic disorders. As discussed in the next section, the prevailing

wisdom at the time was that dopamine depletion produced an overactivation of the anti-kinetic indirect pathway causing a chronic increase in BG-output and a subsequent reduction in movement size and speed. In contrast, hyperkinetic disorders such as Huntington's disease and hemiballismus both selectively impair the indirect pathway to cause excessive jerky movements (Albin et al., 1989).

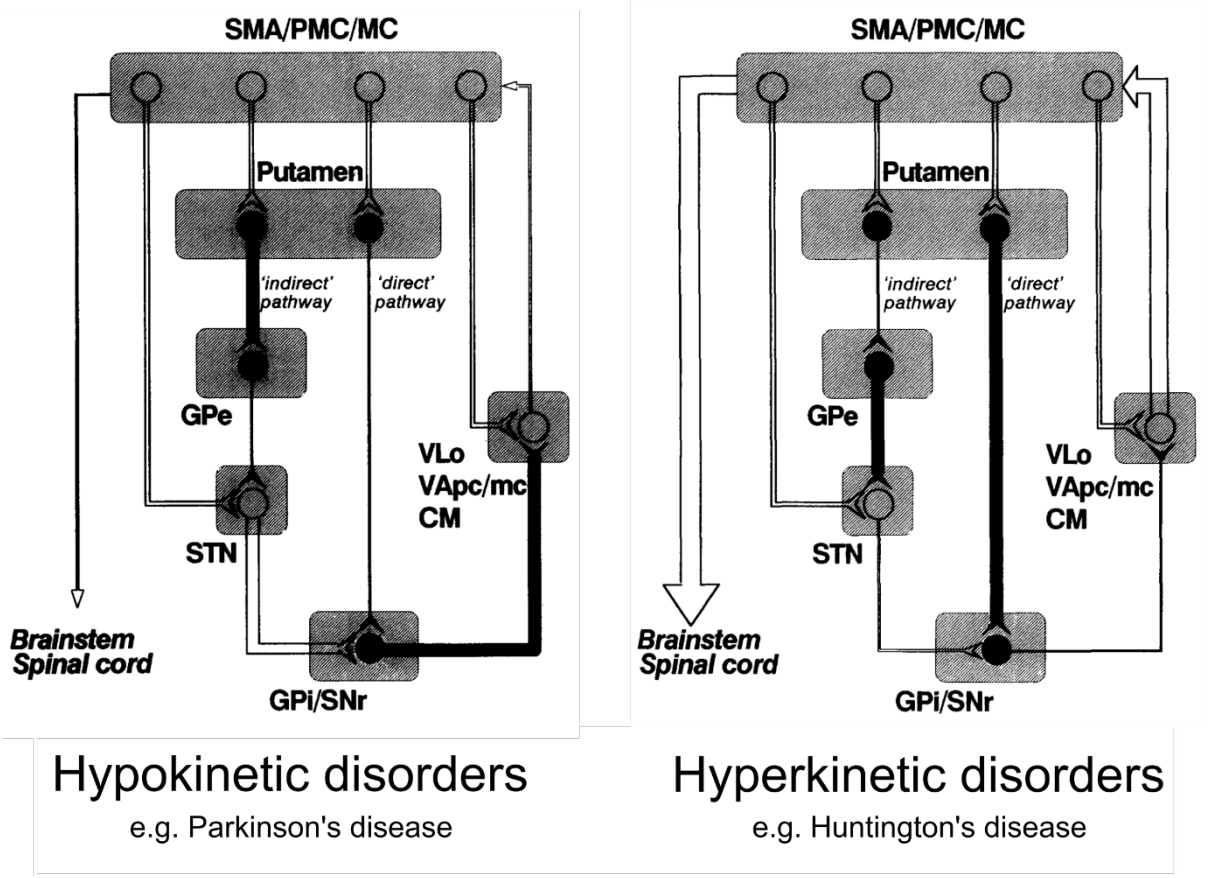


Figure 1-1: Schematic of the basal ganglia (DeLong, 1990)

Schematic representation of neural activity within the motor network in both hypo- and hyperkinetic movement disorders as suggested by DeLong (1990). Under this schema, BG output from the internal globus pallidum (GPi) and substantia nigra pars reticulata (SNr) determines the size and speed of movements. BG output is governed by two opposing striatal pathways termed the "direct" and "indirect" pathway, which promote or inhibit movement respectively. It was proposed that an imbalance between these two pathways was responsible for kinetic disorders, with Parkinson's disease producing overactivation of the indirect pathway (left) and Huntington's disease over activating the direct pathway (right). Line thickness represents relative neural activity, sold lines represent inhibitory connections, and hollow lines represent excitatory connections.

1.1.4 The proposed role of dopamine

A key mechanism underpinning the Albin/DeLong hypothesis is the dichotomous effect of dopamine innervation on striatal output. By 1990, it had long since been known that dopamine was critical for the processing of cortical and thalamic input to the striatum (Kitai et al., 1976; Wilson & Groves, 1981), and that medium spiny neurones (MSNs) were the principle cell type (Fox et al., 1971). It was assumed that MSNs had at least two sub-populations, which Albin et al., (1989) referred to simply as GABA projecting neurons, that belonged to either the direct (dMSNs) or indirect (iMSNs) pathway. Moreover, it was thought that dopamine had an opposing effect on each subpopulation. This prediction was based largely on indirect measures of activity such as gene expression and receptor binding studies in downstream nuclei, since MSN subpopulations were indistinguishable in shape and electrophysiological properties (Gerfen, 1992).

These predictions were proven correct by the discovery of two major subsets of MSN that differ in their expression of dopamine receptors and efferent connections. Specifically, PCR studies showed that D_1 receptor mRNA was found primarily in dMSNs projecting to the substantia nigra, while D_2 receptor mRNA was found in iMSNs projecting to the pallidum (Surmeier et al., 1996). Dopamine receptors are metabotropic G-protein-coupled, meaning that each sub-class of receptor produces a different intracellular response upon ligand binding that is dependent on the G-protein with which it is associated. D_1 receptor activation increases the responsiveness of MSNs to sustained glutamate release from the cortex and thalamus. They do this by altering the expression and properties of AMPA, NMDA, and Ca^{2+} membrane channels, which keeps MSNs in a so-called “up-state”, where their membrane

potential is much closer to their spiking threshold (Surmeier et al., 2007). D_2 receptor activation has the opposite effect, reducing MSN excitability by decreasing AMPA and Ca^{2+} receptor currents, while also reducing presynaptic glutamate release. These studies stratified two sub-types of MSNs and their opposing response to dopamine innervation; which has since been quantified more accurately in transgenic mice using GFP expressed under the control of D_1 or D_2 promotors, confirming the segregation of each receptor subtype to the direct or indirect pathway respectively (Bertran-Gonzalez et al., 2008; Matamales et al., 2009).

They did not however provide any evidence toward the functional role of either pathway. The Albin/DeLong hypothesis predicts that chronic dopaminergic cell loss will produce motor impairments in PD through imbalanced MSN activity, whereby a net increase in iMSN activity produces slowed movements through an indirect pathway-mediated increase in BG-output. In support of this, dopaminergic cell loss causes a reduction in dendritic spine density on striatopallidal MSNs but not neighbouring striatonigral MSNs (Day et al., 2006), as well as an overall increase in striatal D_2-receptor expression relative to D_1-receptors (Gerfen et al., 1990). Microdialysis studies in parkinsonian NHPs also report reduced GABA levels in the STN, providing further cellular evidence that the indirect pathway is overactive in PD (Soares et al., 2004).

1.1.5 The impact of MPTP primate models

The strongest evidence for the Albin/DeLong hypothesis came from the serendipitous discovery of MPTP (1-methyl-4-phenyl-1,2,3,6-tetrahydropyridine), which is a prodrug to the neurotoxin MPP+ that selectively kills dopaminergic cells. MPTP was first identified in 1983 when previously healthy individuals developed PD-

like symptoms immediately after ingesting a synthetic opioid (Langston et al., 1983). It was recognised that MPTP could be utilised in research to produce PD-like symptoms in NHPs via a single systemic injection. MPTP administration produced near identical motor symptoms in NHPs to those observed in PD: bradykinesia/akinesia, rigidity, freezing, impaired gait, tremor and postural disturbances (Burns et al., 1983). As expected, these motor impairments are recovered by dopamine replacement therapy, which also induces dyskinesias following chronic administration (Clarke et al., 1987).

One crucial advantage of primate models of PD is that it is possible to compare network activity in both the healthy and pathological state. Early studies in MPTP primates reported abhorrent activity throughout the indirect pathway, recorded as increased tonic discharge from the STN and GPi, as well as decreased GPe activity (Filion & Tremblay, 1991). Critically, pharmacological lesioning of the overactive STN was found to reverse Parkinsonian motor symptoms (Berman et al., 1990). This evidence fits perfectly with the Albin/DeLong hypothesis and led to development of the rate model, which states that the competing influences of the two striatal pathways on BG-output is encoded by the relative number action potentials they generate. As described above, the dynamic regulation of MSN excitability is lost in PD. The importance of dopamine in modulating MSN output was further underlined by pharmacological studies in MPTP monkeys, where dopamine agonist administration increased GPe activity but decreased firing in the GPi (Filion et al., 1991), while activity in the latter was almost completely silenced during dopamine-induced dyskinesias (Papa et al., 1999).

1.1.6 The introduction of deep brain stimulation

The extensive evidence gathered in patients and primates in support of the Albin/DeLong and rate hypotheses, provided new rationale for surgical intervention in PD. As the principle output of the indirect pathway, the STN was of particular interest, but severe side effects were produced by permanent lesions in patients with hemiballismus (Whittier, 1947). Prior to lesioning a structure, surgeons would typically pass a small amount of current to assess if lesioning it would be successful, and it was noted that high frequency stimulation was particularly effective (historical review: Gardner, 2013). A breakthrough technological advancement came with the advent of deep brain stimulation (DBS) by *Medtronic*, where chronic electrical stimulation of the thalamus was found to reversibly treat tremor in PD (Andy, 1983; Mundinger, 1977). This technique was later extended to the STN when it was proven to reduce rigidity in MPTP monkeys (Benazzouz et al., 1993). As DBS was having a similar effect to lesioning surgery, it was assumed to work in the same way by reducing output from the target structure. It was proposed that high frequency stimulation kept the target structure in a permanent state of depolarisation that blocked cell firing (Benabid et a., 2001). This was supported by recordings taken during electrode localisation in patients, where nearby cells were inhibited during high frequency stimulation (Filali et al., 2004). DBS could be performed bilaterally with relatively few side effects compared to lesions and was found to be remarkably effective in many patients (Krack et al., 2003). Despite this, it was primarily reserved for late-stage PD patients who were still dopamine responsive but suffering from dyskinesias, reduced efficacy, or cognitive side effects such as impulsivity. The location and frequency of stimulation was tailored for each patient, but was typically delivered at high frequency (>130Hz) into the STN. These findings were of particular relevance to the Albin/DeLong hypothesis, as it

suggested that reducing information flow through the indirect pathway could improve hypokinetic motor deficits.

1.1.7 Limitations of the Albin/DeLong hypothesis

PD research has benefited greatly from the unique insight gained from the ability to record from implanted DBS electrodes, but these studies are limited to the implanted nuclei however, and only allow recordings during short periods of time where patients perform extremely limited behaviours. These types of studies are typically low throughput and suffer from a low number of participants, mainly due to a small patient pool and the need to comply with ongoing medical treatment. Furthermore, the testing of novel pharmacological and electrical interventions is limited by regulatory considerations. The practical, technological, and ethical limitations of clinical study mean it is impossible to properly probe BG function using recordings from patients alone.

In order to properly test the depolarisation block hypothesis, recordings were needed in BG-output nuclei during DBS. This exact experiment was conducted in MPTP primates by Hashimoto et al., (2003), who reported an increase in GPe and GPi discharge rates when stimulating STN, thus contradicting many widely accepted views held at the time. This uncertainty as to the mechanism of action through which DBS provides therapeutic benefit was further reflected by the controversial effect of GPe stimulation, which according to Albin/DeLong ought to exacerbate hypokinetic motor symptoms in PD if increasing indirect pathway output. While some studies did report a worsening of symptoms following GPe stimulation or lesion (humans: Munro-Davies et al., 1999; primates: Zhang et al., 2006), others noted a marked improvement (humans: Vitek et al., 2004; primates: Vitek et al., 2012). Despite the wealth of

empirical evidence supporting the rate hypothesis, it had also been noted that it failed to explain several notable features of PD such as the paradoxically therapeutic effect of lesioning the GPi (Baron et al., 1996), which should in theory produce severe dyskinesias. Such observations prompted re-evaluation of several hypotheses surrounding the mechanism of DBS, the rate model, and the long-standing Albin/DeLong framework of BG-function.

Despite the obvious translatability of the MPTP model it is used by relatively few labs worldwide due to the significant economic, logistical, and ethical constraints associated with working with NHPs, and tends to be even lower throughput than their clinical counterparts. The severe restrictions placed upon clinical and primate experiments led to the majority of early studies of BG function to draw conclusions from an overly simplistic model that does not take into account many potentially important connections between structures; nor does it acknowledge cell type heterogeneity within structures. In this regard, experiments in rodents not bound by such restrictions were able to more accurately characterise and record from different cell types within the motor network.

Dopaminergic midbrain neurons in a healthy brain are extremely large with extensive arborisation. When characterised in rodents, the average dopaminergic neurone contributed approximately 370,000 individual synaptic inputs that covered an area of up to 1 mm^3, which equates to roughly 100,000 striatal cells (Arbuthnott & Wickens, 2007). Despite identification of two MSN subtypes that can be segregated by their dopamine receptor expression (Bertran-Gonzalez et al., 2008; Matamales et al., 2009), vast amounts of dopamine is released into the extracellular space for extra-synaptic uptake by local dopamine transporters, giving each individual dopamine cell

a “sphere of influence” that extends further than that it’s individual synaptic connections (Rice & Cragg, 2008). This sphere of influence will contain striatal GABAergic interneurons that are significantly impacted by dopamine depletion (Mallet et al., 2006), yet are excluded from the Albin/Delong model despite powerfully modulating striatal output (Gerfen & Surmeier, 2011). Over simplification of network dynamics is further highlighted along the indirect pathway, which was originally represented as a linear one-directional process but actually exists as a series of reciprocal feedback loops. For instance, pallidostriatal projections are enriched onto GABAergic striatal interneurones and so can widely influence striatal output despite being ‘downstream’ of such activity (Bevan et al., 1998). While the net effect of dopamine release into the striatum may still promote direct pathway activation as predicted by Albin/DeLong, these studies certainly suggest a more nuanced role of dopamine in movement regulation than originally proposed by Albin/DeLong.

Studies in both PD patients and MPTP primates greatly advanced our understanding of BG anatomy, which was not only critical in the development of DBS as a legitimate treatment option, but also gave rise to several key theories of BG function. Despite this, the therapeutic benefit provided by DBS or pallidotomies could not be readily explained by either the Albin/DeLong or rate hypotheses, meaning that a new framework was needed. The advent of optogenetic technologies gave researches the ability to record and modulate individual cells populations in rodents (Boyden et al., 2005), providing unprecedented insight into the role of each striatal pathway.

1.1.8 Optogenetic insights into basal ganglia function

If not rate, then how is information conveyed by both pathways? What is the true function of each pathway? And, what is the specific function of different cell types? These questions must be answered in rodent models where it is possible to monitor and compare activity between both striatal pathways. Methods available to researchers in humans and primates have not been useful for this purpose as iMSNs and dMSNs are indistinguishable in terms of shape, size, and electrophysiological properties (Gerfen, 1992). Modern advances in genetic technology has enabled the insertion of light sensitive ion channels into specific neural populations, allowing researchers to identify and modulate neural activity using light stimulation (Boyden et al., 2005). It has also allowed for optical monitoring of neural activity using fluorescent calcium indicator proteins such as GCaMP3 (Zariwala et al., 2012), which has provided a tool to record the activity of specific neuronal populations during behaviour.

These technologies allowed researchers to directly test the Albin/DeLong hypothesis. The first study to do so found that optogenetic activation of D_2-receptor mediated dMSNs produces PD-like symptoms such as increased freezing, bradykinesia and reduced locomotion, while D_1-receptor mediated iMSN activation reduced freezing and increased locomotion (Kravitz et al., 2010). Similarly, cre-dependent pharmacological ablation of D_1-receptor MSNs in the dorsolateral striatum produces hypolocomotion in mice while D_2-receptor ablation produced hyperlocomotion (Durieux et al., 2012). The same study also found that indirect pathway MSNs were critical for haloperidol-induced catalepsy. Despite these early genetic studies being in support of the rate hypothesis, a landmark study in mice found that dMSNs and iMSNs are concurrently active during movement (Cui et al., 2013),

which has since been corroborated elsewhere (Barbera et al., 2016; Klaus et al., 2017). This finding disproved several longstanding ideas in the field: firstly, the indirect pathway could no longer be viewed as a ubiquitous stream of anti-kinetic activity, and secondly, BG-output could no longer be viewed as a simple gate for thalamic activity that was “opened” during discrete periods to promote action initiation. These conclusions are in line with work in songbirds showing that thalamic and pallidal cell pairs fire continuously at high rates, with individual thalamic spikes entrained to BG output with sub millisecond precision in a behaviourally dependent manner (Goldberg et al., 2012).

The concurrent activation of both pathways provided evidence for a complementary hypothesis however, which states that the direct pathway promotes ongoing motor programmes, while the indirect pathway concurrently inhibits competing schema (Mink, 1996). In support of this hypothesis, mice trained to either push or pull a lever to receive reward were more likely to change strategy when iMSNs were activated by optogenetic light stimulation, while the inverse was true during periods of dMSN activation (Nonomura et al., 2018). In terms of action initiation, optogenetic stimulation during a fixed-ratio lever press task increased the latency to the first lever press regardless of which pathway was stimulated, or whether light stimulation suppressed or activated target cells (Tecuapetla et al., 2016). These manipulations did however disrupt movement in a cell dependent manner, dMSN light stimulation slowed movement initiation, while iMSN stimulation caused initiation to be aborted in favour of other behaviours. The fact that either suppression or activation of either pathway disrupts initiation and execution of actions, suggests that it is the precise pattern of activity across and within pathways, not the overall rate, which is critical for movement regulation.

1.1.9 Rodent models of dopamine depletion

The importance of dopamine in regulating such activity patterns has since been confirmed using parkinsonian rodent models. A pattern of cell death similar to that seen in PD can be recapitulated in rats or mice using the neurotoxin 6-hydroxydopamine (6-OHDA), which selectively destroys monoamine cells when injected directly into the brain (Deumens et a., 2002). It is typically administered alongside a norepinephrine reuptake inhibitor such as desipramine, so that 6-OHDA is selectively transported into dopaminergic neurones only, leading to terminal disruption of mitochondrial function (Rodriguez-Pallares et al., 2007). The pattern of cell loss is therefore highly dependent on injection site and toxin concentration. Near total dopaminergic cell death is achieved by injected 6-OHDA into the medial forebrain bundle (MFB), which destroys all dopamine tracts originating from the midbrain including those belonging to the nigrostriatal, mesolimbic, and mesocortical pathways. This procedure is usually only administered unilaterally, which reduces the severe appetitive and motivational deficits produced by a bilateral lesion (Ungerstedt, 1971). A more selective lesion can be achieved by injecting 6-OHDA directly into the SNc and largely sparing the ventral tegmental area, while a lesion that is milder still is produced by injecting 6-OHDA into the striatum to be taken up by dopamine axonal terminals that project to specific striatal areas. This model produces robust unilateral deficits in paw use, locomotor activity, grip strength, and fine motor control (review: Deumens et al., 2002), which can be ameliorated by dopamine replacement (Dupre et al., 2016; Lundblad et al., 2002; Paillé et al., 2007) and DBS therapy (Dorval & Grill 2014; Mottaghi et al., 2020; Rattka et al., 2016), with the former treatment producing dyskinesias after chronic administration in all of those studies.

Initial experiments in anaesthetised rats that used a combination of *in vivo* cell firing patterns and juxtacellular labelling to identify putative dMSNs and iMSNs, found that dMSNs were inhibited by dopamine lesion, whereas indirect pathway neurons became more activated (Mallet et al., 2006). As discussed however, Cui and colleagues showed that iMSN and dMSN activity in healthy mice is indistinguishable during movement and both populations increase their activity prior to and during locomotion. Building upon these findings, it has been shown that both cell types have local ensembles that coactivate in a movement-specific manner (Parker et al., 2018). Despite dMSNs having suppressed global activity following dopamine depletion, their clear relationship with movement is preserved. Indirect MSNs on the other hand, lose nearly all of their spatial coordination and no longer increase their activity in response to movement due to a tonic increase of baseline activity at rest. Importantly, levodopa administration restored iMSN function at a therapeutic concentration. When given at a higher dose however, it induced dyskinesias that corresponded with a loss of spatial coordination and movement activity kinematics in dMSNs that was comparable to those observed in the iMSN population before treatment. When taken together with the previous section, it becomes clear that the coordination of BG cell activity in both time and space is critical for the regulation of movement and is lost in PD following dopamine depletion.

1.2 Beta oscillations: timing is everything

1.2.1 A brief introduction to oscillations

The BG is responsible for the initiation, regulation, and abortion of ongoing action sequences through continuous control of multiple interconnected nuclei. Not only does this depend on integration of large amounts of diverse sensory and contextual information from across the cortex and thalamus, as well as dopaminergic input from the midbrain, but upon dynamic temporal regulation of the precise patterning of activity across the entire network. Oscillatory activity is the principle mechanism by which the neuronal spiking from multiple brain regions is orchestrated, allowing efficient transfer of information between spatially distributed cell populations (Fries, 2005). Oscillations can be recorded with submillisecond temporal resolution from extracellular electrodes placed either on the skull (electroencephalography, EEG), the brain surface (electrocorticogram, ECoG), or within the brain itself (local field potentials, LFPs). These techniques record the summated electrical potentials due to transmembrane currents from active cells (dendrites, somas, and axons) in the brain area surrounding the electrode. The relative contribution of different current sources and sinks to the overall signal depends on location, orientation and strength of the current source, as well as the tissue resistance and electrode impedance (Buzsáki et al., 2012). Synaptic currents from local population networks are the main contributors to LFP shape as, unlike action potentials, they occur at slow enough timescales to summate in large enough numbers to produce a measurable signal. Thus, the LFP largely reflects synaptic inputs in the brain area in which it is measured. Temporal synchrony of large populations of cells is needed to produce LFP oscillations

and it is generally accepted that they represent ongoing population activity. In general, oscillations have been studied in association with global state changes that are linked to arousal and specific semi-arbitrary frequency bands have been implicated in distinct physiological function (Buzsáki et al., 2002; Buzsáki & Draguhn, 2004; Buzsáki & Wang, 2012; Engel & Fries, 2010; Fries, 2005).

1.2.2 History of beta oscillations in Parkinson's disease

The limitations of the classic Albin/DeLong model led to belief that it was the timing of BG activity which is important for movement regulation. It was noted that dopamine depletion caused pallidal neurones, which were consistently uncorrelated in healthy primates, to become significantly coherent at under 15Hz (Bergman et al., 1998). Several more studies in both patients (Levy et al., 2000) and MPTP primates (Nini et al., 1995) also showed that cells in the BG were abnormally synchronised and tended to fire in bursts of activity. The study of abnormal network synchrony in PD has benefited greatly from surgical interventions, where LFPs can be easily recorded from DBS electrodes typically implanted into the STN or GPi. It was shown that power within, and coherence between, the STN and GPi was dominated specifically by oscillations in the 10 to 35Hz beta band in patients off medication (Brown et al., 2001). Beta activity was reduced by levodopa and replaced by gamma band activity between 70 to 85Hz, which is thought to be a proxy for increased spiking activity. The reciprocal relationship between beta and gamma was further emphasised during movement, which reduced beta band STN-GPi coupling in favour of gamma activity (Cassidy et al., 2002). Robust increases in beta power after dopamine depletion has since been confirmed by extensive studies in humans (Kühn et al., 2004, 2008; Moran et al., 2008; Priori et al., 2002; Silberstein et al., 2003), MPTP primates (Connolly et al., 2015;

Deffains et al., 2016, 2018; Feingold et al., 2015; Leblois et al., 2007; Soares et al., 2004; Stein & Bar-Gad, 2013), and 6-OHDA lesioned rats (Avila et al., 2010; Brazhnik et al., 2012; Cagnan et al., 2019b; Delaville et al., 2015; Dupre et al., 2016; Leventhal et al., 2012; Li et al., 2012; Mallet et al., 2008a, 2008b, 2020; Sharott et al., 2015, 2017).

These studies led to the development of the beta hypothesis, which states that increased beta band activity produced by dopamine depletion holds the network in an anti-kinetic state by reducing pro-kinetic gamma activity (Brown, 2003; Hammond et al., 2007). The temporal dynamics of beta activity during movement support this hypothesis, where beta power is most prominent at rest or when asked to inhibit movements, is supressed prior to and during movement, and rebounds after it is finished (Kühn et al., 2004). Beta desynchronization prior to movement was also shown to correlate with reaction time in this study. In accordance with this, initiation of movements cued during periods of high beta power are delayed (Williams et al., 2005) and their eventual force diminished (Gilbertson et al., 2005), while externally driving the motor cortex (Pogosyan et al., 2009) or STN (Chen et al., 2007) at beta frequency has the same effect. Perhaps the strongest evidence supporting the anti-kinetic role of beta band activity comes from correlative evidence taken from PD patients during treatment. Increased beta power in the STN is reduced by dopamine replacement therapy (Priori et al., 2002; Tinkhauser et al., 2017b), and by DBS therapy, where reductions correlated with the extent of motor improvement (Kühn et al., 2008; Little et al., 2012; Tinkhauser et al., 2017a; Weinberger et al., 2006).

1.2.3 History of beta oscillations in animal models of Parkinson's disease

Unlike humans, increases in beta power following MPTP administration in primates is restricted to a lower frequency band between 8 and 15Hz (Deffains et al., 2016; Feingold et al., 2015; Leblois et al., 2007; Soares et al., 2004; Torrecillos et al., 2018). Despite the difference in frequency, this band is modulated by movement in an similar manner to that recorded in humans (Feingold et al., 2015), is increased for the duration of hold periods (Spinks et al., 2008), and is positively correlated with reaction time (Zhang et al., 2008). Moreover, increased beta power in the STN and GPi is reduced by therapeutic administration of levodopa (Tachibana et al., 2011). It is therefore accepted that activity in this narrower band is comparable to the 13-30Hz activity recorded in humans.

The MPTP primate model provides a unique opportunity to investigate the evolution of abnormal beta activity as the disease progresses. MPTP is typically administered systemically over a period of many weeks or months until motor deficits reach the required threshold, which allows the model to more accurately reflect the chronic progression of PD. This approach is seen as the gold standard in PD modelling in NHPs, as evidence suggests it produces more consistent degeneration in other non-dopaminergic monoamine midbrain systems that are responsible for the non-motor symptoms observed in PD, and even some reports of alpha-synuclein-positive aggregation in the nigrostriatal pathway not seen in the acute model (Masilamoni & Smith, 2018).

Efforts using this approach to establish a correlative link between global beta power and particular motor deficits have been less successful compared to corresponding studies in humans however, with some studies reporting that increased

beta does not appear until after symptom onset (Devergnas et al., 2019; Leblois et al., 2007) and does not positively correlate with symptom severity (Connolly et al., 2015), which could suggest that beta oscillations do not play a causal role in symptom generation. Having said this, primate studies are limited to a single structure and are severely limited by small sample sizes that would not capture the variation typically seen in human studies (Rosa et al., 2011). In this regard, beta synchronisation between GPi and GPe has been shown to increase with disease progression when pooling data from multiple primates, but did not exist on the level of individual animals (Muralidharan et al., 2016). It is also possible that these contradictory findings in monkeys represent the evolution of PD over time and that oscillatory abnormalities only begin to affect movement after a certain level of dopamine depletion is reached that cannot be compensated for using physiological processes such as neuronal plasticity. This framework may partly explain the delayed emergence of increased beta power relative to symptoms not only in MPTP primates (Leblois et al., 2007), but also in rodent models of PD (Mallet et al., 2008b).

An increase in beta power following dopamine depletion has also been recorded in rodents over a wide frequency range that likely depends on experimental methodology and behavioural context. Increased activity between 13 and 20Hz has been recorded in anaesthetised rats (Mallet et al., 2008a, 2008b; Sharott et al., 2017) and those performing well-learned tasks (Lemaire et al., 2012; Leventhal et al., 2012), while recordings in awake freely moving rats has recorded increased power anywhere between 20Hz (Li et al., 2012; Sharott et al., 2005) and 40Hz (Avila et al., 2010; Brazhnik et al., 2012; Delaville et al., 2015). Investigation into beta oscillations in rodents has been primarily restricted to rats, due to the controversial relationship between dopamine depletion and parkinsonian pathophysiology in mice, where some

studies report strong beta activity (McCarthy et al., 2011; Sanders & Jaeger, 2016) and others do not (Lobb & Jaeger, 2015). Despite the wider range of frequencies seen in rodents when compared to NHPs, rodent beta power is modulated by movement (Avila et al., 2010), is reduced by levodopa (Dupre et al., 2016) and DBS therapy (Li et al., 2012), and remains within the range of frequencies seen in individual PD patients (Quinn et al., 2015; Tinkhauser et al., 2017a). The frequency difference observed between patients, NHPs, and rodents could be seen as simple species variation, or it could be the result of a more focal dopamine lesion when compared to the myriad of cellular changes produced by a chronic neurodegenerative disorder.

1.2.4 The role of beta oscillations in network stabilisation

Using the influential communication through coherence framework (Fries, 2005) and a wealth of evidence from patients and PD animal models, the beta hypothesis was refined further to better incorporate a physiological role in signal processing. Beta activity is thought to promote existing motor states by inhibiting the processing of new movements (Brittain et al., 2014; Engel & Fries, 2010). They do this under physiological conditions by temporarily restricting the information coding capacity of the BG in time and space, as individual cells can only fire at specific phases of the oscillation, once released from this rhythm, cell populations can once more fire dynamically with movement. If beta oscillations do indeed dynamically control information coding, you would expect to observe a gradiated response in activity during motor tasks that scale inhibition in terms of force or number of sensorimotor areas involved (e.g. holding one finger in place will recruit fewer neurones than a clenched fist). As predicted, beta suppression has been shown to scale with exerted force during a gripping task in medicated PD patients (Tan et al., 2013), while in

healthy primates beta power is scaled with the complexity of gripping movement (Spinks et al., 2008). Importantly, firing rate in the motor cortex was inversely correlated with beta activity and positively correlated with gamma band activity.

As previously discussed, the precise timing and pattern of cell firing throughout the BG is critical for regulating ongoing movement. Increased beta power in STN LFPs represents an increase in the number of cells oscillating at beta frequencies, which in theory could produce the motor impairments seen in PD by rigidly entraining population firing during periods critical for movement. In line with this, a significant proportion of STN and GPi cells have been shown to persistently oscillate at beta frequency (Baaske et al., 2019; Moran et al., 2008; Weinberger et al., 2006, 2012), a feature which correlates with several parkinsonian motor symptoms such as akinesia and rigidity (Little et al., 2012; Sharott et al., 2014; Tinkhauser et al., 2017a). This has been shown to be a network wide phenomena in awake MPTP treated primates where more extensive recordings are possible, and it is estimated that between 30 and 80% of neuronal spiking in the motor cortex is locked to ongoing beta activity (Baker et al., 1997, 2003; Murthy & Fetz, 1996), while this number is estimated at 60% in the striatum (Courtemanche et al., 2003). Taken together, these studies provide strong evidence that increased beta band activity massively reduces the information coding capacity of the entire motor network in PD.

In rats, a similar increase in beta power following dopamine depletion has been recorded over a wide frequency range that likely depends on experimental methodology and behavioural context. Increased beta power has been recorded throughout the network in cortex (Sharott et al., 2005), striatum (Sharott et al., 2017), STN (Sharott et al., 2005), GPe (Mallet et al., 2008a), and SNr (Avila et al., 2010). It

has been shown in the STN that neurones phase-lock their firing to the beta band specifically (Baaske et al., 2019) and increased coherence has been recorded across the STN in spatially distributed populations (Mallet et al., 2008b). Studies using complex time-locked behaviours found that beta oscillations were not rigidly linked movements but were robustly increased following cues used to determine motor output (Leventhal et al., 2012). While the behavioural context here may not translate perfectly to human experiments, it supports the dynamic role of beta in network stabilisation rather than a specific 'anti-kinetic' signal.

1.2.5 The transient nature of beta activity

Many of the early studies linking beta power to motor symptoms did so using global averaging techniques that typically represented beta band activity as being continuously elevated. In reality, beta power fluctuates over time, giving rise to bursts of activity that are locked both temporally to ongoing movement and spatially within and between BG structures (Cagnan et al., 2019b; Tinkhauser et al., 2017a, 2017b). A beta burst is typically defined as a period in which beta power exceeds a certain threshold, usually defined in terms of standard deviations away from the mean power. Burst amplitude increases with duration, which is indicative of the progressive recruitment of local neuronal populations over time, suggesting that it is longer bursts that represent the potentially pathological recruitment of large cell populations.

In accordance with this hypothesis, Tinkhauser et al., 2017a found that UPDRS scores positively correlated with the number of longer bursts (>0.6ms) recorded from the STN, while negatively correlated with shorter bursts (≤0.6ms). Both Levodopa (Tinkhauser et al., 2017b) and conventional DBS therapy (Tinkhauser et al., 2017a) were shown to truncate longer bursts, which led to a corresponding increase in the

total number of short bursts. Reaching tasks in medicated PD patients show that the presence of bursts before movement onset reduced peak velocity in a burst amplitude dependent manner, while increased reaction times were associated with bursting immediately after the GO cue (Torrecillos et al., 2018). This suggests that even though beta oscillations wax and wane over short time scales they are capable of interfering with action initiation and movement regulation. This is unsurprising when you consider data showing that beta bursts synchronize across structures to produce a network-wide phenomenon (Cagnan et al., 2019b).

1.2.6 Where is pathological beta activity generated?

The original depolarisation block hypothesis of DBS action states that it provides therapeutic benefit by inhibiting STN activity. As discussed, this was largely rebuked by evidence showing that both GPi and GPe firing rates were increased by high frequency stimulation. In light of this finding, and extensive work correlating beta activity with motor impairment in PD, it has been suggested that DBS provides therapeutic benefit by disrupting beta oscillations (Hammond et al., 2007). It is important to remember that the BG exists as a series of functional loops, such that its motor output to the thalamus will directly affect the input it receives to the striatum and STN via multiple feedback pathways. And while clinical studies have greatly expanded our understanding of BG function and the role oscillations play in orchestrating neural activity, it remains unclear as to the structure and mechanism by which abhorrent beta activity is generated and propagated in a circuit that is cyclic in nature.

The cortex (Li et al., 2012), striatum (McCarthy et al., 2011; Sharott et al., 2017), GPe (Mallet et al., 2008a; Crompe et al., 2020), GPe-STN loop (Nevado-Holgado et al., 2014; Tachibana et al., 2011), and GPe-striatal loop (Corbit et al., 2016) have all

been implicated in the generation, amplification, and/or propagation of beta rhythms. DBS is highly efficacious when delivered to the STN or GPi and reduces elevated beta band activity throughout the network, which suggests a strong subcortical drive, and makes the STN-GP loop the most obvious candidate for propagating pathological rhythms. The anatomical architecture of the BG certainly supports this theory. As one of the two major BG-input nuclei, the STN receives huge glutamatergic drive from the cortex via the hyperdirect pathway, as well as indirect striatal input via inhibitory GPe projections. It can therefore be viewed as a central hub of the BG as it integrates information from across the network, and it has been proposed to pathologically propagate beta oscillations generated by the cortex (Hammond et al., 2007).

This is due, in part, to the lack of historical evidence of increased beta in the striatum of MPTP primates (the other cortical target), but also because the STN directly influences downstream BG-output activity (Deffains et al., 2016) and is particularly susceptible to ongoing beta activity in the cortex (Baaske et al., 2019; Sharott et al., 2005). In support of this, a study of patients with electrodes implanted into both GP and STN found that local beta power was modulated by the alignment of oscillatory activity between structures. Specific alignments (i.e. phase differences) consistently increased beta power, the magnitude of which correlated with the duration of phase locking (Cagnan et al., 2015). Importantly, L-Dopa reduced the frequency and duration that both structures spent in beta-promoting alignments, suggesting that excessive synchrony driven by the STN propagates beta oscillations in the parkinsonian state.

Early models of BG function that portrayed the indirect pathway as a linear process have been shown to be overly simplistic. The GPe, for example, is made up

of two distinct cell types that have unique firing properties (Mallet et al., 2008a), anatomical connections (Mallet et al., 2012), and functional roles (Mallet et al., 2016). Prototypic cells make up an estimated two-thirds of the overall population and represent classical GPe cells that project predominantly to STN, while the remaining third is largely made up of arkypallidal cells that provide negative feedback to the striatum (Mallet et al., 2012). These two cell populations have been shown to fire reliably in anti-phase in anaesthetised rats, which suggests that there is also strong lateral inhibition within the GPe that is potentially driven by prototypical cells (Crompe et al., 2020). Moreover, the GPe and STN are also reciprocally connected, with STN providing positive feedback via glutamatergic axons that presumably project to both GPe subpopulations unequally (Koshimizu et al., 2013a; Nevado-Holgado et al., 2014). Considering that studies in multiple species have shown both structures oscillate robustly and synchronously at beta frequency following dopamine depletion, and that both structures make connections throughout the network, it has been suggested that the GPe-STN loop acts as a central pattern generator for BG activity and propagates pathological beta activity (Mallet et al., 2008a; Nevado-Holgado et al., 2014). Computational studies show that any negative feedback loop with delays can generate oscillatory activity patterns (Ermentrout et al., 2001). In terms of synaptic connectivity, individual GPe cells only sparsely innervate the STN (Mallet et al., 2012), and so under physiological conditions are unlikely to be recruited in large enough numbers to widely synchronise STN. In PD however, increased STN synchrony driven by ongoing cortical beta activity would recruit substantial GPe populations, which in theory could amplify pathological activity and propagate it throughout the network. Elevated beta activity is also consistently found in the GPe (Mallet et al., 2008a), and perhaps unsurprisingly given the anatomical connectivity of the GPe-STN loop, the

proportion of synchronous GPe and GPi neurones also increases significantly after MPTP administration (from 16.7% to 46.9%), making it impossible to tease apart the contributions of each individual structure in humans or primates (Heimer et al., 2002). In 6-OHDA rats however, optogenetic silencing of STN or M1 had no effect on beta activity, while light stimulation of GPe significantly reduced beta power throughout the network (Crompe et al., 2020). Moreover, artificially entraining the network at 20Hz recapitulated pathological phase-locking of GPe neurones only when delivered to the GPe itself, and not after cortical or STN stimulation.

While this evidence points towards the role of GPe in propagating beta rhythms, it does not rule out indirect contributions from connected areas such as the striatum. Recent evidence in anaesthetised rats, where it is possible to segregate MSN sub-populations, show that iMSNs become preferentially phase-locked to the trough of cortical beta oscillations following dopamine depletion (Sharott et al., 2017). This finding suggests that iMSNs are particularly susceptible to dopamine depletion and is in accordance with studies reporting a pathological loss of their temporal and spatial coordination in response to movement (Parker et al., 2018). As the largest BG nuclei, striatal iMSNs converge onto target GPe neurones with a synaptic density of approximately 50-fold greater than that of STN (Fujiyama et al., 2011; Koshimizu et al., 2013; Oorschot, 1996). Indirect MSNs are therefore perfectly placed to widely coordinate GPe activity and become excessively synchronised to ongoing cortical beta oscillations after dopamine depletion.

Rhythmic striatal input to GPe must then produce rhythmic pallidostriatal feedback via prototypic neurones that is likely to reinforce such activity, which a combination of computational (Corbit et al., 2016) and optogenetic studies (Crompe et

al., 2020) suggests is critical for beta generation. Pallidostriatal neurones have been shown to synapse at GABAergic interneurons that powerfully modulate striatal output (Bevan et al., 1998; Gerfen & Surmeier, 2011). Complementary studies suggest that abhorrent striatal activity is primarily driven changes in interneuron connectivity and synchronisation in response to dopamine depletion (Gittis et al., 2011; Mallet et al., 2006; McCarthy et al., 2011). It has been shown that pharmacological (McCarthy et al., 2011) or optogenetic (Kondabolu et al., 2016) stimulation of striatal interneurons induces PD-like increases in beta activity that are accompanied by motor deficits. Taken together, these studies implicate the dysfunctional indirect pathway in the amplification and propagation of abnormal oscillatory activity generated in the cortex, which has direct consequences for the pattern of activity generated by BG-output nuclei.

In order to better understand the temporal relationship between structures in the motor network, Cagnan et al., (2019) compared BG spiking activity to ongoing beta activity in parkinsonian rats. High frequency oscillations in LFP waveforms are thought to represent the activation of large neuronal ensembles that can be quantified in the absence of suprathreshold cell spiking using background unit activity (BUA). Critically, temporal alignment of the ECoG and STN BUA precedes individual cortical beta bursts and follows their temporal evolution. When probing this relationship further, it was found that abrupt changes in phase difference between structures (termed phase slips) preceded the evolution of a beta burst, and that the phase difference immediately after each phase slip was maintained for the entire burst duration. These conditions were consistently found in striatum, STN, and both GPe cell types, which at the very least, suggests that specific interactions between the indirect pathway nuclei provide the conditions through which beta can propagate around the network.

1.2.7 The role of cortical beta-band oscillations

The majority of studies investigating BG dynamics in patients are restricted to the STN due to the practical limitations of neurosurgery. The other major site accessible in patients is the primary motor cortex (M1), which can be recorded using non-invasive scalp EEG as well as subdural ECoG strips. As discussed, it has been proposed that BG nuclei pathologically propagate beta oscillations generated by the cortex, and that DBS provides therapeutic benefit by disrupting network-wide entrainment (Hammond et al., 2007). In support of a cortical generator, evidence in dopamine depleted rats (Li et al., 2012; Sharott et al., 2005) and primates (Goldberg et al., 2004), show that pyramidal cells fire in pathological bursts that are phase-locked to ongoing beta oscillations, and that BG nuclei such as the STN (Baaske et al., 2019) and striatum (Sharott et al., 2017) become pathologically locked to cortical activity specifically in the beta frequency range.

Unlike subcortical structures, there is only limited evidence of a global increase in cortical beta power in humans however (de Hemptinne et al., 2013, 2015), with some evidence even suggesting it is reduced (Stoffers et al., 2007). Having said this, M1 beta power is modulated by movement in a similar manner to that recorded in the STN, where power is suppressed prior to and during movement, and then rebounds after action termination (Miller et al., 2012). This dynamic response of cortical beta during movement has been shown to be affected in PD patients (de Hemptinne et al., 2015; Labyt et al., 2005). The effect of DBS on cortical beta activity remains unclear however, with contradictory studies reporting either suppression (Fraix et al., 2008; Whitmer et al., 2012) or amplification of beta activity in M1 (Melgari, 2014), while one large study reported no change at a group level (de Hemptinne et al., 2015).

High frequency stimulation of STN will not only depolarise neuronal soma and axons local to the electrode, but also the dendritic terminals of the hyperdirect pathway. Cortical activation has been recorded in humans during STN DBS that is potentially driven by antidromic activation of the hyperdirect pathway (Fraix et al., 2008; Kuriakose et al., 2010), while similar observations in rats correlate with motor improvements (Dejean et al., 2009). Building upon this work, it has been shown that DBS produces antidromic spiking in the cortical pyramidal neurones of 6-OHDA rats that reduced cortical beta power, restored tonic pyramidal cell firing, and correlated with DBS efficacy (Li et al., 2012). It was also shown that antidromic cell firing modulated pyramidal cell firing probability, opening up the possibility that DBS provides therapeutic benefit by directly desynchronising cortical input to the BG.

The original beta hypothesis was based on the reciprocal relationship between beta and gamma oscillations that were framed for simplicity as two discrete frequency bands acting in opposition. Beta oscillations do not, of course, exist in isolation but continuously interact with multiple frequency bands that are all affected by a myriad of cell activity throughout the network. Slower oscillations, such as those in the beta band, are thought to modulate the excitability of neuronal ensembles, biasing cell firing to specific phases of the oscillation. Activation of large neuronal cell populations produces high frequency LFP content in the gamma band (60-250Hz), which is supported by evidence correlating this activity with single-neuron spiking (Manning et al., 2009) and blood oxygenation level dependent signal activation (Scheeringa et al., 2011).

If beta oscillations do indeed restrict information encoding in time and space, you would expect to see a significant interaction with ongoing gamma activity.

Significant phase-locking of high-frequency gamma band activity to the peak of ongoing M1 beta oscillations, termed phase-amplitude coupling (PAC), is observed in PD but not in hyperkinetic disorders such as dystonia (de Hemptinne et al., 2013). Moreover, it has also been shown to occur within the STN (Yang et al., 2014) and between STN and cortex (Shimamoto et al., 2013). Importantly, beta-gamma coupling in the motor cortex has been shown to correlate with rigidity in PD and, unlike cortical beta power, is consistently reduced by therapeutic DBS (de Hemptinne et al., 2013, 2015).

It has been shown that beta oscillations in the parkinsonian motor cortex have sharper peak features relative to the trough when compared to healthy adults, which creates a more asymmetric non-sinusoidal waveform feature that correlates with gamma-beta PAC (Cole et al., 2017). It has been proposed that this sharp beta peak is generated by synchronous afferent BG input onto cortical pyramidal cells (Sherman et al., 2016). In line with this, increased coherence between the GPi and cortex was recorded in PD patients that was reduced by therapeutic DBS (Wang et al., 2018). The cortical beta waveform becomes smoother and more symmetric after DBS, suggesting that it disrupts pathophysiological network entrainment. These findings fit nicely with the idea that computational power is reduced throughout the motor network in PD. They also support the idea that synchronised burst firing originating in the cortex rigidly entrains the network to beta frequencies through subcortical propagation.

1.3 Closed-loop phase-locked stimulation: a future therapy?

1.3.1 Introduction to closed-loop approaches for Parkinson's disease

DBS therapy is remarkably effective in many cases but is limited by the cost and risk associated with surgery (Appleby et al., 2007; Hariz et al., 2008; A. Williams et al., 2010), which may explain why only 2% of patients undergo surgery (Kestenbaum et al., 2015). One study investigating the long-term effects of DBS found that it reduced symptoms by approximately 40% on average after four years, but also reported stimulation-induced side effects in up to 50% of patients (Volkmann et al., 2009). Common side effects include speech intelligibility (Tripoliti et al., 2011), impaired executive functioning (Hershey et al., 2004; Jahanshahi et al., 2000, 2013), and a paradoxical worsening of symptoms in unaffected limbs (Chen et al., 2006).

DBS provides continuous high frequency stimulation that does not fluctuate with either symptom severity or the appearance of side effects, both of which wax and wane over time depending upon multiple factors such as treatment regiment, stress, sleep, and diet (Jankovic, 2005). If DBS could be applied only during periods when symptoms are present, or better still, before they occur, then the amount of stimulation delivered to the brain could be massively reduced. The advantages of such a treatment strategy would be manyfold, but most importantly it would reduce side effects by allowing physiological activities to continue mostly undisturbed and limiting the spread of current to non-target structures (e.g. Little et al., 2016). It may also improve the safety and cost of treatment by reducing the number of compulsory surgeries needed through

increasing battery life, and by minimising the need to change stimulation parameters due to a loss in efficacy caused by habituation to stimulation.

In order to stimulate only when necessary, the application of current must be driven in real time by a biomarker of the disease, which is commonly referred to as closed-loop DBS or adaptive DBS. Closed-loop DBS has been successfully implemented using various technologies and signals in both cardiac arrhythmias (Sutton et al., 2007) and epilepsy up to now (Jobst et al., 2017). In terms of PD however, closed-loop technologies are in their embryonic stages and several potential biomarkers of disease action are being explored. Behavioural measures such as using an accelerometer to track tremor provide ground truth of symptom severity, but offer no mechanistic insight and are difficult to implement in most cases. In the unique case of tremor, where it is possible to easily track symptom severity automatically in a quantifiable manner, preliminary closed-loop studies show that synchronising stimulation to ongoing tremor activity can be particularly efficacious (Brittain et al., 2013). This approach is simply not possible for more complex motor impairments such as bradykinesia or postural disturbance, where a neurophysiological marker of disease action is needed.

Perhaps the most immediately obvious candidate biomarker of ongoing symptom severity would be dopamine levels in the striatum, which can be accurately measured using intracranial microdialysis (Kilpatrick et al., 2010), a technique which can now be integrated into a stimulation electrode (Zhang et al., 2016, 2018). Not only is this approach limited by significant technical barriers such as avoiding tube blockages and miniaturising analysis hardware onto an implantable device, but is also unlikely to have the temporal resolution needed to continuously track fleeting changes

in symptom severity. When considering these limitations, by far the most practical solution is to utilise the recording electrode itself to track electrophysiological biomarkers of disease action.

1.3.2 Beta as a biomarker

Beta oscillations are increased throughout the motor network in PD, are reduced by therapeutic treatment, and correlate with symptom severity. They also represent an ideal pathophysiological biomarker of disease action from a practical point of view, as oscillations are stable and consistent LFP features that can be recorded indefinitely. Moreover, activity within each frequency band is thought to have a specific function depending upon the structure(s) and task(s) involved, allowing closed-loop approaches to tune into and target specific processes. This approach was first validated by Little et al., (2013), where high frequency STN stimulation delivered only during periods of high beta power provided therapeutic benefit comparable to continuous DBS despite using half as much power. Interestingly, when comparing how either treatment strategy interacted with ongoing beta activity, they were found to have different mechanisms of action, whereby only closed-loop DBS reduced the number 'long' beta bursts (>0.6s) that correlate with PD severity (Tinkhauser et al., 2017a).

Despite the comparative success of these studies, the implementation of continuous stimulation during periods of high beta power is a relatively crude approach for several reasons. In its current form, threshold detection is carried out using an externalised CPU that can only trigger stimulation after a delay of approximately 500ms. This not only prevents its use in a clinical setting as the hardware must be miniaturised and installed onto existing DBS systems, but the stimulation delay also provides theoretical limitations to its potential efficacy. Firstly, even if longer bursts are

pathological, it is entirely possible that the delay in stimulation onset will limit efficacy by delaying burst suppression during critical periods for movement. Considering that beta levels rise and fall in a movement dependent manner, more extensive testing during periods of natural movement is needed to fully understand the extent of this limitation. Secondly, by waiting for beta amplitude to reach a certain threshold, the closed-loop system described above is permitting a certain level of entrainment in both time and space that is arbitrarily set by the experimenter. Computational studies show that larger amplitude oscillations are harder to disrupt and that it would be most energy efficient to disrupt neural ensembles before they become entrained and not afterwards (Weerasinghe et al., 2019). While it is possible to optimise this threshold further, the current feedback mechanism will always miss the optimal window for suppression. Finally, even though stimulation is restricted only to periods of high beta power, it is still delivering continuous high frequency stimulation over long intermittent periods that will undoubtedly disrupt non-pathological processes throughout the network; and is therefore likely to produce similar side effects to standard DBS therapy. The limitations described above should be viewed in a positive light however, as it leaves ample room for improvement upon a closed-loop system that is already potentially providing substantial benefit. The importance of their findings should also not be understated and, at the very least, they show that beta oscillations provide a reliable biomarker with which to limit stimulation time without compromising on efficacy.

If beta oscillations are truly pathological, then the optimal solution would be to interact and supress activity in this band with minimal interference to other independent processes. A landmark study in MPTP primates delivered single or trains of pulses to the GPi in response to action potentials recorded from the motor cortex (Rosin et al., 2011). This strategy outperformed standard DBS when reducing low

frequency oscillatory activity and discharge rates in the pallidum (including those in beta band) and was also more effective in reducing akinesia. In support of the role of increased network synchrony in PD pathophysiology, reductions in akinesia were associated with oscillatory changes but not discharge rates in the GPi. Importantly, this study proved that by accurately targeting underlying network dynamics it is possible to provide superior treatment benefit with massively reduced electrical input. Using spiking activity to time stimulation is not a translatable strategy however, as action potentials cannot be reliably recorded over long periods from a DBS electrode. Moreover, the need to record from multiple sites would significantly increase surgical complexity and risk. This study also used a delay of 80ms from cortical spike detection to GPi stimulation in an attempt to coincide pulses with pathological bursting activity. Shorter delays, as well as instantaneous stimulation using GPi as both referencing and stimulation site, provided detrimental results, highlighting the importance of a stable biomarker that can accurately target a specific neural process over long periods of time.

1.3.3 Rationale for phase-locked stimulation

Several lines of evidence over the past decade have identified phase-locked stimulation as the most efficient way to modulate synchronous network activity. Open-loop stimulation at or close to the target frequency will drift slowly in and out of phase with the target oscillation, allowing post-hoc comparison of how stimulation at each phase affects oscillatory amplitude. The first study to utilise such an approach targeted peripheral tremor recorded from an accelerometer, which is highly synchronous with cortical activity at the same frequency so can be used as a proxy of pathological neural activity. Unlike DBS which applies direct electrical current, transcranial alternating

current stimulation (TACS) oscillates current at a chosen frequency to supposedly interact naturally with cortical oscillations. Post-hoc analysis of open loop TACS at tremor frequency showed that tremor amplitude was bidirectionally modulated in a phase dependent manner, such that specific phase differences (not absolute phase) suppressed tremor while others amplified it (Brittain et al., 2013). Locking TACS to the phase of maximal suppression produced a mean tremor reduction of 52%.

A similar study using tremor frequency thalamic DBS in order to stimulate once at a random phase per cycle, found that pulses delivered to one half of the cycle suppressed the oscillation while the other half exaggerated it (Cagnan et al., 2013). Unlike the TACS study that used phase cancellation to suppress tremor oscillations, the effects reported here were in anti-phase and may be produced by interactions with the sinusoidal pattern of neuronal excitability seen in the thalamus at tremor frequencies. Interestingly, when stimulation happened to hit consecutive suppressive phases it caused up to a threefold increase in suppression, suggesting that more accurate phase tracking could massively improve efficacy. While the suppression observed in these studies fell short of being clinically useful and was only tested over extremely short periods, they provided preliminary evidence of the beneficial effect of phase-locked stimulation, especially when you consider the detrimental effect of open-loop low frequency stimulation on essential tremor (Constantoyannis et al., 2004).

Direct evidence supporting phase-locked stimulation in PD has since been recorded using the same technique described above but stimulating at beta frequency in the STN (Holt et al., 2019). Here, the beta cycle was split into four semi-arbitrary segments, and it was found that stimulation delivered to the descending phase reduced oscillatory amplitude while the ascending phase increased it. As expected,

consecutive stimulation pulses in the same segment led to an augmented suppressive response, which was increased further still by greater phase precision. Moreover, STN BUA only began to reduce after four consecutive suppressive phase pulses, implying that consistent phase-locked stimulation is needed to decouple the network. These findings suggest that stimulation delivered consistently to a specific suppressive phase could powerfully modulate beta oscillations. Importantly, this strategy would only use a small amount of electrical current that is unlikely to affect other activity parameters, as evidenced by the negligible effect of single pulse stimulation of firing rate in the above study. In line with this, oscillatory activity and burst firing are potentially regulated by independent mechanisms (Chan et al., 2011), and other closed-loop studies have shown dissociable effects of these parameters on motor performance (Rosin et al., 2011).

1.3.4 Examples of phase-locked stimulation

Phase-tracking technologies not only have potential clinical relevance but provide invaluable tools for selectively interacting with physiological processes to probe network dynamics. The earliest example of phase-locked stimulation targeted hippocampal theta rhythms, where the slow speed and stability of the oscillation make temporal resolution less important (Siegle & Wilson, 2014). Historical evidence from a wide range of studies suggests that neural activity is highly structured around slower rhythms, such that firing rates of genetically defined cell types peak at different phases of the theta cycle (Buzsáki & Wang, 2012). It has been suggested that hippocampal theta oscillations act to segregate incoming information from various sources. In particular, they help differentiate between activity encoding new information about the outside world and that which encodes the retrieval of stored information (Hasselmo,

2005; Hasselmo et al., 2002). Under this schema, input from the entorhinal cortex (EC) encodes new information about current state of the environment and is phase-locked to the trough of hippocampal theta, while memory retrieval processes encoded by CA3 cell firing are locked to the peak (Colgin et al., 2014). Siegle and Wilson (2014) used a H-maze to dissociate between these two processes, as mice must first memorise their starting position (information encoding – EC dependent) before using this memory during the choice portion of the maze to find reward (information retrieval – CA3 dependent). By stimulating in a phase-locked manner at either the peak or trough of ongoing theta oscillations while mice traversed specific portions of the maze, they were able to differentially impair performance by disrupting either retrieval or encoding of information respectively. Despite this system lacking the required responsiveness to have utility for less stable oscillations or those at higher frequencies, it provided strong evidence that phase-locked stimulation can affect behaviour using relatively sensitive perturbations. It also beautifully demonstrates the role oscillations play in orchestrating multiple streams of activity converging onto a single input structure with diverse functional meaning.

More recently, a system has been developed by Kanta et al., (2019) that can partially track the phase of high frequency gamma oscillations (40-70Hz) in real time. It works by first isolating the frequency of interest using a bandpass filter, the derivative of which is then is used to detect the peak (or trough) of the filtered oscillation by tracking when the derivative signal crosses from positive to negative (or negative to positive). This system has limited phase targeting granularity allowing stimulation to be triggered off either the peak or trough of an oscillation, which at high gamma frequency means the majority of stimulation pulses tend to occur on descending or ascending phases due to small stimulation delays. Furthermore, while the system was

implemented on a field programmable gate array (FPGA), allowing fast signal processing, algorithmic delays due to traditional filtering approaches still served to limit the responsiveness of the system. Nevertheless, this system is capable of reliably tracking oscillations up to 55 Hz and has been used to modulate gamma band activity in the basolateral amygdala. This activity is critical for emotional memory consolidation, and bidirectional modulation of oscillation amplitude during the consolidation phase of a memory task produced corresponding changes in performance. Taken together, these studies confirm the utility of phase-locked stimulation in a variety of settings that provide a basis with which to investigate the importance of neural dynamics on behaviour.

In relation to PD, efforts are currently ongoing across several labs to develop phase-tracking technology with the temporal resolution needed to modulate parkinsonian beta oscillations in real time. A recent study confirmed that phase-locked stimulation can modulate beta power in a bidirectional manner (Sanabria et al., 2020), but only recorded over extremely short periods of time (10 second bins), meaning that the magnitude of changes produced by persistent phase-locked stimulation remains unclear. It is also remains to be seen if real-time beta band modulation affects behavioural performance, which would establish a causal relationship between beta oscillations and motor impairment for the first time. In an attempt to address this question, one study applied phase-locked stimulation during periods of artificially high beta power in two healthy monkeys performing a reaching task (Peles et al., 2020). They did so using a brain-machine interface to train both subjects to volitionally increase their cortical power in order to initiate reaching trials. Stimulation targeting the descending phase suppressed beta power and reduced reaction times during this task. Although this study provides encouraging evidence that phase-locked stimulation

can improve motor performance through beta suppression, it did not accurately reflect a parkinsonian-like pathophysiological state. As such, further testing in PD models is necessary to investigate if similar behavioural improvements can be reproduced when interacting with endogenous activity.

1.3.5 The effect of phase-locked stimulation on neural dynamics

Through what mechanism does phase-locked stimulation modulate oscillatory activity and the underlying network activity? As discussed, oscillations under 100Hz are thought to arise from synchronous synaptic inputs to neuronal ensembles near the electrode. Modulating oscillatory activity therefore acts as a method of controlling activity both entering and exiting the target structure. In terms of PD, it has been shown that input to cortical neurones is typically synchronised to the peak of ongoing beta oscillations in a manner that correlates with symptom severity (de Hemptinne et al., 2013, 2015). Slower oscillations such as those in the beta band are therefore critical in regulating the timing of spiking activity that is critical for Hebbian-style synaptic plasticity. In principle, synapses are strengthened when pre-synaptic cells fire before the post-synaptic neuron and are weakened if it arrives afterwards (Feldman, 2012). Phase-locked stimulation has been shown to produce either phase advances or delays depending on when in the cycle pulses are delivered, which significantly alters neuronal synchrony but not firing rate (Nicholson et a., 2018). Phase shifts such as this may alter the recruitment of neurons in the target structure to ongoing network oscillations and could therefore produce long-lasting effects on regional connectivity via alterations in plasticity.

To study the effect of oscillatory synchrony in more detail, cortically evoked potentials (CEPs) produced at a “triggering” site were compared before and after

single pulse stimulation was delivered to an anatomically connected “stimulating” site (Zanos et al., 2018). Critically, the stimulation was phase-locked to either the peak or trough of ongoing beta oscillations. It was found that trough stimulation, when cell activity was at its peak, produced larger CEPs when compared to pre-stimulation baseline, while peak stimulation reduced CEP amplitude. Larger evoked potentials from identical stimulation pulses indicates increased information transfer between sites (i.e. increased synaptic strength). These effects were only present when stimulating during increased oscillatory activity and outlasted burst duration by up to 1.5 seconds, suggesting that oscillations are critical for synchronising input into target structures. Importantly, the more consistently stimulation hit the target phase the larger the evoked potential, which adds to multiple lines of evidence that highlight the importance of accurately tracking phase. Finally, increased CEPs were also observed in all areas connected to the stimulation site providing they had coherent oscillatory activity. The effect was independent of their spatial distribution, adding to several hypotheses implicating oscillations in the coordination of spatially distributed structures (Fries, 2005). They also provide a mechanism by which the elevated beta band activity observed in PD could have wide ranging effects on synaptic plasticity throughout the network. As expected, abnormal levels of LTP and LTD have been observed in PD that correlate with disease severity (Udupa & Chen, 2013). It is therefore possible that increased oscillatory activity and activity dependent plasticity throughout the network drive each other during the progression of PD. If true, phase-locked stimulation could provide extremely low-current persistent disruption of this positive feedback loop via network desynchronization. The changes elicited by phase-locked stimulation at a network level are likely to be quite different to those produced

using conventional DBS (Nicholson et al., 2018; Siegle & Wilson, 2014; Zanos et al., 2018), meaning that target networks must be carefully considered.

1.4 Aims

The literature described in the previous section uses a variety of phase specific methodologies and provides strong rationale for this project. While phase specific interactions with ongoing oscillatory activity has been demonstrated (Cagnan et al., 2013; Holt et al., 2019; Kanta et al., 2019; Peles et al., 2020; Sanabria et al., 2020), many questions remain about the precise properties of sustained accurate phase-locked stimulation on oscillatory modulation. Furthermore, the utility of such an approach when targeting beta oscillations in PD remains unclear. Although preliminary evidence using closed-loop stimulation to target beta activity provides encouraging evidence (Little et al., 2013; Rosin et al., 2011; Tinkhauser et al., 2017a), phase-locked stimulation promises to provide a tool for selectively targeting specific generators of pathological activity. We hypothesise that phase-locked stimulation will suppress beta-band oscillations in parkinsonian rats leading to an improvement in motor function.

To achieve this, we have developed a highly responsive system to produce continuous online phase-estimation. We utilise this system in an attempt to modulate beta activity in dopamine depleted rats during behaviour, thus directly testing the causal relationship between beta and motor impairment. In line with substantial evidence implicating the GPe and STN in propagating cortically generated beta activity in PD, we deliver stimulation subcortically to either structure that is phase-locked to

ongoing cortical beta oscillations. The remainder of this report is dedicated to the following experiments that were carried out in chronically implanted rats following unilateral dopamine lesion:

- Determined system accuracy with and without stimulation enabled;
- Quantified the cortical modulation produced when stimulating subcortically at different phases of the beta cycle;
- Determined the effect of beta modulation on system output;
- Compared the modulation produced by open-loop and closed-loop stimulation;
- Assessed spontaneous forelimb use during phase-locked stimulation that amplified or suppressed cortical beta power;
- Assessed gait performance during phase-locked stimulation that amplified or suppressed cortical beta power.

2 Materials and methods

Experimental procedures were carried out on 15 weight-matched male rats (Lister-Hooded, 350-400 g, Charles River, UK) and were conducted in accordance with institutional guidelines and the Animal (Scientific Procedures) Act 1986 (UK). Animals were kept on a 12-hour light-dark cycle at constant temperature and humidity, while food and water was provided *ad libitum*.

2.1 Surgical procedures

Each rat underwent two separate recovery surgical procedures performed under deep anaesthesia using isoflurane (4 % induction, 0.5 - 2 % maintenance) and oxygen (2 l/min). Local anaesthetic (Marcaine, 2 mg/kg, 2.5 mg/ml) and non-steroidal anti-inflammatories (Metacam, 1 mg/kg, 5 mg/ml) were administered subcutaneously at the beginning of all surgeries, while opioid analgesia (Vetergesic, 0.3 mg/ml, 0.03 mg/kg) was also provided for three consecutive post-operative days. The first procedure produced a unilateral dopamine lesion by injecting 6-hydroxydopamine (6-OHDA) directly into the substantia nigra pars compacta (SNc) using stereotaxic coordinates 4.9 mm posterior and 2.3 mm lateral from bregma at a depth of 7.8 mm from the brain surface. The neurotoxin 6-OHDA was dissolved immediately before use in phosphate buffer solution containing 0.02 % w/v ascorbate to a final concentration of 6 mg/ml. Between 1 and 1.5 µL of 6-OHDA solution was injected at a rate of 0.1 µL/min through the pipette, which was left in place a further 5 minutes before being

withdrawn. A subset of animals from early experiments were given desipramine (25 mg/kg, intraperitoneal; Sigma, Germany) approximately an hour before 6-OHDA at the beginning of surgery. In accordance with the 3Rs (*https://www.nc3rs.org.uk),* desipramine was discontinued due to poor post-operative recovery. Following full recovery and not less than 13 days later, those with the greatest reduction in contralateral paw-use during the cylinder task underwent a second procedure to implant pairs of stainless steel electrodes (California Fine Wire, stainless steel, bifilar, heavy formvar insulation, 127 µm strand diameter) into the external globus pallidus ([GPe], AP: -1.4 mm, ML: 3.2 mm, DV: -5.2 mm) and subthalamic nucleus ([STN], AP: -3.85 mm, ML: +2.5 mm, DV: -6.5 mm). The GPe is anatomically distinct from the entopeduncular nucleus in rodents, which is the homologue of the human GPi and located more posteriorly within the internal capsule, thus we could be sure that stimulation was restricted to the external segment only. Four M1.4 stainless steel ECoG screws were inserted bilaterally over the motor cortex (AP: [+1.5, +1.5, +4.6, +4.6] mm, ML: [-2.0, +2.0, -1.6, +1.6] mm), as well as two reference screws inserted over the cerebellum. The implant was then anchored to the skull at height of approximately 20 mm using bone cement. Neurotoxin injections, electrical stimulation, and ECoG recordings were all performed on the right hemisphere.

2.2 Closed-loop phase-locked stimulation

2.2.1 Real-time phase tracking and closed-loop trigger algorithm

A novel approach was developed by Colin McNamara to track phase within a band of interest in real time. A continuous transform was performed directly on the

digital values produced by the sampling analogue to digital converter (ADC). A sample rate of 20 kHz per channel was used in order to record the full detail of the stimulation artefacts aiding their removal in post hoc analysis. However, for phase tracking, the data was downsampled by producing a single sample from the sum of 8 to 12 (n_{dn}) successive samples, since tracking beta-band phase did not require such a high number of samples per cycle. Thus, the phase tracking component ran at sample rates in the range 1.67 to 2.5 kHz (varying the sample rate was one of the ways to achieve different target oscillation centre frequencies). Performing a continuous transform allowed a phase estimate to be instantaneously produced corresponding to each value of the downsampled data stream. A bandlimited complex estimate of the signal was generated from the downsampled wideband data stream by, on receipt of each sample, updating a complex weight register that maintained the relationship between the estimate of the signal and a pair of continuously oscillating reference sine and cosine waves. The error between the real part of the estimate signal and the current ADC sample was used to update the weight register for use with the next ADC sample. The centre frequency of the band of interest was set by the frequency of the reference waves. This depended on the downsampled sample rate and the number of values in the lookup table containing a quarter of a sine wave used to generate the reference waves (n_{points}, 11 to 15 values per quarter cycle were used). Thus the centre frequency of the phase tracker pass band was given by ($fc = 20000/n_{dn}/n_{points}/4$). The width of the band of interest was set by a coefficient on the error term used to update the weight register. This essentially smoothed the reference wave by dampening the rate of convergence between the estimate and the signal. Finally, a continuous phase estimate was produced by calculating the polar angle of the complex signal estimate using a CORDIC (Volder, 1959). A real-time trigger was generated when the phase

estimate passed into the target phase range unless it had been less than 0.8 of a target frequency period since the most recent passing into the target phase range. This was important to reduce stimulation at times of poor phase estimates for instance at times of low power in the target frequency range. A phase shift corresponding to half the stimulation width (100 μs) was subtracted from the phase estimate causing the stimulation to be triggered early allowing the middle of the stimulation to occur at the desired target phase. Additionally, to reduce the effect of electrical stimulation artefacts on the phase estimate, a digital hold circuit operating on the 20 kHz data stream held the sample preceding the stimulation trigger on the input of the phase tracking circuit for 600 μs from the start of the trigger. An offset removal digital filter was also implemented on the input to the phase tracker to remove any residual offset remaining from the analogue front end.

2.2.2 Data acquisition and electrical stimulation

Electrocorticogram (ECoG) signals measured from M1.4 screws referenced to two cerebellar M1.4 screws. These signals were amplified and digitised using a RHD2000 family amplifying and digitising headstage connected to a RHD USB Interface Board by a RHS Stim SPI Interface Cable all from *Intan Technologies* (*intantech.com*). A stimulation wire was wrapped around the recording cable using a three-stranded braid and epoxy added between the junction of the tether and headstage to provide structural support. Electrical stimulation was driven using a fully isolated current source (battery powered with an optically coupled trigger, A365RC, World Precision Instruments) with the source and sink terminals connected to the adjacent strands of the pair of stainless steel wires forming the stimulation electrode. Stimulation events were biphasic consisting of two consecutive pulses of opposite polarity between 30 and 70 μA in amplitude and 95 μs in duration separated by 10 μs.

To achieve closed-loop stimulation, a custom designed digital circuit was used to access the digital data stream from the headstage, track phase within a band of interest in real time, and generate digital pulses to activate the optically coupled trigger of the stimulation current source. The custom designed digital circuit was implemented using extra available digital circuitry within the field programmable gate array (FPGA) located on the RHD USB Interface Board.

2.3 Open field recording protocol

Before undergoing behavioural assessment during phase-locked stimulation, a number of standardised recording sessions were performed in order to optimise stimulation parameters in each rat. These extensive recordings form the basis of the analyses performed in chapters one and two. During data acquisition which took place over multiple days, rats freely explored a 90 by 50 cm open field surrounded on five sides with electrical shielding located in a dedicated recording room. Three to six recording blocks were performed per rat. Recording blocks consisted of eight pairs of recordings with a different real-time target phase applied in each pair. Target phase order was randomised across blocks. Stimulation was enabled in the first recording of each pair (stimulation recordings) and disabled in the second (baseline recordings). Stimulation recordings were approximately 4.5 minutes in duration and baseline recordings were approximately 2 minutes in duration. The real-time system generated triggers during 20 second epochs (on epochs) separated by 5 second trigger free epochs (off epochs) and was in operation across all recordings. Generating real-time triggers in the absence of closed-loop stimulation during baseline recordings allowed

comparison of the real-time system performance between open-loop and closed-loop operation. These recordings also provided the opportunity to assess baseline physiology in the absence of stimulation. Embedding short epochs lacking stimulation within stimulation recordings provided an internal comparison point to assess the effect of stimulation without the need to correct for changes occurring over longer time frames such as arousal, brain state, general movement levels and external electrical noise.

2.4 Stimulation parameter selection

The centre frequency for real-time phase tracking for each block was chosen at the start of the block based on power spectra generated from previous recordings from the same rat and was in the range 34 to 38 Hz. In order to match or slightly exceed the charge density produced by therapeutic DBS in humans (~30 μC/cm^2), we kept stimulation amplitudes between 30 and 70 μA, which equates to a comparable charge density in rodents when taking into account differences in electrode size and stimulation pulse width (e.g. a 50 μA 100 μs pulse produces ~40 μC/cm^2). The highest amplitude within this range was selected that did not produce out-of-band spectral contamination, which we define as stimulation-dependent spectral peaks outside of the target band (± 5 Hz of centre frequency). Such events tended to occur when stimulating at high amplitudes on suppressing phases.

2.5 Electrophysiological analysis

Post hoc analysis of ECoG spectral properties and stimulation phase including statistical tests were performed using SciPy (scipy.org). Text values are reported as mean ± standard deviation and error bars in plots show mean ± standard error of the mean unless otherwise stated. First stimulation artefacts were removed from the 20 kHz recordings by interpolation between the sample immediately preceding the stimulation and the sample 1.7 ms later. The resulting signals were downsampled to 1 kHz in two steps using finite impulse response anti-aliasing filters (designed using remez, combined pass band ripple less than 0.001 dB below 420 Hz, stop band attenuation greater than 90 dB above 498 Hz). All spectra and phase calculations were performed on the artefact removed and downsampled signal. Post hoc trigger phase in the beta-band was calculated by filtering (firwin, numtaps = 513) the signal between ±5 Hz of the centre frequency (fc) chosen for real-time phase tracking. The trigger phase was then calculated as the polar angle of the Hilbert transform analytic signal at the midpoint of the biphasic trigger. Power spectral density (PSD) calculations were performed using Welch's method (Welch, 1967) with a resolution of 1 Hz spectral bins. Changes in beta-band power were calculated from the respective PSDs (mean of fc bin ± 5 bins inclusive, i.e. mean of 11 bins total) in dB. The Watson-Williams test was performed using pycircstat (*pypi.org/project/pycircstat*).

2.6 Behaviour

Using knowledge gained from the open field experiments described in the previous section, we selected two phases that produced maximal amplification and maximal suppression to target during behaviour. It also allowed us to select the stimulation amplitude that produced the strongest modulation without generating out-of-band spectral peaks. Certain animals were excluded from analysis due to poor modulation or poor behavioural performance, details of which can be found in Table 2-1 and are more accurately described at the start of each experimental chapter (section 3.2.1, 5.2.1, and 5.2.2).

2.6.1 Cylinder assessment

The cylinder task was used to assess paw use asymmetry pre- and post-lesion to establish dopamine lesion severity *in vivo*, as well as post-implant to assess motor impairment during closed-loop stimulation studies. The ability of each rat to weight-bear on its affected contralateral (to the lesion) fore paw during rearing was manually scored during three 10-minute sessions of free exploration of a clear cylindrical arena (diameter 200 mm, height 505 mm). Contralateral paw use was recorded using post-hoc video analysis and defined as the number of times the left paw contacted the arena walls as a percentage of the combined total of left and right touches.

2.6.2 Gait assessment

Apparatus

A custom-designed setup was developed using a modified *CatWalk XT* (Noldus, Netherlands) to assess locomotion in parkinsonian rats. The standard

CatWalk system consists of glass walkway raised above a high speed camera (100 fps). The glass plate is illuminated by green light that reflects within the glass at points being touched, allowing for semi-automated detection of footprints as rats traverse the walkway. Several modifications from its off-the-shelf form were needed to allow concurrent recordings in behaving rats:

1. To ensure that a minimum of two footprints per paw were captured by the camera, we added a 3D-printed circular platform to either end for sugar pellet delivery – this meant the entirety of the glass track could be used for locomotion.

2. The walkway is formed by two plastic walls that needed to be raised using aluminium sheeting to stop rats climbing out of the arena and to provide electrical shielding.

3. A large rectangular aluminium sheet was attached around the sides and back of the platform to provide further electrical shielding.

4. The CatWalk XT lid contains red strip lighting that provides contrast to ensure detection of the rat moving across the track and increases footprint clarity. This was removed in place of a zip line system needed to hold the recording tether, which was essential for stopping wire tangling and allowing the rat to move freely across the length of the track.

5. Curtains enclosing the area beneath the platform were added to reduce glare, while red ambience lighting in place of the red strip light helped increase footprint contrast.

Behavioural protocol

During the training period that lasted no more than 4 days, tethered rats were allowed to freely explore the glass walkway and reward areas at either end for 15-minutes per day until they consistently crossed the walkway to collect reward. Only runs in which the animal moved with consistent speed for two complete step cycles were included in analysis (i.e. each paw contacted the ground at least twice). A block of testing was divided into four equal sessions, one for each experimental condition: no stimulation, high frequency stimulation at 130 Hz, amplifying-phase stimulation, and supressing-phase stimulation. Three out of seven rats completed one block per day consisting of sessions that were 20 minutes in length. One rat completed up to two blocks per day consisting of sessions that were 5 minutes in length. The remaining three rats completed up to two blocks per day consisting of shorter sessions that lasted until 8 runs were completed or 14 minutes had passed. The quality of runs across each of three groups was similar, but the optimised session length in the final group allowed us to maximise the number of completed runs across all four conditions equally. The phase of maximal amplification/suppression and stimulation amplitude were pre-selected using historical data recorded from each rat.

Analysis

Although some manual corrections were needed due to the number of modifications made to the hardware, the *CatWalk* software automatically records

footfall patterns from each individual run for analysis. We were able to compare global locomotive function during each of the four stimulation conditions, as measured by changes in running speed and style, as well as individual paw parameters such as stand time, stride length, swing speed, and maximum contact area. We did so by comparing mean performance and variance on the injured left side (contralateral to the lesion) relative to the uninjured right. Definitions of each measure were as follows:

Average speed (cm/s)

Distance the animal has travelled in each step cycle (i.e. distance from one left front contact to next) divided by the time taken to do so. An average is taken for each complete step cycle to calculate the overall average speed of each run.

Walking

Rats were said to be walking if one forelimb contact was followed by one hindlimb (e.g. LF → RH → RF → LH). Only runs in which this held true for over 50% of the run were classified as walking.

Bounding

Rats were said to be bounding if one forelimb contact (or hindlimb) was followed by the other (e.g. LF → RF → LH → RH). Only runs in which this held true for the entire run were classified as bounding.

Mixed

Runs were classified as a mixed style if they contained between 50 and 99% of the bounding style.

Stand (s)

The duration of contact of a paw with the glass plate.

Stride length (cm)

Distance between successive placements of the same paw.

Swing speed (cm/s)

Stride length divided by time spent without that paw in contact with the glass plate.

Maximum contact area

Maximum area of a paw that contacts the glass plate.

2.7 Tissue analysis

Rats were deeply anaesthetised with isoflurane (4%) and pentobarbital (3 ml, Pentoject, 200 mg/ml) and transcardially perfused with phosphate-buffered saline (PBS) followed by fixative (paraformaldehyde dissolved in PBS, 4%, wt/vol). To preserve structural integrity of electrode tracts following perfusion, the head with electrodes still in place was post-fixed in 4% w/v PFA for at least 24 hours before extracting the brain and cutting it into 70 µM thick coronal sections. Lesion severity was verified using antibodies to tyrosine hydroxylase to visualise unilateral cell body loss in the SNc and loss of dopaminergic innervation in the dorsal striatum (rabbit anti-TH primary; diluted 1:1000; Millipore Cat# AB152, RRID:AB_390204; donkey anti-rabbit Alexa Fluor 488 secondary; diluted 1:1000; *Thermo Fisher Scientific* Cat# A-21206, RRID:AB_2535792).

TH staining was performed on eight equally spaced coronal sections across the rostral-caudal axis to record the full extent of the lesion. Those sections containing electrode tracks were stained for either parvalbumin (guinea pig anti-parvalbumin primary; diluted 1:1000; Synaptic Systems Cat# 195-004, RRID:AB_2156476; donkey anti-guinea pig Cy3 secondary; diluted 1:500; *Jackson ImmunoResearch* Cat# AB_2340460, RRID: AB_2340460) or FoxP2 (rabbit anti-FoxP2 primary; diluted 1:500; Sigma Cat# HPA000382 RRID:AB_1078908; donkey anti-rabbit Alexa Fluor 488 secondary; diluted 1:1000; *Thermo Fisher Scientific* Cat# A-21206, RRID:AB_2535792) to confirm their location within the GP and STN respectively; their final position in three-dimensional space was calculated using Paxinos & Watson (2007). Where electrodes missed their intended target, the nearest border of each structure was located using immunohistochemistry and, alongside other histological landmarks, used to calculate relative electrode position. The electrode position for each individual rat is documented in Table 2-1 alongside inclusion data for each chapter.

Rat	Included for analysis?			Globus pallidum (external)			Subthalamic nucleus		
	Electrophysiology (Chapters 1 & 2)	Cylinder	Catwalk	AP -1.0 mm	ML +3.1 mm	DV -6.4 mm	AP -3.5 mm	ML +2.5 mm	DV -8.0 mm
GPe									
1	✓			-0.44	-0.15	-1.15	0.02	0.3	-0.75
2	✓			0.64	-0.3	0.2	0.5	0.2	-0.05
3	✓		✓	0.04	0.1	-0.4	0.5	0.3	-0.55
4			✓	1	-0.1	-1	0.14	0.86	-0.86
5		✓	✓	0.88	-0.03	-0.14	2.06	-0.51	-0.64
6	✓	✓		0.52	0.15	0.42	0.38	0.18	-0.64
7	✓			0.04	-	-	0.38	0.14	-0.61
8	✓	✓	✓	0.4	-0.36	0.7	0.26	-0.01	0.97
9	✓	✓	✓	0.4	-0.13	0.37	0.5	0.16	0.87
STN									
6		✓	✓	0.52	0.15	0.42	0.38	0.18	-0.64
10		✓	✓	0.52	0.45	0.09	0.58	0.5	0.54

Table 2-1: Subjects list and electrode placement data

The location of electrodes targeting the GPe and STN were calculated relative to the ideal position (coordinates in header) using a combination of immunohistochemisty and careful analysis of anatomy using Paxinos & Watson (2007). For example, the actual AP coordinate for the GPe electrode implanted into rat 1 is -1.44 mm, as it is -0.44 mm from the ideal position (-1.0 mm). Different groupings of rats were used for electrophysiology, cylinder, and *CatWalk* testing due to practical, technical, and behavioural issues throughout the course of experimenting, details of which can be found in the first three sub-columns. Rat 6 received GPe and STN stimulation at various timepoints and so is included once per group. The precise electrode position is unavailable for rat 7 due to tissue damage during analysis, as such the ML and DV coordinates are marked as unknown (-).

Chapter 1

3 Physiological response to phase-dependent stimulation

3.1 Introduction

Rhythmic brain activity plays a fundamental role in information processing by orchestrating cell activity in both the spatial and temporal domains (Fries, 2005). It can be measured in local field potentials as oscillatory activity and is thought to represent the summation of synaptic input to a target structure, which can synchronise in large enough numbers at slow enough timescales to produce a measurable signal (Buzsáki et al., 2012). Importantly, genetically identifiable cell populations with unique functional roles “tune-in” to specific frequencies, becoming phase-locked to ongoing activity in that band as it fluctuates over time (Colgin et al., 2009). This dynamic engagement of networks through phase-locked cell firing not only allows for efficient information transfer across widely distributed brain regions but also helps to segregate unrelated activity that is converging onto the same node (Siegle & Wilson, 2014). As such, activity in semi-arbitrary frequency bands has been found to correlate with various motor, sensory, and cognitive functions (Buzsáki et al., 2002; Buzsáki & Draguhn, 2004; Buzsáki & Wang, 2012; Engel & Fries, 2010; Fries, 2005).

To date, various methodologies have been utilised in order to probe the functional importance of oscillatory activity. One of the most obvious and convenient ways to do so, is to externally drive networks at a target frequency by either electric or

optogenetic means. Such a method has been utilised to show that holding cortical networks at beta frequencies using transcranial alternating current stimulation can slow movements in healthy subjects (Pogosyan et al., 2009). Beta activity fluctuates over short timescales however, meaning that driving the network continuously irrespective of its presence, will not faithfully mimic naturally occurring activity. Furthermore, applying continuous stimulation over long periods will undoubtedly alter overall neuronal excitability and must caveat any conclusions drawn from such an approach. In order to infer a causal relationship between oscillations and specific functions it is also necessary to disrupt ongoing activity. The only option currently available to researchers in this regard is to silence whole regions via physical, chemical, electrical or optogenetic perturbations. Not only does this extreme approach indiscriminately disturb cellular function around the target area but may also permanently suppress oscillatory activity across the entire network. Taking these considerations together, the perfect tool would enable researchers to selectively amplify or suppress physiological bursts of activity in a specific frequency band in real time.

Various proof-of-principle studies in humans have shown it is possible to modulate ongoing oscillations by delivering pulsatile stimulation as little as once per cycle (Cagnan et al., 2017; Holt et al., 2019). These early studies relied upon post-hoc analysis of open-loop continuous stimulation that was free to drift slowly in and out of phase with the ongoing target oscillation. Each pulse produced either amplification or suppression of activity depending on when in the target cycle it was delivered, with consecutive pulses arriving at the same phase compounding the modulatory effect. Optogenetic studies *in vitro* have since provided further evidence that phase-locked stimulation can modulate oscillatory amplitude (Nicholson et al., 2018). This was done

in a highly controlled environment however, where artificial closed-loop feedback was produced by locking excitatory input to externally generated oscillations. The transient nature of oscillations *in vivo* means that highly responsive phase estimations must be produced near instantaneously in order to deliver true phase-locked stimulation consistently. This is particularly true for high frequency oscillations in the gamma band for example, where transient bursts of activity can reach up to 150 Hz (Colgin et al., 2009). The first published example of *in vivo* phase-locked stimulation was used to target low gamma activity in mice completing a fear conditioning task (Kanta et al., 2019). Their system can detect oscillatory peaks or troughs by calculating when the derivative of the filtered signal changes polarity. Despite stimulation being restricted to just two phases it was able to modulate 50 Hz activity in a bidirectional manner.

One potential clinical use for phase-tracking technology is in the treatment of PD, where it has been conclusively shown that cell populations across the motor network become rigidly entrained to beta oscillations that propagate throughout the network (Hammond et al., 2007). By reducing the ability of neurons to fire dynamically with movement in both time and space, beta oscillations act to limit the information coding capacity of the BG (Brittain et al., 2014; Engel & Fries, 2010). Importantly, activity in this band is reduced by dopamine replacement and DBS therapy, the extent of which correlates with motor improvement (Kühn et al., 2008; Little et al., 2012; Tinkhauser et al., 2017a; Weinberger et al., 2006). If increased beta oscillations are indeed pathological then it stands to reason that specifically suppressing such activity will improve treatment efficacy while also reducing the side effects commonly produced by conventional DBS (Volkmann et al., 2009). In support of such an approach, high frequency stimulation applied only during periods of high beta power was as effective as classic DBS despite reducing total stimulation by almost half (Little

et al., 2013). Phase-locked stimulation promises a more energy efficient and spectrally specific way to suppress beta oscillations in PD, yet has not been realised up until now due to the technical challenges involved in accurately tracking phase in real time.

Here, I utilise a highly responsive system that provides continuous online phase estimation. By performing *in vivo* electrophysiological recordings in freely moving 6-OHDA rats, I first set out to demonstrate the efficacy of our phase-tracking system when targeting beta-band oscillations that are exaggerated in parkinsonian rats. Once the accuracy of our system was confirmed, I was able to test whether or not phase-locked stimulation can modulate oscillations in a bidirectional manner. I summarise my findings in the next section, evaluate the utility of our system, and discuss potential mechanisms of action. Later, in chapter 3, I attempt to establish a causal link between beta frequency activity and parkinsonian motor impairment. Before doing so, I look more closely at the interactions between brain and system when using our closed-loop approach (chapter 2).

Summary:

Figure 3-1 – Histological verification of dopamine lesion and electrode placement
Figure 3-2 – Increased cortical beta power is present on the lesioned side
Figure 3-3 – Phase-tracking accuracy in freely moving parkinsonian rats
Figure 3-4 – Example traces of phase-locked stimulation
Figure 3-5 – Modulation of cortical beta power by pallidal phase-locked stimulation

3.2 Results

All experiments were carried out in 6-OHDA hemi-lesioned rats, which accurately reproduces the dopamine depletion and exaggerated beta-band activity commonly observed in PD (Sharott et al., 2005). Those animals with substantial reductions in spontaneous forelimb use after recovering from surgery were implanted with stimulating electrodes into the GPe and STN, as well bilateral surface screws above the motor cortex (input) and cerebellum (reference). Thus, stimulation delivered to either subcortical nuclei was phase-locked to ongoing beta activity originating from the motor cortex. In chapters 1 and 2, we assess the efficacy of our system using GPe stimulation only, while the final chapter assesses motor impairment during stimulation of either GPe or STN.

To allow comparisons across all animals, phases, and timepoints, a strict recording protocol was used to evaluate the efficacy of phase-locked stimulation. Each recording session consisted of eight stimulation blocks lasting 270 seconds, with each block targeting one of eight phases equally spaced across the cycle. The order in which each target phase occurred was chosen at random before each session. Stimulation was delivered in repeating 20 second cycles termed ‘on-epochs’, that were separated by 5 second ‘off-epochs’ where no stimulation was delivered. Each stimulating block was followed by 130 seconds without stimulation, where the target phase was tracked but with stimulation disabled.

This chapter begins with an overview of the animals used across all three chapters, characterising the lesion and assessing electrode placement accuracy (Figure 3-1). The above protocol was then used to conduct extensive recordings

during free exploration of an open field, which allowed us to determine the accuracy and reliability of our system during periods with and without stimulation enabled (Figure 3-2 and 3-3). We could then compare beta-band modulation across multiple phases when stimulating in the GPe (Figure 3-4 and 3-5).

3.2.1 Histological verification of dopamine lesion and electrode placement

A total of 15 rats underwent two separate surgeries before data collection began, one to produce a unilateral lesion of dopaminergic neurones in the SNc, and the other to implant stimulating electrodes into the GPe and STN. A combination of electrode placement data, spectral profiling, responsiveness to stimulation, and motor assessments were used to determine which animals were included for electrophysiological (chapters 1 and 2, n = 7) and behavioural analysis (chapter 3, n = 7). Although an equal number of rats were used in both sections, each group contains a different combination of subjects due to the practical and technical challenges associated with developing phase-locked stimulation in behaving animals, details of each group can be found in the methods (Table 2-1).

Lesion strength varied between rats, the extent of which can be seen in Figure 3-1, which shows representative examples of relatively strong (example 1) and weak dopamine lesions of the right hemisphere (example 2). In both cases, histological analyses confirmed a total loss of dopamine cell bodies within the lateral SNc following 6-OHDA administration, while a small amount of immunoreactive cells in the medial portion remained in a subset of rats (e.g. Figure 3-1B, bottom panel). Tyrosine hydroxylase positive cells were also noticeably reduced in the VTA but to a much lesser extent than the SNc. The dopamine depletion observed here is therefore comparable to that recorded from post-mortem analysis of human tissue (German et

al., 1989; Goto et al., 1989). This pattern of cell death within the midbrain produced a gradient of loss in the projecting fibres terminating at the striatum, which was strongest in the dorsolateral portion and weakest ventromedially. Importantly for our model, the dorsolateral striatum receives dense innervation from cortical sensorimotor areas in particular (McGeorge & Faull, 1989) and is thought to be critical for motor function (Tecuapetla et al., 2016).

Electrode position was determined using a combination of immuno-histochemistry (Figure 3-1C, D) and the stereotaxic atlas (Paxinos & Watson, 2006). The mean distance from the centre of GP (AP: -1.00 mm, ML: +3.10 mm, DV: -6.40 mm) to the electrode tip was 0.87 mm ± 0.26 mm (mean ± s.d., n = 15), while the mean distance from the centre of STN (AP: -3.5 mm, ML: +2.5 mm, DV: -8.0 mm) was 1.15 mm ± 0.85 mm (mean ± s.d., n = 15). Only rats with electrodes in or close to the target structure and that were responsive to stimulation were included for analysis, we can therefore be confident that electrical stimulation engaged the motor network.

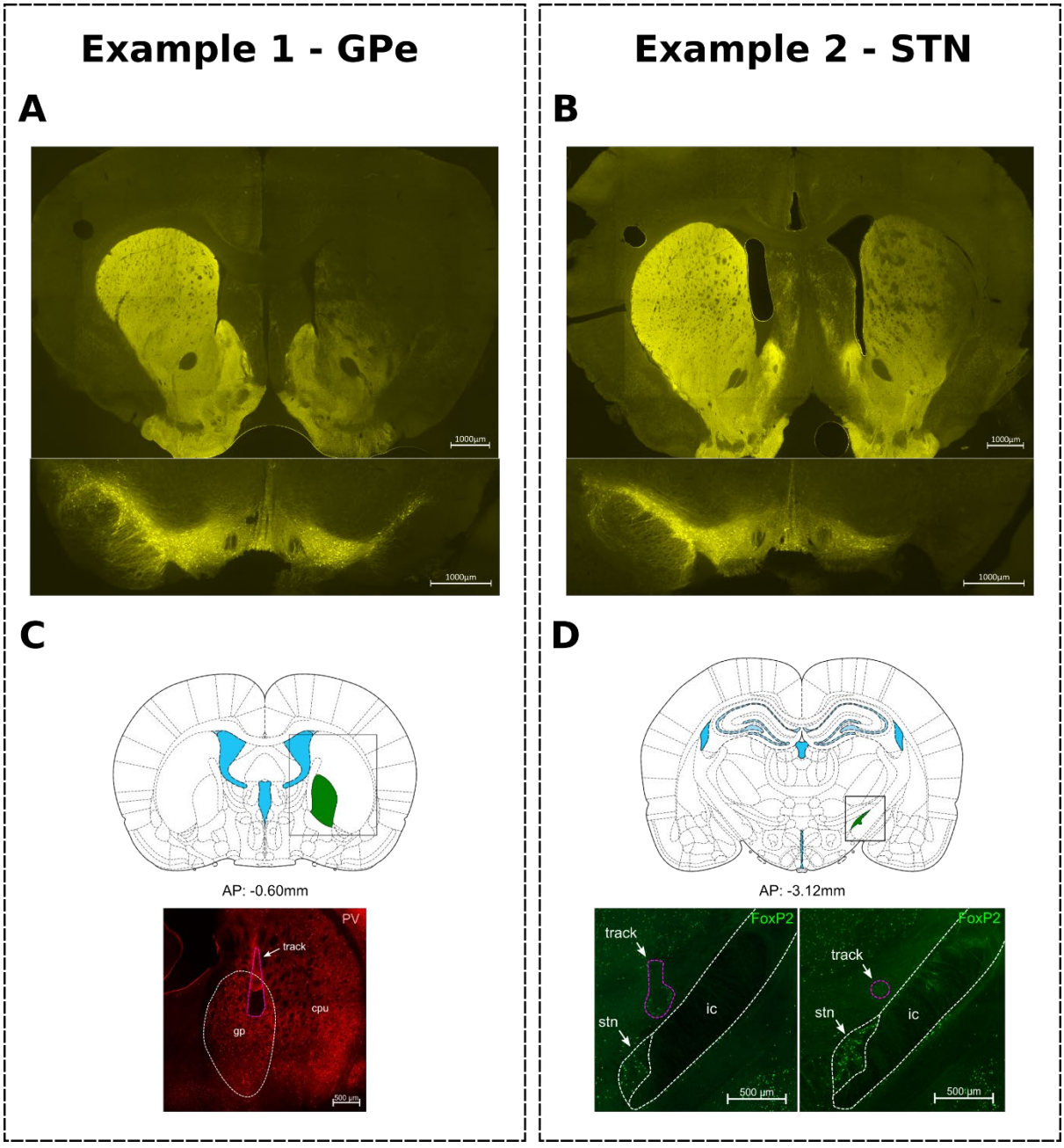


Figure 3-1: Histological verification of dopamine lesion and electrode placement

Immunohistochemisty was used to assess lesion severity and electrode position. Tyrosine hydroxylase (TH) staining was performed on eight coronal sections equally spaced across the rostral-caudal axis of the striatum and SNc, with representative sections shown in A and B. Unilateral 6-hydroxydopamine injection into the right SNc destroyed all cell bodies around the injection site (bottom panel of A and B), producing a gradient of loss in the fibres projecting to the striatum that was strongest in the dorsolateral portion and weakest ventromedial portion (top panel of A and B). Electrode position was confirmed using a combination of Paxinos & Watson (2007) and either parvalbumin (PV) or FoxP2 staining for the GPe (C) and STN (D) respectively. Representative examples are shown in C and D, where white dotted lines are used to aid visualitation of the target structure and purple dotted lines outline the electrode track.

3.2.2 Phase-tracking accuracy in freely moving parkinsonian rats

Before testing the efficacy of our phase-tracking closed-loop system, we first had to establish the presence of increased beta oscillations in dopamine depleted awake rats. A prominent beta peak centred around approximately 35 Hz was observed in the right ECoG that was remarkably consistent across animals (Figure 3-2B). Although a small increase can be observed in the dopamine-intact left hemisphere (Figure 3-2A), this is not comparable to the lesioned side in terms of amplitude and is likely produced by signal conduction from the lesioned hemisphere. We can therefore conclude that exaggerated activity within this band is a direct result of 6-OHDA lesion, a finding which is supported by previous studies in awake moving rats (Avila et al., 2010). The system could then be calibrated for each rat to target oscillatory activity within 5 Hz of the spectral peak (centre frequency: ~35 Hz). In order to assess the accuracy of our phase-tracking system, the actual phase of each stimulation pulse calculated post-hoc was plotted relative to intended target phase when stimulating in GPe (Figure 3-3). This analysis was performed for baseline recordings where phase-tracking occurred but with stimulation disabled (brown line) and also for stimulation blocks where data from across all target phases were combined (black line). The histograms for each condition are near identical, meaning that the presence of electrical artifacts does not impair system performance. Using the pooled stimulation data, 60.78 ± 4.28 % (mean ± SD) of the stimuli were delivered within a quarter of a cycle of the target phase. In addition, the rate of real-time triggers in baseline recordings (23.92 ± 2.37 Hz, dashed horizontal lines) and stimulation recordings (23.78 ± 2.66 Hz) were not different ($p = 0.55$, paired t-test, $t_6 = 0.64$) and were considerably less (31 %) than the theoretical maximum trigger rate (the centre frequency selected for phase tracking).

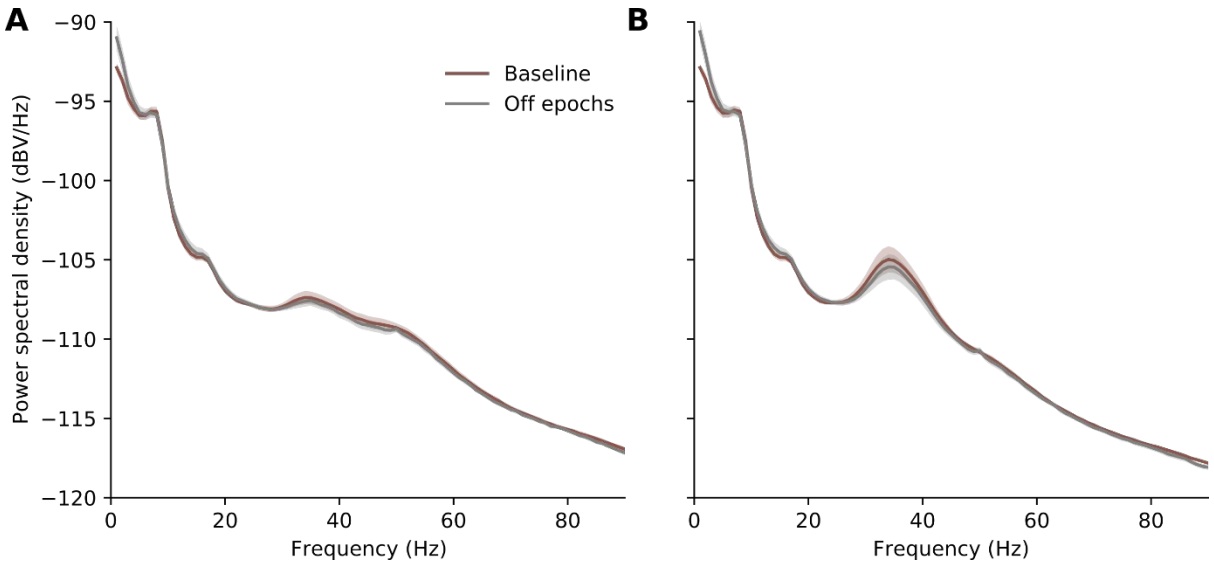


Figure 3-2: Increased cortical beta power is present on the lesioned side

Power spectral density plots (mean ± SEM, n = 7 rats) showing elevated beta-band power in the absence of stimulation recorded from frontal ECoG screws located either contra- (A) or ipsilateral (B) to the 6-OHDA lesion. Elevated beta-band power on the lesioned side was present in short (5 s) epochs with stimulation intentionally disabled embedded in stimulation enabled recordings (grey). The power in these epochs was very similar to that in longer baseline recordings without stimulation (brown).

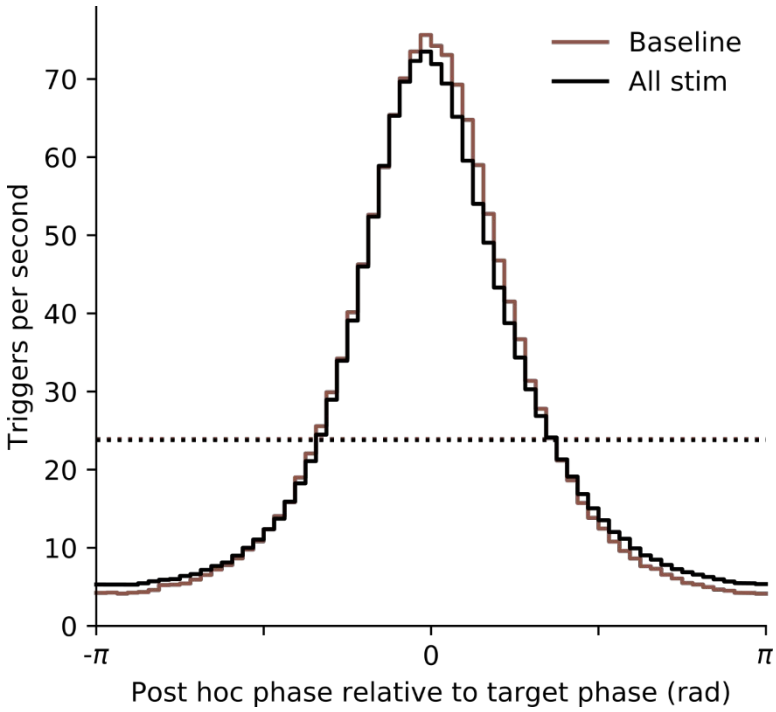


Figure 3-3: Phase-tracking accuracy in freely moving parkinsonian rats

Trigger accuracy histogram of ECoG phase on the lesioned side calculated post hoc and plotted relative to target phase. The accuracy and mean trigger rate (dotted lines) of the real time generated triggers, without stimulation enabled (brown) and with stimulation delivered to the globus pallidus (black) were almost identical, demonstrating that the system was able to maintain full accuracy in the presence of electrical artefacts and physiological perturbation produced by stimulating.

3.2.3 Example traces of phase-locked stimulation

Having successfully demonstrated the accuracy of our system, we next addressed whether stimulation phase-locked to ongoing cortical beta oscillations is able to modulate beta power when delivered to the GPe. Our data is in line with previous studies that show beta as a relatively unstable oscillation that waxes and wanes over time (e.g. Tinkhauser et al., 2017a). Upon inspection of raw traces, we found that certain target phases amplify and prolong high 'bursting' activity (Figure 3-4C), while others kept beta power consistently low (Figure 3-4B). This is particularly clear when looking at those raw traces when filtered around the centre frequency used for phase tracking (traces directly beneath raw signal).

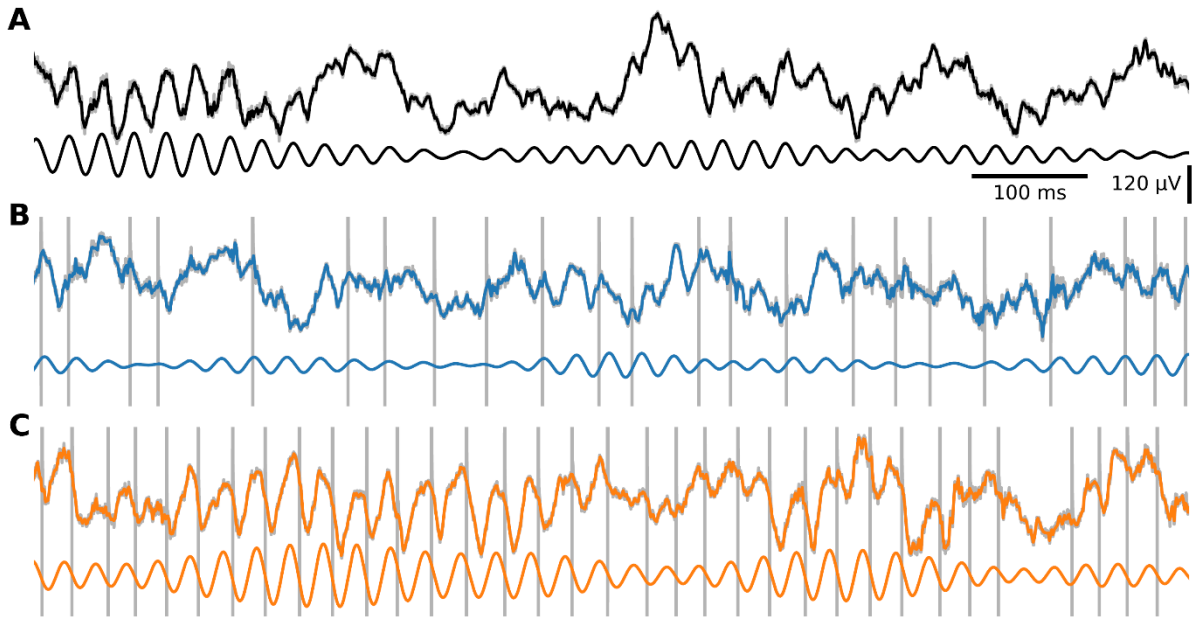


Figure 3-4: Example traces of phase-locked stimulation

Example one second duration typical ECoG traces with (A) no stimulation, (B) stimulation delivered to the globus pallidus targeted to a suppressing phase of the ECoG and (C) stimulation targeted to an amplifying phase. Each panel shows the wideband signal down sampled to 1 kHz after removal of stimulation artefacts (coloured) superimposed on top of the original recording sampled at 20 kHz (grey). The stimulation artefacts visible as grey vertical lines are truncated in amplitude to aid visualisation of the physiological activity. The artefact free signal, filtered in the beta-band post hoc is shown below each trace. Note the mean beta-band amplitude compared to the no stim condition is reduced with suppressing stimulation and increased with amplifying stimulation.

3.2.4 Modulation of cortical beta power by pallidal phase-locked stimulation

To quantify changes in beta-band activity we calculated power spectral density (centre frequency ± 5 Hz) during on- and off-epochs for each of the eight target phases. The modulation of beta power was approximately sinusoidal with power increasing linearly from the phase of maximal suppression to the phase of maximal amplification (Figure 3-5A). Absolute target phase significantly modulated beta-band power ($p = 0.0013$, one-way ANOVA, $F_{7, 48} = 4.12$) and the absolute phase of maximal suppression and maximal amplification was different ($p = 0.0022$, Watson-Williams test, $F_{1, 12} = 15.09$). They were also nearly always in anti-phase and were broadly similar between subjects (Figure 3-5B). Maximal amplification (−1.41 ± 1.08 dB) generally occurred when targeting just after the peak (1.36 ± 0.39 π rad), while maximal suppression (2.32 ± 0.80 dB) occurred just after the trough (0.28 ± 0.32 π rad). To better visualise the modulation produced by phase-locked stimulation, mean power spectral densities for on-epochs targeting phases that produced maximal amplification (orange) or suppression (blue) were compared to mean power during off-epochs (Figure 3-5C, D). Phase-locked stimulation targeting the suppressing phase flattened the spectral peak at 35 Hz, whereas amplifying stimulation produced a robust increase. Taken together, it is clear that our system can bidirectionally modulate cortical beta power consistently in real time when stimulating in the GPe.

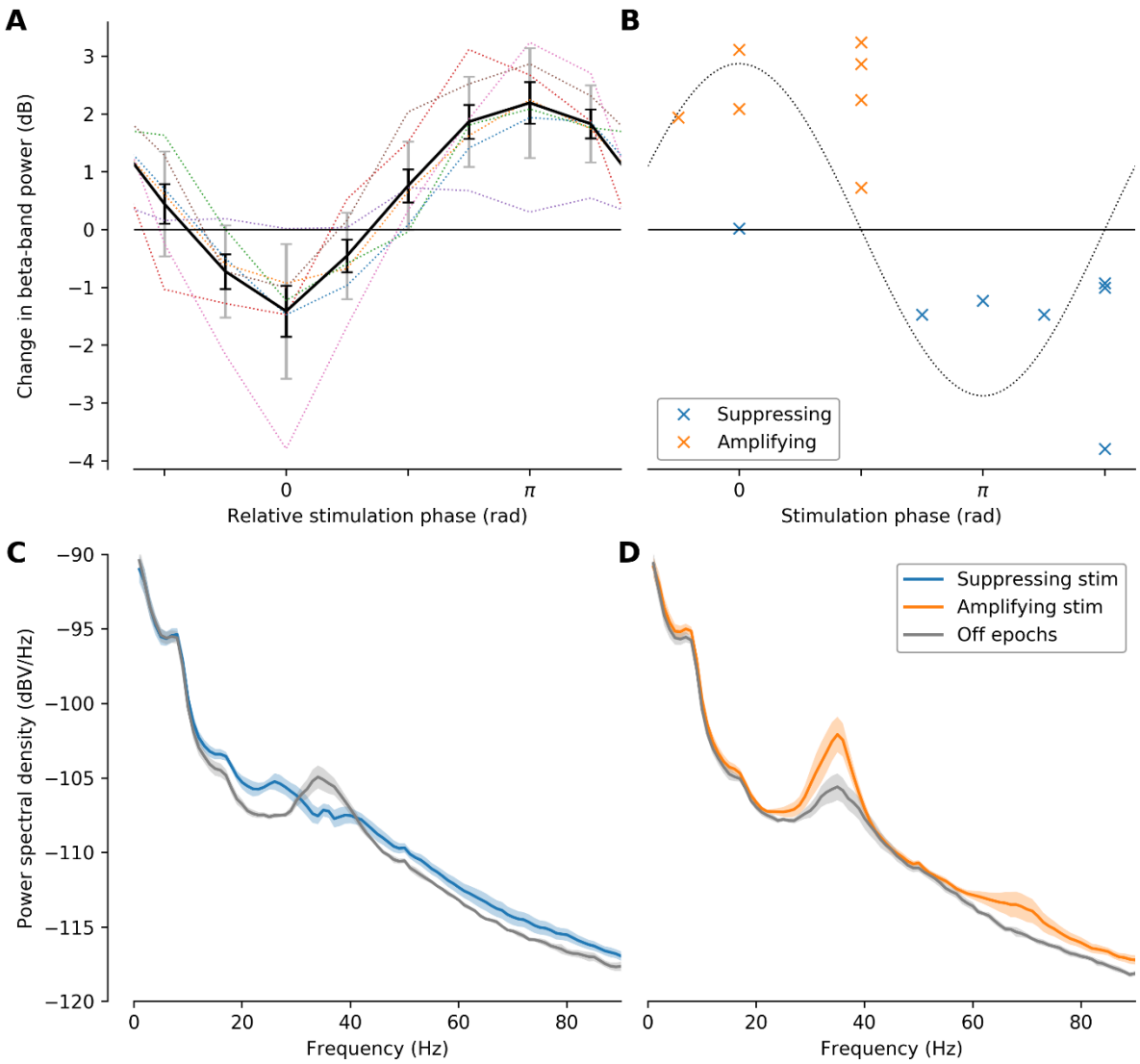


Figure 3-5: Modulation of cortical beta power by pallidal phase-locked stimulation

(A) Change in beta-band power due to stimulation across 7 rats for 8 target phases aligned by the most suppressing target phase for each rat. The change in beta-band power for each recording was calculated in dB as the ratio of the mean beta-band power in repeated short (5 s) epochs of no stimulation to the mean beta-band power in the longer intervening (20 s) epochs with stimulation enabled. The dotted lines show the values for each rat with the mean ± SEM in black and standard deviation in grey. (B) Absolute phase versus beta-band power of the most suppressing and most amplifying target phases for each rat. The dotted line provides a visual aid showing the location of the peak and trough of the beta-cycle. (C, D) Power spectral density plots (mean ± SEM, n = 7 rats) showing (C) a reduction in the beta-band spectral peak when stimulation was applied to the most suppressing target phase (blue) compared to stimulation disabled short epochs embedded in the same recordings (grey) and (D) an increase when stimulation was applied to the most amplifying target phase

3.3 Discussion

The main finding in this chapter is that phase-locked stimulation can bidirectionally modulate exaggerated beta oscillations in freely moving 6-OHDA rats. Pallidal stimulation arriving just after the peak amplified cortical beta oscillations, while stimulation arriving just after the trough suppressed them. By leveraging accurate phase-tracking whereby 60% of pulses occurred within a quarter cycle of the target phase, robust bidirectional modulation was achieved by stimulating well under once per cycle using relatively little current.

To understand how phase-locked stimulation in the pallidum modulates ongoing beta oscillations in the cortex we must first consider the neural circuitry involved. The GPe is made up of two distinct cell types that have unique firing properties, anatomical connections, and functional roles (Mallet et al., 2008a, 2016). The prototypic cell population innervate nuclei across the basal ganglia including 'classic' downstream targets such as STN and SNr, while the vast majority of arkypallidal neurones project upwards to densely innervate the striatum (Mallet et al., 2012). While prototypic neurones also innervate the striatum, they do so with approximately 10 to 20-fold less synaptic density than arkypallidal neurones (Mallet et al., 2012). An important consideration when interpreting the impact of phase-locked stimulation in this study is the antiphase relationship in cell firing between each pallidal population. Prototypic neurones fire at the trough of ongoing beta oscillations, while arkypallidal neurones fire at the peak, which is highly suggestive of strong lateral inhibition. It is therefore extremely likely that stimulation arriving at a specific phase will engage the two populations differently and affect the temporal relationship between them. For example, stimulation arriving during the active phase of one

population could reinforce the local oscillation and synchronise their output, while stimulation arriving out-of-phase may disrupt the oscillation and desynchronise that population. Phase-locked stimulation would therefore have a significant impact on GPe output at the level of individual action potentials and, as evidenced in this chapter, a significant impact on overall network dynamics.

The cortex (Li et al., 2012), striatum (McCarthy et al., 2011; Sharott et al., 2009), GPe (Corbit et al., 2016; Mallet et al., 2012), and STN (Deffains et al., 2016; Nevado-Holgado et al., 2014), have all been implicated in the generation and propagation of pathological beta oscillations in PD. The results in this chapter support a subcortical driver however, as phase-locked stimulation was able to amplify (or supress) beta-band activity throughout the network by continuously energising (or disrupting) pathological rhythms within the GPe. Although the mechanism of action is presumably different, a similar reduction in beta-band synchronisation is observed throughout the network following subcortical DBS therapy (Kühn et al., 2018; Vitek et al., 2012). Assuming that phase-locked stimulation does indeed modulate GPe output, how might this correspond to reduced beta activity in the motor cortex? It has been proposed that the GPe-STN loop acts as a central pattern generator for the motor network (Nevado-Holgado et al., 2014). In terms of synaptic connectivity, juxtacellular labelling of individual GPe cells reveal relatively sparse innervation of STN (Mallet et al., 2012), and so under physiological conditions are unlikely to be recruited in large enough numbers to widely synchronise STN output. Pallidal cells exhibit up to a 100-fold increase in beta synchronisation following dopamine depletion however, which is driven by both STN (Goldberg et al., 2004; Heimer et al., 2006; Mallet et al., 2008a; Nini et al., 1995) and striatal inputs (Corbit et al., 2016; Sharott et al., 2017). The reciprocal connection between GPe and STN means that either structure will receive

highly-synchronised anti-phase beta frequency feedback from the other in the pathological state. The consequence of which is that the GPe-STN loop becomes locked to beta frequency rhythms in a positive feedback cycle. By helping to synchronise (or desynchronise) the circuits involved, phase-locked stimulation should in theory enhance (or suppress) ongoing oscillations originating from either structure and keep (or stop) them reverberating throughout the network.

Another feedback loop implicated in the propagation of pathological beta oscillations is formed between the GPe and striatum. Considering that iMSNs converge onto GPe neurones with a synaptic density of approximately 50-fold greater than that of STN, they are perfectly placed to widely coordinate GPe activity (Fujiyama et al., 2011; Koshimizu et al., 2013; Oorschot, 1996). In turn, ascending pallidal projections synapse onto GABAergic striatal interneurons to provide powerful and wide-reaching coordination of MSN output (Bevan, 1998). Computational models predict that it is these specific pallidostriatal projections that propagate beta activity in the dopamine depleted state (Corbit et al., 2016). Recent evidence shows that iMSN activity becomes phase-locked to cortical beta oscillations following dopamine depletion in rats (Sharott et al., 2017), which means that arkypallidal and prototypic neurones will be driven at beta frequencies that serve to further reinforce local iMSN synchrony via interneurone disinhibition. In support of pallidostriatal generator, optogenetic inhibition of both GPe cell populations completely suppressed cortical beta activity in rats, whereas cortical or subthalamic inhibition had no effect (Crompe et al., 2020). Moreover, artificial beta frequency optogenetic stimulation only reproduces the firing patterns and phase relationships between subcortical structures when stimulating the GPe. As will be discussed in more detail in chapter 3, we were able to produce equally effective modulation of cortical beta using STN stimulation in

a small cohort (n = 2). These results do not rule out the possibility that modulation was driven by secondary effects on GPe circuitry however, and it is entirely feasible that phase-locked subthalamic stimulation modulates cortical beta oscillations indirectly by enhancing or disrupting prototypic synchrony. The lateral connections between both pallidal populations have yet to be defined, nor those projecting from STN, making it hard to predict how stimulation of one population will affect the others. It is therefore difficult to tease apart the contributions of either population using the current methods. This is particularly true when using electrical input, where STN stimulation can directly influence the GPe through antidromic activation of prototypic synaptic terminals. Future single unit activity analyses from across the motor network is in preparation, which will provide ground truth evidence of the impact of phase-locked stimulation on GPe output and should help isolate the impact of each individual cell population.

The findings in this chapter highlight the utility of phase-locked stimulation, which was able to powerfully modulate oscillatory activity using much smaller amounts of current than conventional DBS by targeting specific cellular processes. In MPTP-lesioned primates, GPi stimulation triggered by rhythmic cortical firing at a fixed delay was able to supress pathological oscillatory activity and ameliorate parkinsonian symptoms (Rosin et al., 2011). The fixed delay was manually chosen so that stimulation coincided with oscillatory bursting in BG output nuclei. While cortical phase was not tracked, and stimulation was delivered to the GPi, it seems likely that the effect was produced through similar mechanisms to those produced here. Considering the behavioural improvement achieved using their approach (and others e.g. Little et al., 2013), it is tempting to predict that phase-locked stimulation will produce a comparable if not greater improvement in motor performance by specifically targeting the cell populations responsible for beta generation.

Chapter 2

4 Closed-loop properties of the system

4.1 Introduction

Typical electrophysiological studies take snapshots at set intervals of neural activity (e.g. LFPs) and then measure any changes in response to a perturbation (e.g. stimulation). Closed-loop experiments by definition should also consider the inverse response, measuring how changing neural activity impacts upon system output. Changes in this direction are often overlooked while the development of closed-loop systems remain in the embryonic stages. One potential closed-loop approach for treating PD is to apply high frequency stimulation only when beta power reaches a predefined threshold (Little et al., 2013). While our system can be adapted to stimulate in such a manner, the approach used in chapter 1 attempts to continuously interact with the ongoing signal, dampening or energising biological activity by stimulating up to once per cycle. This means it must rapidly adapt to changes in the input signal that it itself is modulating.

One intuitive prediction we can make about phase-locked stimulation is that pulses arriving at phases that suppress the oscillation will impair future phase estimation, thus reducing the accuracy of upcoming stimulation. This would then limit system efficacy through unintended stimulation at amplifying phases. In an attempt to safeguard against stimulating during periods with unstable phase estimation, our

system was setup to only trigger stimulation if 80% of a target frequency has passed since the most recent occurrence of that target phase. In the case of stimulation on suppressing phases we predict that if a stable state equilibrium can be achieved, then the number of stimulation events will be reduced due to a drop in the accuracy of phase prediction.

In contrast, amplifying stimulation will improve future phase estimation and increase the likelihood of stimulating at the next cycle. It is therefore entirely possible from a theoretical point of view that our system enters into a positive feedback loop when targeting amplifying phases, leading to continuous beta frequency stimulation over long periods. The dynamic nature of neural circuits combined with external noise makes this scenario less likely, as suggested in chapter 1 where the trigger rate during all stimulation periods (23.78 ± 2.66 Hz) remained well below the theoretical maximum rate (target frequency: 35 Hz). Nonetheless, several lines of evidence suggest that amplifying pathological beta rhythms in such a manner is likely to significantly worsen symptoms in PD (Pogosyan et al., 2019; Torrecillos et al., 2018; Zhang et al., 2008). It also has important implications for other disorders such as epilepsy, where recent studies show DBS to be particularly effective at reducing seizure rate (Jobst et al., 2017) and phase-locked stimulation has potential clinical utility. The positive feedback loop described above could be particularly dangerous as prolonged seizures (status epilepticus) are associated with cell death (Meldrum & Brierley, 1973), cognitive deficits (Helmstaedter et al., 2007), and increased morbidity (Treiman & Walker, 2006). It is therefore vital to start addressing such considerations before implementing closed-loop algorithms in future brain-computer interfaces.

By stimulating only when a stable phase estimate is present, our system adapts to changes in cortical activity in a cycle-by-cycle manner, stimulating up to once per cycle to either invigorate or disrupt activity as it occurs naturally within the brain. It will therefore stimulate at near beta frequency over long periods, which has the potential to drive potentially harmful cycles of positive feedback, or will produce a stable state equilibrium between brain and system that defines a true closed-loop system. Relatively little is known about such interactions and if they are affected by behavioural state or arousal. Attempts to address such questions have not been possible up to now due to the lack of a reliable system and model. This chapter investigates how each target phase impacts upon system output and then looks in detail at the patterns of activity generated by phases that produce maximal amplification or maximal suppression.

Summary:

Figure 4-1 – Effect of target phase on the accuracy and rate of stimulation

Figure 4-2 – Effect of target phase on future stimulation

Figure 4-3 – Triggering open-loop stimulation using closed-loop activity patterns

Figure 4-4 – Quantification of closed- and open-loop beta-band modulation

4.2 Results

In the previous chapter we established system efficacy, proving that it can target particular phases with the required accuracy to modulate exaggerated beta-band activity in a bidirectional manner. In order to better understand how changes in cortical activity influences the output of our system (and vice-versa), stimulation trains produced when targeting each of the eight phases equally spaced across the cycle were compared in terms of accuracy, regularity, and number of pulses (Figure 4-1 and 4-2). We then looked more closely at the stimulation patterns generated when targeting the phases that produce maximal amplification and maximal suppression. If each phase produces an inherently unique pattern of activity as predicted, then each pattern may interact differently with ongoing beta activity irrespective of phase, in a manner that simply reflects the number and/or regularity of pulses. In order to investigate this hypothesis, the stimulus trains produced by amplifying and suppressing phases during closed-loop stimulation blocks were reapplied in an open-loop manner, allowing us to compare any differences in modulation between phases and to see if identical patterns of stimulation produce the same electrophysiological response independent of phase-locking (Figure 4-3 and 4-4).

4.2.1 Effect of target phase on the accuracy and rate of stimulation

Having confirmed that stimulation artifacts do not impact upon system accuracy (Figure 3-3), we again analysed mean histograms of actual phase calculated post-hoc relative to intended real-time target phase. All stimulation blocks combined (black) was compared to on-epochs targeting either the phase of maximal amplification (orange) or maximal suppression (blue, Figure 4-1A). Amplifying stimulation in contrast to suppressing stimulation had a higher mean stimulation rate (amplifying 25.75 ± 4.06, suppressing 21.19 ± 2.33, $p = 0.0045$, paired t-test, $t_6 = 4.42$) and a greater accuracy measured as percentage of stimulation within a quarter cycle of the target phase (amplifying 74.96 ± 6.97 %, suppressing 47.29 ± 7.00 %, $p = 0.0003$, paired t-test, $t_6 = 7.26$).

Since the absolute phase of amplifying and suppressing stimulation was similar across animals (but not identical), differences in the mean trigger accuracy histograms from panel A remained evident (Figure 4-1B). Interestingly, each target phase had a distinct histogram shape that exhibited step-wise improvements in trigger accuracy and number from peak suppression just after the trough to peak amplification on the descending phase. When taking these results together with the previous chapter, it is clear that each target phase generates a unique pattern of activity – arising from the effect of the stimulation on the biological system (i.e. the modulation of beta-band power) – demonstrating that the electronic and biological systems enter into a combined closed-loop state, producing activity in each that would not have been possible in either, without the presence of the other.

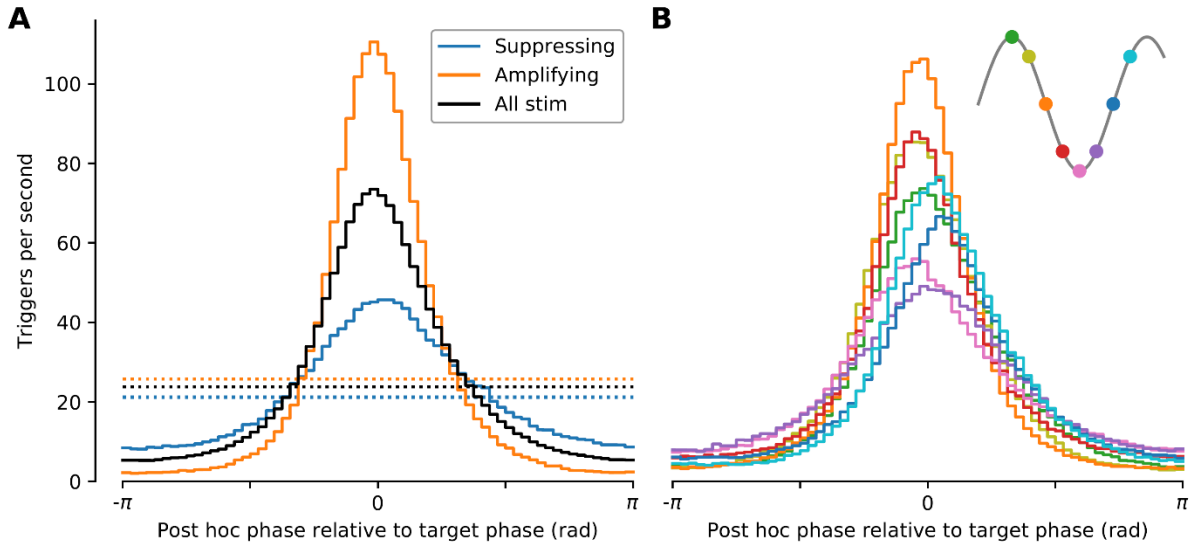


Figure 4-1: Effect of target phase on the accuracy and rate of stimulation

(A) Trigger accuracy histogram of ECoG phase calculated post hoc plotted relative to target phase. Stimulation targeted to the most amplifying phase (orange) produced a higher rate of stimulation on the correct phase (0 rad) and a higher mean stimulation rate (dotted lines) compared to the mean across all target phases (black). Stimulation targeted to the most suppressing phase (blue) led to reduced accuracy and a lower mean stimulation rate (dotted lines) reflecting the systems success in suppressing the oscillation. (B) Mean trigger accuracy histograms for each target phase across all 7 rats plotted relative to target phase with inset showing the target phase of each trace.

4.2.2 Effect of target phase on future stimulation

Plotting mean trigger accuracy histograms in the previous section highlighted clear differences in stimulation accuracy and rate when targeting amplifying or suppressing phases. In order to better understand how phase-locked stimulation impacts upon future stimulation in a cycle-by-cycle manner, we next calculated triggered averages of the frontal ECoG for a 200-millisecond window centred on the stimulation trigger (Figure 4-2A). In the 100-milliseconds preceding stimulation onset the amplitude of beta oscillations was near identical and only differed in terms of the phase at time zero. Phase had no effect on oscillation amplitude in the cycles proceeding trigger onset when stimulation was disabled, but produced a clear range of modulation when enabled that was most evident when comparing maximal amplification and suppression (Figure 4-2A, bottom panel). Strikingly, the contribution to the mean of oscillations in the beta band were completely suppressed after just one cycle when stimulating on the ascending phase in this example.

It is evident from the above analysis that phase-locked stimulation powerfully modulates oscillation amplitude, which should lead to phase-dependent changes in phase estimation on subsequent cycles. Differences in the temporal dynamics of the amplifying and supressing stimulation trains can be seen in their auto-correlograms (Figure 4-2B). When targeting the phase of maximal amplification (orange) a strong beta-frequency sinusoidal rhythm was observed that reflects the beta rhythmicity of the stimulus train. A similar yet much weaker rhythm was produced when stimulating at the maximal suppressing phase (blue). The stable rhythm produced by amplifying stimulation was larger in terms of peak-to-trough amplitude (i.e. trigger accuracy), as well as absolute trigger number (i.e. trigger number), when compared to supressing

stimulation. This was particularly evident in the distribution of inter-trigger intervals when limited to the first trigger, where amplifying phases (dotted line) produced a large amplitude peak on the first beta cycle following stimulation at time zero, reflecting an increased likelihood of successive stimulation when compared to suppressing phases (dashed line). These results show that phase-dependent modulation of oscillatory amplitude strongly impacts future phase estimation on a cycle-by-cycle basis.

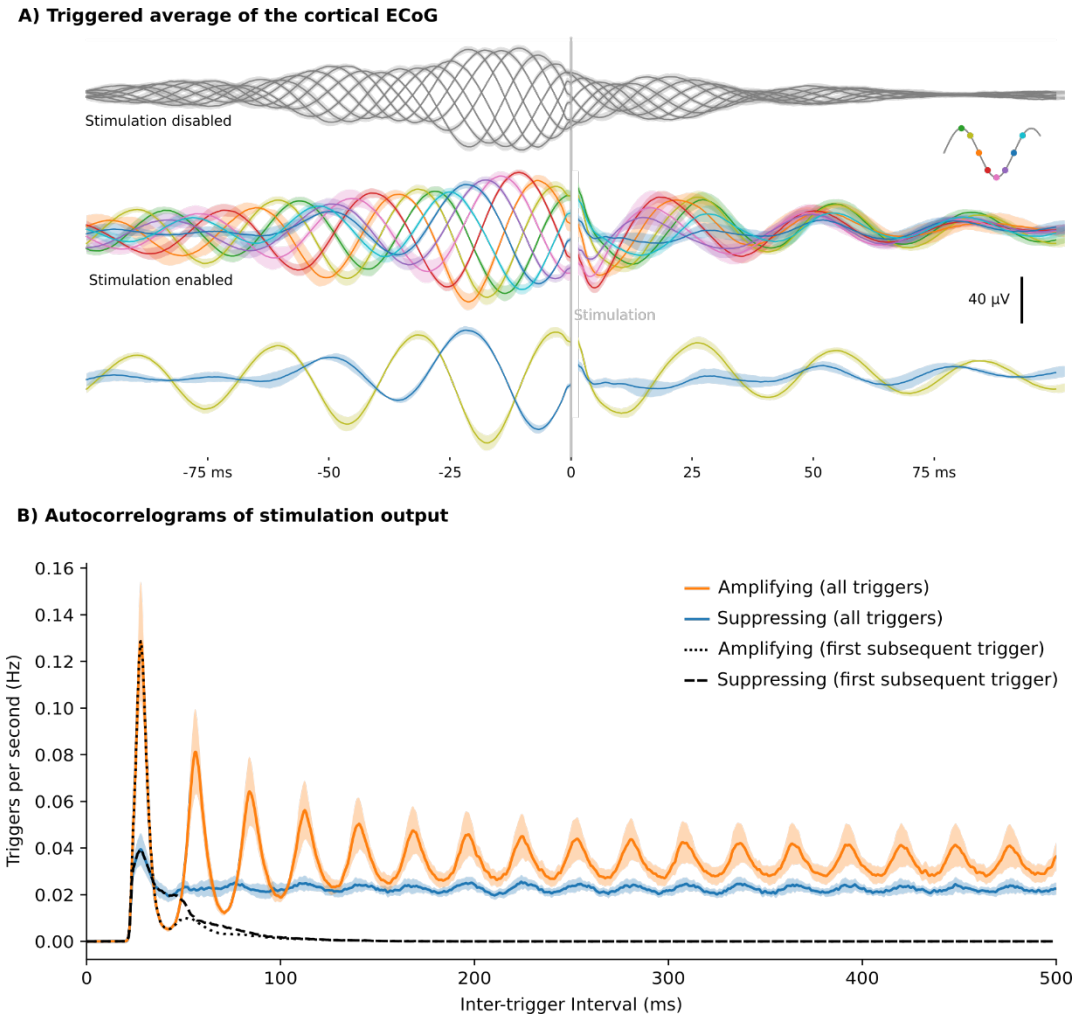


Figure 4-2: Effect of target phase on future stimulation

(A) Representative example of evoked potentials produced in the ECoG when aligned to trigger onset for each target phase (mean ± SEM). A spectrum of modulation was produced by stimulation (middle panel), with large differences produced when comparing the phase of maximal amplification (green) to the phase of maximal suppression ([blue], bottom panel). (B) Distribution of inter-trigger intervals to all subsequent triggers (autocorrelogram, solid lines) and limited to the immediately subsequent trigger (standard ISI, dotted lines) normalised by total duration of active stimulation (on-epochs) and smoothed using a Gaussian (sigma = 0.5 ms, n = 7 rats).

4.2.3 Triggering open-loop stimulation using closed-loop patterns

Considering that stimulation at each individual phase produces inherently different patterns of activity in terms of the number and rhythmicity of pulses, we next looked at the impact these parameters have on beta-band modulation when delivered open-loop (i.e. not phase-locked). To do so, we first applied phase-locked stimulation at the most amplifying (Figure 4-3B, solid orange) and most suppressing phases (Figure 4-3D, solid blue) to reproduce the bidirectional beta modulation characterised in chapter 1 (n = 3 rats). We then re-applied the identical stimulus trains generated during these closed-loop sessions but in an open-loop manner (dashed orange/blue). In order to quantify the modulation produced by each condition, we calculated changes in power within 5 Hz of the centre frequency (Figure 4-4). Both amplifying and suppressing stimulus trains significantly increased beta power when delivered open-loop ($p \leq 0.001$, t-tests to zero), but not when compared to each other ($p = 0.51$, t-test, $t_{12} = 0.66$), confirming that differences in the rate of stimulation were not responsible for the differences in beta modulation produced during closed-loop experiments. As expected, closed-loop suppressing and closed-loop amplifying stimulation were significantly different ($p = 9.3e^{-11}$, t-test, $t_{12} = 10.63$), while both outperformed their open-loop equivalent (closed-loop amplifying vs open-loop amplifying: $p = 0.0012$, paired t-test, $t_{12} = 4.20$; closed-loop suppressing vs open-loop suppressing: $p = 9.1e^{-08}$, paired t-test, $t_{13} = -10.60$). These results show that phase-locked stimulation is essential for suppressing ongoing oscillations and is crucial for maximising the amplification of such activity.

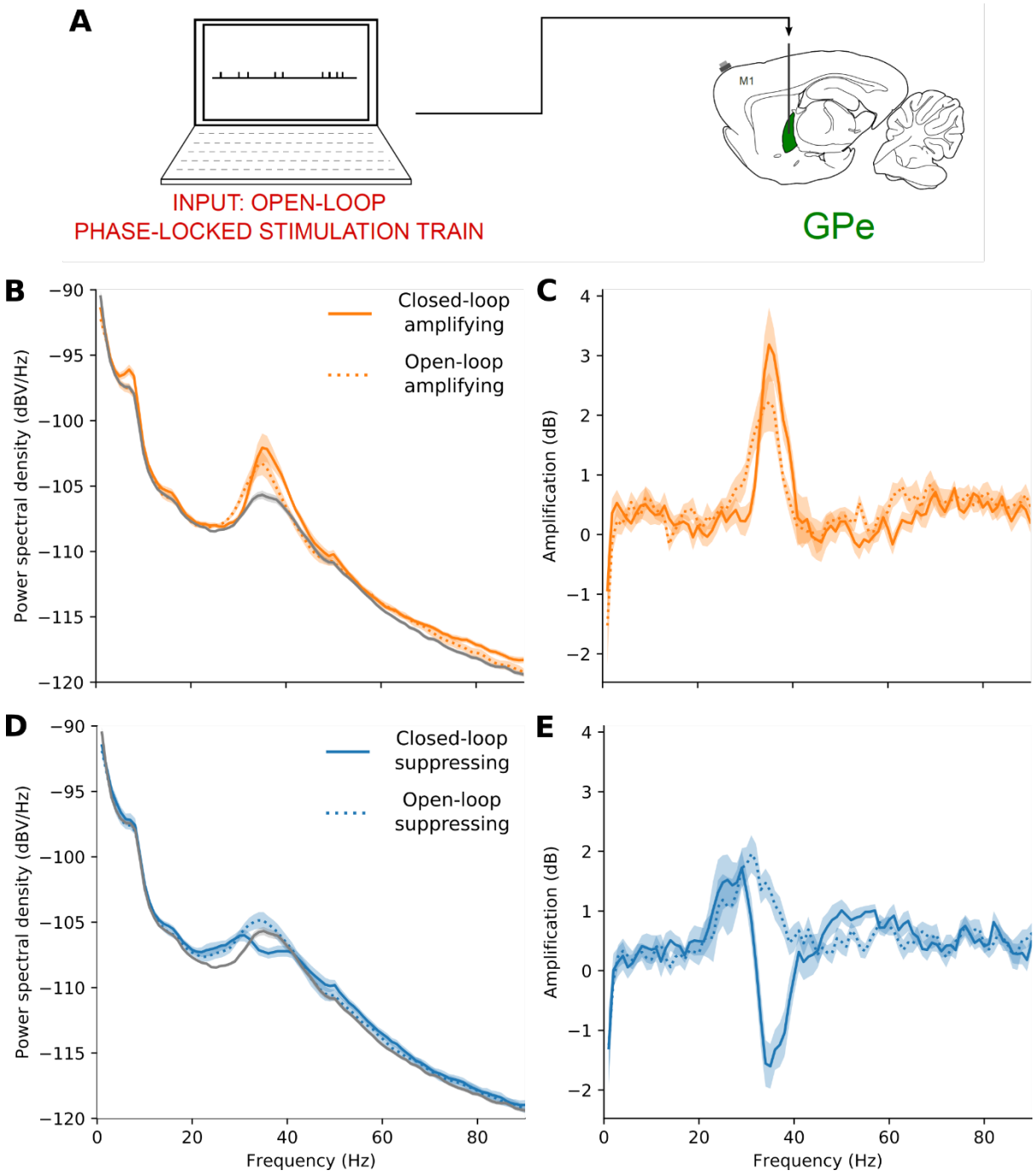


Figure 4-3: Triggering open-loop stimulation using closed-loop activity patterns

(A) The exact stimulus trains produced by phase-locked stimulation were reapplied in an open loop manner to investigate the importance of the interaction between stimulation and the online phase. (B, D) Power spectral density plots (mean ± SEM, n = 3 rats) show that phase-locked stimulation was able to amplify (solid orange) or suppress (solid blue) beta-band activity as expected. When reapplied open-loop, both amplifying (dashed orange) and suppressing (dashed blue) target phases produced amplification in the target band. (C, E) When normalised against the no stimulation condition, power spectral density in the beta-band was strongly reduced by phase-locked suppressing stimulation (solid blue) when compared to all other conditions.

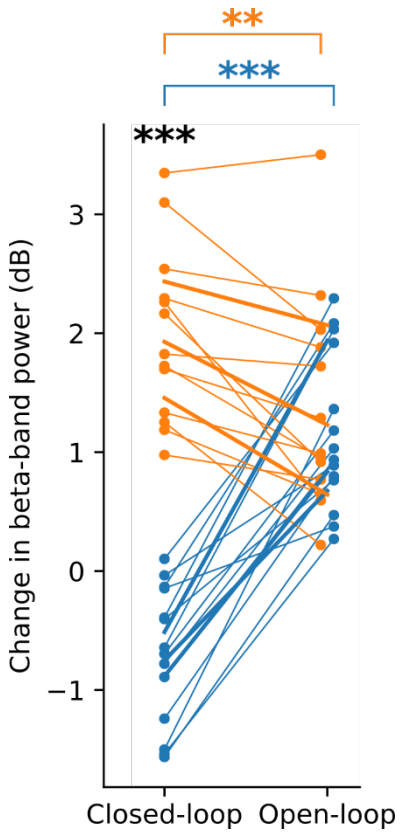


Figure 4-4: Quantification of closed- and open-loop beta-band modulation

The exact stimulus trains produced by phase-locked stimulation were reapplied in an open loop manner to investigate the important of phase. Amplifying (orange) and suppressing (blue) closed-loop stimulation is therefore paired with the identical open-loop equivalent. To quantify the modulation produced by each of the four stimulation conditions we calculated the change in beta-band power in a 10 Hz window centred around the target frequency (approximately 35 Hz). Each scatter point represents one recording, while the bold lines represent the group mean for each rat (n = 3). Closed-loop amplifying and suppressing stimulation were significantly different (black stars, $p = 9.3e^{-11}$, t-test, $t_{12} = 10.63$), while both outperformed their open-loop equivalent (closed-loop amplifying vs open-loop amplifying: orange stars, $p = 0.0012$, paired t-test, $t_{12} = 4.20$; closed-loop suppressing vs open-loop suppressing: blue stars, $p = 9.1e^{-08}$, paired t-test, $t_{13} = -10.60$).

4.3 Discussion

We provided evidence in chapter 1 that phase-locked stimulation can modulate beta power in a bidirectional manner by stimulating well under once per cycle. In doing so, our system must adapt to changes to the input signal that it itself seeks to create. The results in this chapter show that each target phase produces a unique pattern of stimulation that varies in terms of number, accuracy, and rhythmicity. Despite inherent differences in each pattern, amplifying and suppressing stimulation produced near identical levels of beta-band amplification when delivered open-loop, but failed to match that produced by phase-locked stimulation. When taken together, the results in this chapter show that brain and system enter into a state of equilibrium that is dependent on target phase, and that consistent phase-locking is essential for modulating oscillatory activity.

When all stimulation data was combined in chapter 1, the trigger rate was around 10 triggers per second below the theoretical upper bound dictated by the pre-set closed-loop centre frequency. This was possible because our system prevented stimulation delivery if 80% of a target frequency had not passed since the most recent trigger (as opposed to stimulating on every possible cycle). On-epochs targeting the phase of maximal suppression had a reduced trigger rate when compared to all phases combined, presumably because reductions in beta amplitude led to more periods where stimulation was prevented due to poor phase estimation. In contrast, on-epochs targeting the phase of maximal amplification produced an increased trigger rate. This remained well below the theoretical upper bound however, suggesting that stimulation acted to energise ongoing physiological activity as it fluctuated naturally

over time and did not get locked into potentially harmful artificial cycles of activity. Not only did stimulation occur more often during amplifying stimulation but, as shown by the phase histograms, with much greater accuracy. These results suggest that amplifying oscillations in the target range improved future phase estimation as expected. In accordance with this, the auto-correlograms of system output showed that amplifying target phases led to increased likelihood of stimulation on subsequent beta cycles when compared to suppressing stimulation. Evoked potentials calculated using the ECoG support this view and highlight the consistency with which stimulation at each phase modulates ongoing activity. A spectrum of stimulation profiles was produced in between the phases of maximal suppression and amplification, with each target phase producing a unique pattern of activity that was driven by the modulation produced when stimulating at that particular phase.

Stimulation patterns that produced beta suppression when phase-locked failed to do so when delivered open-loop, providing strong evidence that controlling stimulation phase is essential for disrupting oscillations in real time. In absolute terms, both open-loop conditions produced near identical amplification of beta power despite not tracking phase, which is perhaps unsurprising considering stimulation was delivered near the resonant frequency of the target oscillation. Interestingly, the amplification produced by each open-loop condition was quite different from a qualitative standpoint when analysing the spectral plots in Figure 4-3. Open-loop amplifying stimulation produced a sharper beta peak that was higher in amplitude than that produced by suppressing stimulation, which produced a wider spectral peak. The contrasting effects produced by amplifying and suppressing open-loop stimulation could reflect the differences in trigger patterns. Here, we show that phase-locked amplifying stimulation generates triggers more often with greater rhythmicity when

compared to suppressing phases, which may correspond to a sharper spectral peak when delivered open-loop. When you consider that beta frequency stimulation powerfully increases beta power, as evidenced by open-loop stimulation in this chapter, the modulation achieved here using phase-locked suppressing stimulation is particularly impressive. Not only do the results in this chapter highlight the efficacy of our system, but also the reliability. We used three independent recording sessions that were separated by at least 24 hours to generate mean spectral plots for both closed- and open-loop recordings (Figure 4-3B, D). The power changes produced by each of the three stimulation trains was remarkably consistent when delivered open-loop. The variability in stimulation patterns produced by phase-locked stimulation was therefore extremely small both within and between subjects, which again suggests that brain and system enters into a stable equilibrium that is dependent on target phase. The ability of a closed-loop system to produce and maintain a stable state of equilibrium with the biological system under modulation is likely to be particularly important in clinical applications of phase dependent stimulation, where stability is required over days and weeks.

The evidence in chapters 1 and 2 provide strong evidence for the efficacy of phase-locked stimulation over a period of minutes, yet provide little evidence of how stimulation affects beta activity over shorter timescales that are thought to influence motor function (Torrecillos et al., 2018). In this regard, triggered averages of the ECoG show that near total suppression of beta activity can be achieved after a single cycle when stimulating just after the trough. Stimulation on subsequent cycles is therefore likely to be massively reduced due to poor phase estimation, which is supported by triggered averages of stimulation output that show successive stimulation occurs much less often at suppressing phases when compared to amplifying phases.

Beta activity is not a stable rhythm but waxes and wanes over time, with periods of increased amplitude often referred to as ‘bursts’ of activity (Tinkhauser et al., 2017a). The above analyses highlight the responsiveness of the system to changes in oscillation amplitude before and after stimulation delivery, and suggest it is capable of disrupting beta activity within one or two cycles of burst generation. It has been argued that longer beta bursts are pathological in nature, based mainly on the evidence that burst duration positively correlates with motor impairment in PD (Tinkhauser et al., 2017a). This conclusion is drawn using data from a previous closed-loop study, where high frequency stimulation delivered only during periods of high beta power was found to be as efficacious as conventional DBS (Little et al., 2013, 2015). When the authors analysed in greater detail, their closed-loop stimulation reduced the number of longer bursts lasting over 0.6 seconds and increased those lasting between 0.2 and 0.4 seconds; suggesting that their approach provides benefit by truncating longer pathological bursts (Tinkhauser et al., 2017a). Although we do not directly report when each burst starts, the analysis in this chapter suggests that phase-locked stimulation is able to truncate bursts within one or two cycles. The approach used by Little and colleagues allows a certain level of pathological entrainment before stimulation occurs due to the use of a threshold, whereas our system attempts to continuously stimulate once per cycle. Computational studies predict that stimulating during low beta power is the most energy efficient way to disrupt pathological entrainment and provides rationale for the approach used here (Weerasinghe et al., 2019). It remains to be seen whether suppressing beta activity at the timescales reported here can provide therapeutic benefit but, from a theoretical perspective, the results presented here support the use of phase-locked stimulation in the treatment of PD.

Chapter 3

5 Assessment of motor function during closed-loop stimulation

5.1 Introduction

The pathological role of beta-band activity in PD was first proposed nearly twenty years ago (Brown et al., 2001). It rose to prominence over the following decade thanks to extensive empirical evidence that correlated beta power with motor impairments (Kühn et al., 2004). Importantly, the benefits of DBS therapy correlated with reductions in beta activity (Kühn et al., 2008) and stimulating only during periods of high beta activity is as effective as high frequency stimulation despite using half as much current (Little et al., 2013). Although supported by substantial associative evidence, the beta hypothesis has not been tested directly *in vivo* due to technical limitations. The closest direct evidence comes from externally driving the motor cortex (Pogosyan et al., 2009) or STN (Chen et al., 2007) at specific frequencies, which slows movement in healthy adults only when delivered in the beta-band. While this study does infer causality on some level, their perturbation does not reflect the transient nature of beta bursts, the stimulation will alter overall neuronal excitability, and does not allow for suppression. Here, we overcome these limitations by using phase-locked stimulation to bidirectionally modulate ongoing oscillatory activity in real-time and, in doing so, attempt to establish the first evidence of a causal relationship between beta-band oscillations and parkinsonian motor impairment.

In order to test this hypothesis we first had to consider how best to quantify motor impairment while also recording concurrently from across the brain. Traditional assessments of motor performance include spontaneous (cylinder test) or forced (stepping test) forelimb use, reaching tasks (staircase test), or drug-induced rotational analysis (review: Deumens et al.,2002). While all have their merits, none accurately measure a translatable deficit observed in PD, are oftentimes intrusive, and use low resolution performance measures. Nevertheless, deficits in cylinder scores correlate with lesion severity (Sutton et al., 2013) and have been ameliorated by classic high frequency stimulation in some instances (Dorval & Grill, 2014; Mottaghi et al., 2020; Shi et al., 2004) but by no means all (Rattka et al., 2016). Gait disturbances such as shuffling gait, postural instability, and freezing become more common as PD progresses, meaning that falling is a serious problem and a major cause of morbidity in advanced PD (Balash et al., 2005; Hely et al., 2005). Quantitative analysis of walking patterns in PD show that gait disturbances are driven by reductions in speed, cadence, and stride length; with increased step-to-step variability in the latter measure driving gait instability and freezing (Blin et al., 1990; Hausdorff et al., 2003). Despite some difficulties in comparing bipedal gait impairments with the quadrupedal equivalent, walking performance can be quantitatively assessed in rodents using video tracking software such as the *CatWalk XT* to evaluate footfall patterns (*noldus.com/catwalk-xt*). Like humans, lesioned rats also walk with reduced speed and cadence, spend longer in well supported walking configurations, and have altered stride patterns. These deficits are apparent in both bilateral (Westin et al., 2012) and unilaterally lesioned rats (Boix et al., 2018; Chuang et al., 2010); and while restricting the lesion to one hemisphere may diminish model faithfulness in some respects, it is not uncommon for patients to have lateralised motor deficits (Plotnik et al., 2005), and also

allows the healthy side to be used as a within subject control. While previous studies make it clear that the *CatWalk* system can capture strong motor deficits in 6-OHDA rats, there is relatively little evidence that it can be rescued by high frequency stimulation. One study did however find that DBS increased walking speed across the *CatWalk* (Vlamings et al., 2007), while step-by-step deficits in stride length and speed have been recovered by dopamine replacement therapy (Westin et al., 2012). Despite the lack of *CatWalk* specific evidence, high frequency stimulation has been shown to recover normal locomotion in several studies that utilise a treadmill (McConnell & Grill, 2013; Shi et al., 2006). Treadmill walking may not be the perfect model of gait impairment however, as it provides significant input to the motor system and acts as an external pacemaker to improve performance in humans (Frenkel-Toledo et al., 2005). Nevertheless, gait performance during natural walking provides a sensitive measure of motor impairment that is comparable in both rodents and humans, and can be quantitatively assessed alongside concurrent stimulation.

Continuous high-frequency stimulation ameliorates motor deficits in both gait (Li et al., 2012; Vlamings et al., 2007) and spontaneous forelimb use (Dorval & Grill, 2014; Mottaghi et al., 2020) when delivered to the STN. It therefore stands to reason that these behavioural paradigms will capture the therapeutic benefit of phase-locked stimulation if beta-band activity is indeed pathological. The recent development of phase-tracking algorithms here (and by others: Kanta et al., [2019] and Sanabria et al., [2020]) is the first step towards realising this potential, yet benefits of such a strategy remain unknown and must first be tested in the relevant animal models. Early studies using some form of phase-locked stimulation have provided encouraging evidence that stimulating just once per cycle can produce behavioural change despite using relatively little current. In humans, open-loop thalamic stimulation arriving at the

optimal suppressing phase reduced tremor by nearly a third (Cagnan et al., 2013). In mice, suppressing gamma activity in the basolateral amygdala using phase-locked stimulation impaired memory recall during a fear conditioning task (Kanta et al., 2019); whereas stimulation locked to hippocampal theta cycles bidirectionally modulated reward retrieval during a simple maze task (Siegle & Wilson, 2014). The latter study highlights the unparalleled specificity of phase-locked stimulation, as behavioural modulation was achieved by timing stimulation to target the activity of two distinct hippocampal input pathways using stimulation locked to either the peak or trough of ongoing theta oscillations. Despite producing significant behavioural modulations, the effect sizes observed in the above rodent studies were modest, while those in humans fell short of being clinically useful. The ability to consistently target specific phases across the entire cycle over long periods may be the differentiating factor required to deliver the desired behavioural effects. The experimental results in chapters one and two showcase the accuracy, reliability, and efficacy of our system; providing the foundation with which to form a yet unestablished causal link between cortical beta oscillations and specific motor deficits in PD. In this chapter, we use knowledge gained from those experiments to stimulate at the optimal phase for either suppression or amplification in behaving rats.

Summary:

Figure 5-1 – Effect of stimulation on spontaneous paw use during the cylinder task

Figure 5-2 – Effect of phase-locked stimulation on cortical beta power on the *CatWalk*

Figure 5-3 – Effect of 130 Hz stimulation on cortical beta power on the *CatWalk*

Figure 5-4 – Effect of stimulation on average speed

Figure 5-5 – Effect of stimulation on average speed relative to no stimulation

Figure 5-6 – Effect of stimulation on running style

Figure 5-7 – Effect of running style on average speed

Figure 5-8 – Relationship between average speed and bounding

Figure 5-9 – Effect of stimulation on gait asymmetry

Figure 5-10 – Effect of stimulation on within-run variance

5.2 Results

Critically for our hypothesis, and for the translatability of our model, toxin-induced dopamine depletion produced a robust increase in cortical beta activity that could be modulated by GPe stimulation in a bidirectional manner (Chapter 1). Rats were only included in behavioural analyses if they had a detectable spectral peak in the beta-band that was modulated by phase-locked stimulation in a bidirectional manner. The significant technical and practical challenges associated with combining electrophysiology and behaviour meant that this was not achieved for every animal however. A combination of lesion variability, implant damage, erroneous target phase selection, and deterioration of the tissue-electrode interface over time, led to a limited number of rats meeting the pre-determined inclusion criteria. As such, a subset of rats that received phase-locked STN stimulation were included for analysis. Although not

shown in chapter 1, subthalamic and pallidal stimulation were equally effective, meaning that subjects from both target sites could be combined when assessing the importance of cortical beta oscillations on behaviour. Different shaped markers have been used where appropriate when plotting data to differentiate between those receiving GPe (circle markers) and STN stimulation (triangle markers).

Unilateral 6-OHDA administration into the SNc produced visible motor deficits in spontaneous paw use and gait that were evident in the home cage. In particular, the most successful lesions caused the left hindlimb to lag far behind the unaffected right hindlimb, presumably due to a weakness in the limbs contralateral to the lesion. In order to quantify this motor deficit in a formal setting, we trained rats to traverse a narrow corridor to collect reward. The *CatWalk XT* provides automatic footfall detection software, allowing us to measure average running speeds and styles during locomotion (Figure 5-4 to 5-8). It also allows for left versus right comparisons of gait performance using translatable measures such as stride length and swing speed (Figure 5-9 and 5-10). Spontaneous forelimb use was also recorded using the cylinder task, which provided a complimentary measure of motor impairment (Figure 5-1). Importantly, it was possible to carry out both tests alongside concurrent phase-locked stimulation and, as a result, the effect of each stimulation condition on cortical beta power is also assessed (Figure 5-2 and 5-3). The four stimulation conditions used during testing were: phase-locked amplifying stimulation, phase-locked suppressing stimulation, no stimulation, and open-loop high frequency stimulation at 130 Hz.

5.2.1 Effect of stimulation on paw use during the cylinder task

Spontaneous forelimb use during cylinder testing provided our primary measure of lesion severity *in vivo*, and was used alongside visual inspections to decide which animals to implant. No preference in left or right paw use was observed in the eight implanted rats pre-lesion (46.5 % ± 7.1, $p = 0.68$, one sample t-test, $t_7 = -0.42$). Of those eight, phase-locked stimulation produced bidirectional modulation in five, which includes both STN and GPe cohorts. Of that five, one received STN and GPe stimulation in two separate experiments, which are treated as independent data points during this analysis. Unilateral dopamine depletion produced a marked decrease in contralateral (left) forelimb use in all rats (11.3 % ± 7.1, pre-lesion vs post-lesion: $p = 0.0004$, paired t-test, $t_4 = -10.34$), which was not significantly affected by implantation (9.5 % ± 6.8, post-lesion vs no stim: $p = 0.51$, paired t-test, $t_5 = -0.70$). Rats with the strongest ipsilateral (right) bias during pre-lesion testing were more strongly affected by implantation however, using their contralateral limb very little post-implant (see the two markers below 5% during stimulation testing in Figure 5-1). None of the four stimulation conditions produced a significant change in contralateral paw use across animals ($p = 0.37$, one-way repeated measures ANOVA, $F_{3, 15} = 1.10$).

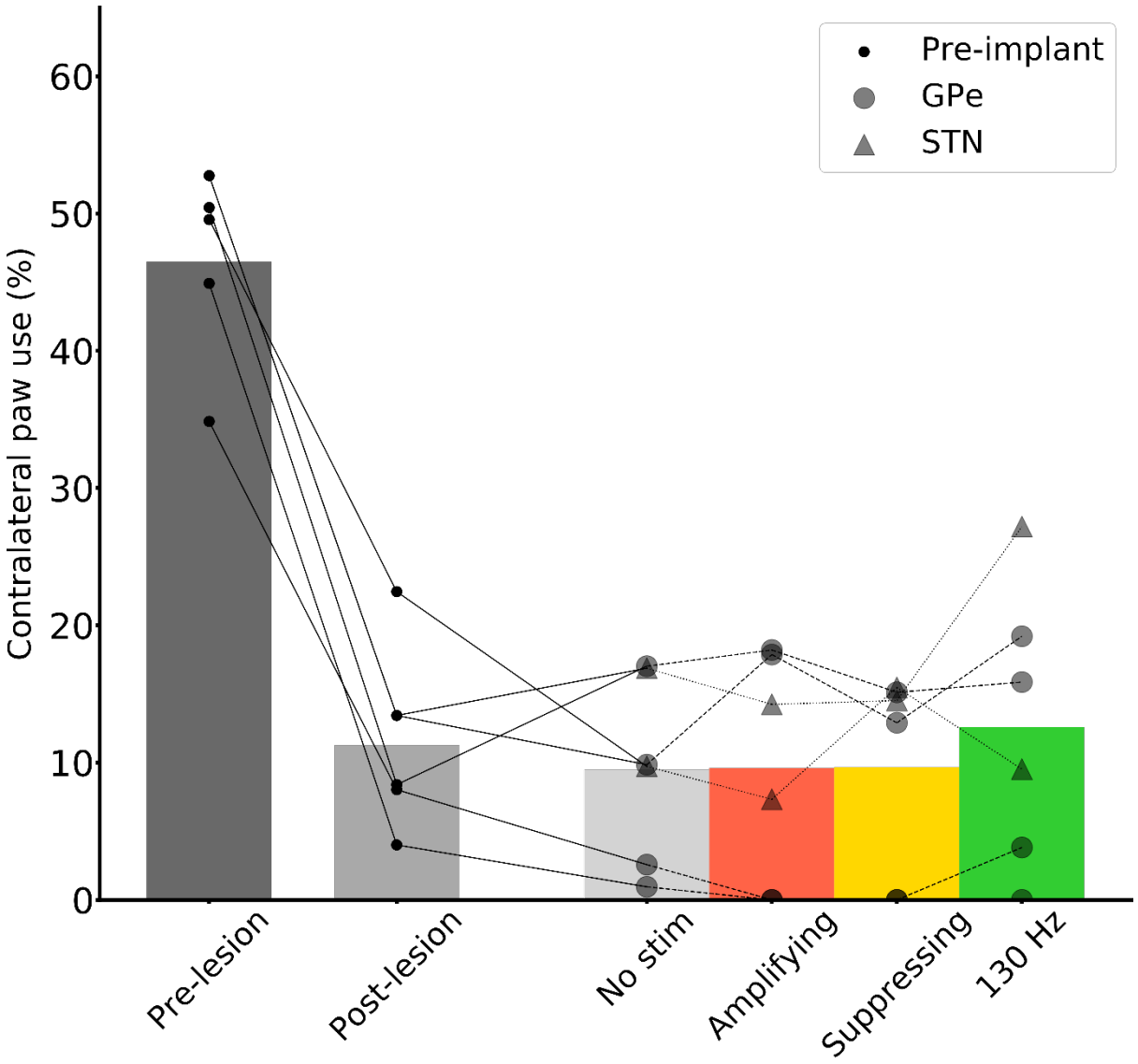


Figure 5-1: Effect of stimulation on paw use during the cylinder task

Spontaneous forelimb use was measured by the cylinder test before (dark grey) and after (grey) unilateral lesion of the right SNc to determine which animals to implant. The number of weight bearing touches of the cylinder walls using the paw contralateral to the lesion were calculated as a percentage of the total. The cylinder test was repeated post-implant during tethered sessions where four stimulation conditions were tested: no stimulation (light grey), phase-locked amplifying stimulation (red), phase-locked suppressing stimulation (gold), and high frequency 130 Hz stimulation (green). Bars represent group means for each condition, while individual scatter points represent the performance of each rat. Stimulation was delivered to either the STN (n = 2, triangles) or GPe (n = 4, circles), with one rat included in both groups as it received stimulation in both target sites during two separate experiments.

5.2.2 Effect of stimulation on cortical beta power on the CatWalk

Before analysing the effect of phase-locked stimulation on locomotion, we first had to confirm system efficacy in rats completing the behavioural task on a new rig (the cylinder task was performed in the same faraday cage as open field recordings in chapter 1). Although aluminium sheeting was installed around the *CatWalk* walkway, electrical noise in the recording room produced a sharp spectral spike at 50 Hz. This spike did not interfere with phase-tracking despite being relatively close to the target centre frequency (34 - 41 Hz), highlighting the accuracy with which our system targets the band of interest. Of the eleven rats that underwent gait assessment, phased-locked stimulation produced bidirectional modulation in seven (Figure 5-2), which is made up of both STN (n = 2) and GPe target groups (n = 5). The absolute phase of maximal amplification and suppression, as well as the magnitude of modulation, were broadly similar between rats regardless of target structure. In contrast, high frequency 130 Hz stimulation failed to modulate cortical beta power in 6 out of the 7 rats (Figure 5-3). When you consider that all stimulation conditions were amplitude matched, these results support a novel mechanism of action when delivering phase-locked stimulation that was more effective in modulating cortical beta power than classic 130 Hz stimulation.

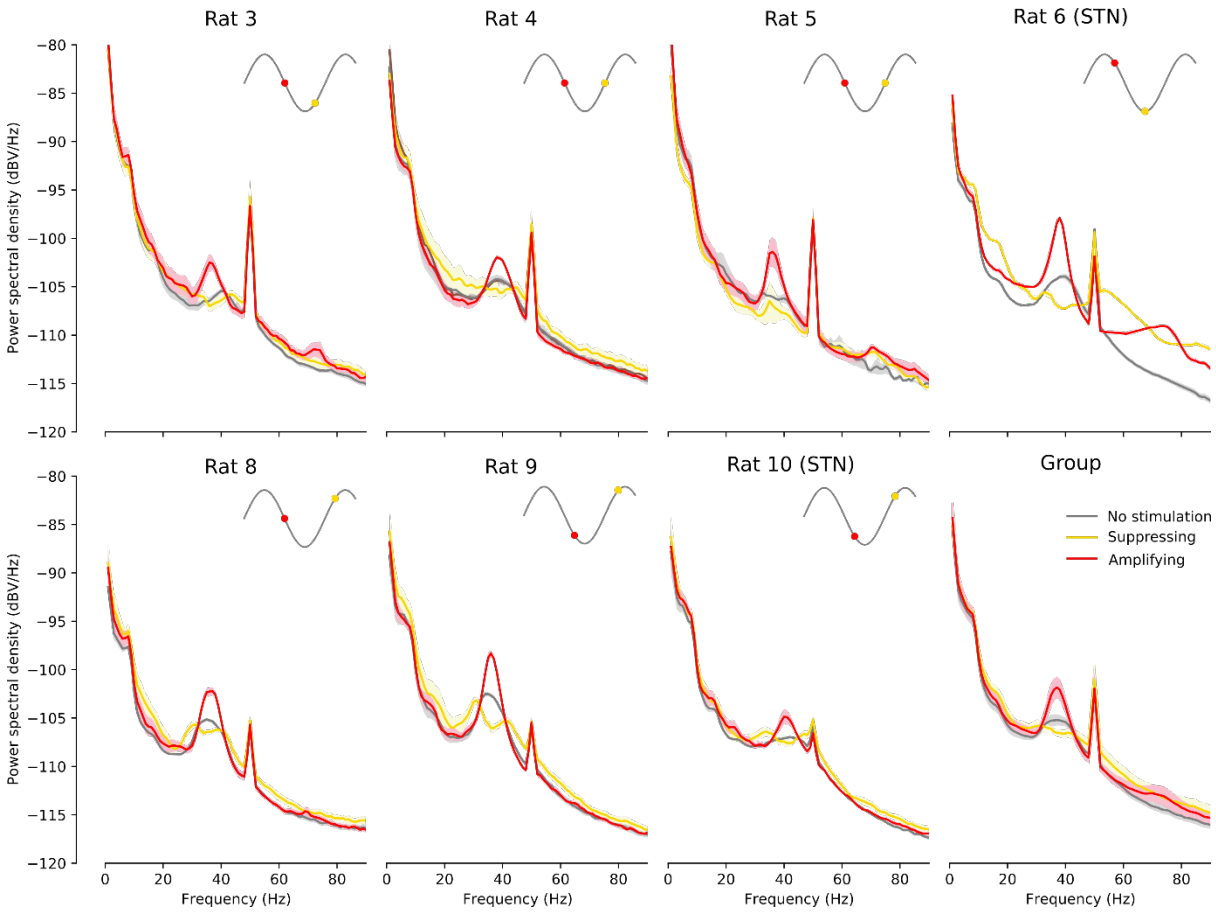


Figure 5-2: Effect of phase-locked stimulation on cortical beta power on the CatWalk

Power spectral density plots (mean ± SEM, n = recordings) recorded from the frontal ECoG screw located ipsilateral to the 6-OHDA lesion. Spectra were calculated from sessions lasting between 5 to 20 minutes, where rats traversed the CatWalk walkway to gain reward. Elevated beta-band power was observed across all rats during the no stimulation condition (grey), which was modulated in a bidirectional manner by phase-locked GPe or STN stimulation. The inset on each panel shows the phase of maximal amplification (red) and maximal suppression (gold), which were individually selected for each rat using knowledge gained from their previous open field recordings. Each rat is named as per Table 2-1 in the Methods and group data is shown in the bottom right panel (mean ± SEM, n = rats).

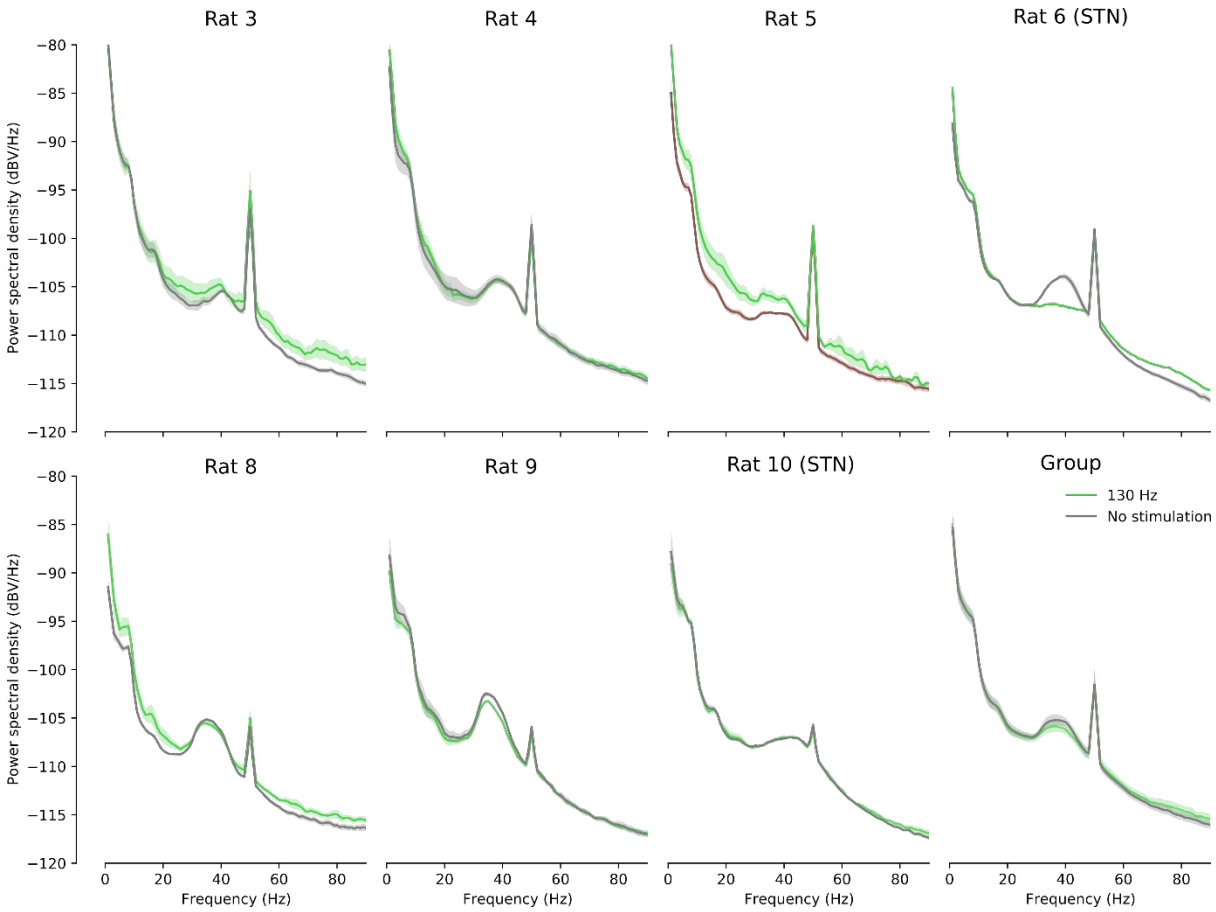


Figure 5-3: Effect of 130 Hz stimulation on cortical beta power on the CatWalk

Power spectral density plots (mean ± SEM, n = recordings) recorded from the frontal ECoG screw located ipsilateral to the 6-OHDA lesion. Spectra were calculated from sessions lasting between 5 to 20 minutes, where rats traversed the CatWalk walkway to gain reward. Elevated beta-band power was observed across all rats during the no stimulation condition (grey), which was not modulated by 130 Hz GPe or STN stimulation (green). Each rat is named as per Table 2-1 in the Methods and group data is shown in the bottom right panel (mean ± SEM, n = rats).

5.2.3 Effect of stimulation on average speed

Rats freely traversed the 90 cm *CatWalk* to collect reward after only a couple of training days, moving at a wide range of speeds anywhere from 20 to 140 cm/s (Figure 5-4). Despite visible gait disturbances following surgery, deficits were less clear during goal-directed behaviour with rats routinely reaching high speeds. Nonetheless, the average speed observed during this task (67.2 cm/s ± 16.9) was comparable to those reported in previous lesion studies (Boix et al., 2018), and fell below those previously reported in healthy controls, who reach average speeds of around 70 to 80 cm/s (Koopmans et al., 2007). As shown by the bottom right panel in Figure 5-4, the effect of stimulation on average speed was modest but consistent ($p = 0.0007$, one-way repeated measures ANOVA, $F_{3, 18} = 8.91$). Post-hoc comparisons (paired t-tests) show that amplifying stimulation significantly reduced speed when compared to no stimulation (61.5 cm/s ± 15.7, $p = 0.008$, $t_6 = -3.85$). It also reduced average speed when compared to suppressing stimulation ($p = 0.003$, $t_6 = -4.63$), which did not differ from the no stimulation condition ($p = 0.67$, $t_6 = -0.44$). Finally, 130 Hz stimulation also reduced average speed when compared to suppressing stimulation (64.5 cm/s ± 18.3, $p = 0.03$, $t_6 = -2.90$), but failed to reach significance relative to no stimulation ($p = 0.09$, $t_6 = -2.04$). The consistent deficits produced by amplifying stimulation were particularly evident when comparing average speed as a percentage of no stimulation (Figure 5-5), with 6 out of 7 rats moving at lower speeds. Amplifying stimulation reduced speed by 8.4% ± 5.9 on average, compared to a 4.4% ± 5.4 reduction during 130 Hz stimulation. These results show that phase-locked stimulation can impair motor performance when amplifying cortical beta activity. Crucially, reductions in average speed were only produced when stimulating just after the peak at amplifying phases and not when stimulating at supressing phases.

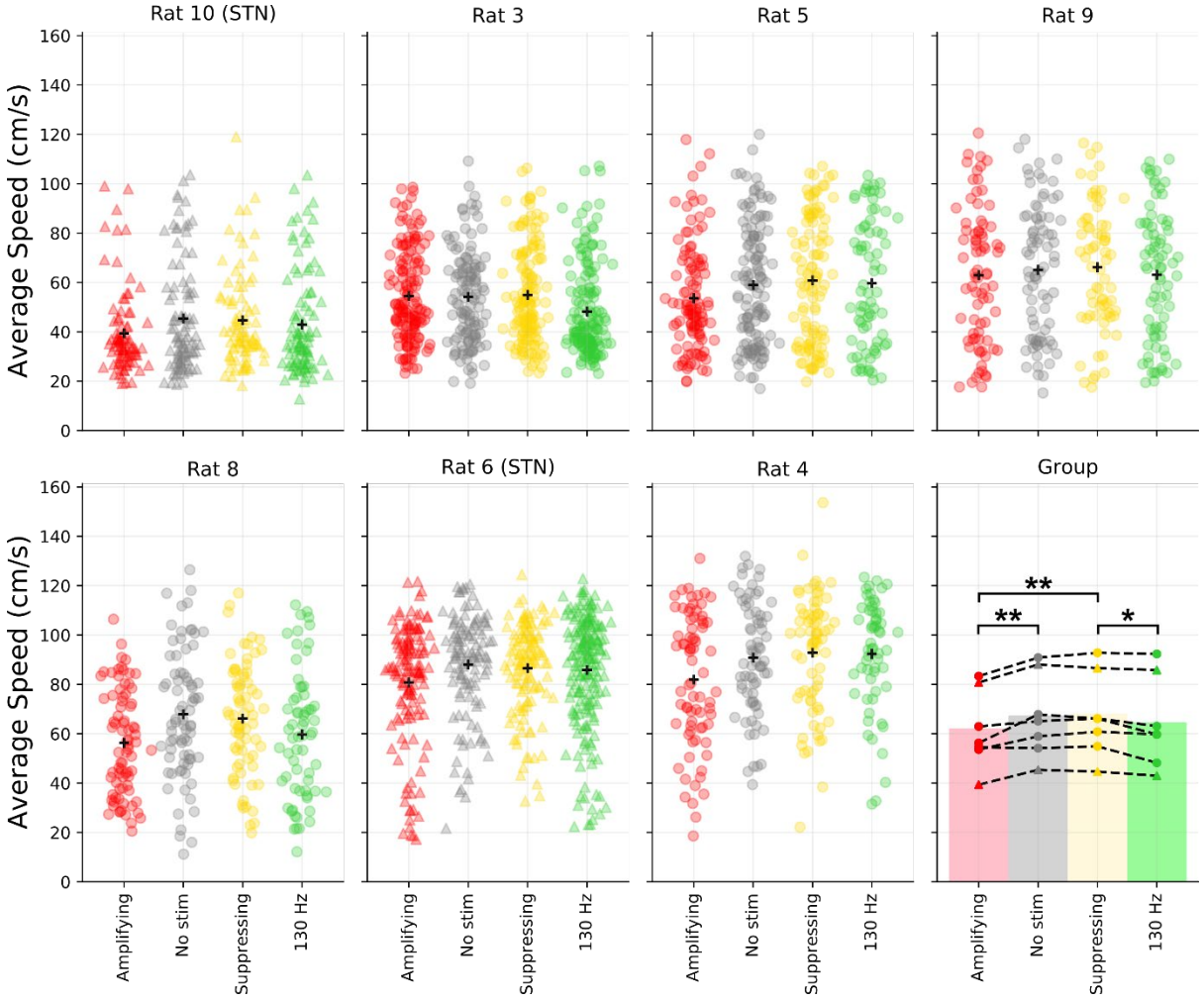


Figure 5-4: Effect of stimulation on average speed

The average speed of each individual run (scatter points) produced by each rat (panels) was recorded automatically by the *CatWalk XT*. Sessions of equal length were recording during phase-locked amplifying (red) and suppressing (gold) stimulation, as well as no stimulation (grey) and 130 Hz stimulation (green). Rats are ordered by ascending average speed during no stimulation, as denoted by the black cross for each condition, with the slowest rat in the top left. Group data is shown by the bar chart in the bottom right panel with scatter points representing individual rats receiving either STN (triangles) or GPe stimulation (circles). The effect of stimulation on average speed reached significance ($p = 0.0007$, one-way repeated measures ANOVA, $F_{3, 18} = 8.91$), with amplifying stimulation (61.5 cm/s ± 15.7) reducing average speed compared to both no stimulation (67.2 cm/s ± 16.9, $p = 0.008$, paired t-test, $t_6 = -3.85$) and suppressing stimulation (67.5 cm/s ± 17.0, $p = 0.003$, paired t-test, $t_6 = -4.63$).

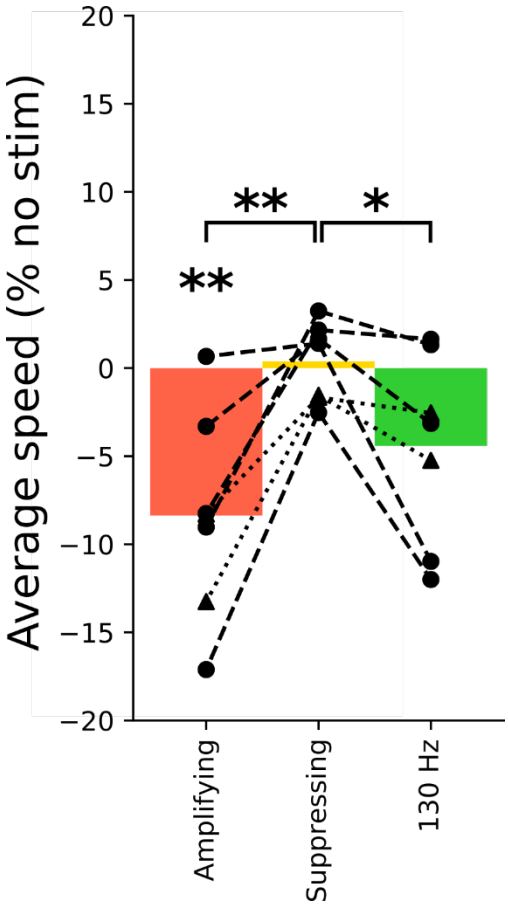


Figure 5-5: Effect of stimulation on average speed relative to no stimulation

The average speed for each rat on the *CatWalk XT* as a percentage change from the equivalent no stimulation condition for both STN (triangles) ad GPe (circles). The bars represent the group mean, while scatter points represent individual rats. Only phase-locked amplifying stimulation was significantly different from control (-6.2 % ± 7.3, p = 0.008, paired t-test, t_6 = -3.85), while suppressing stimulation (0.38 % ± 2.25) was significantly different from both phase-locked amplifying stimulation (p = 0.003, paired t-test, t_6 = -4.63) and 130 Hz stimulation (p = 0.03, paired t-test, t_6 = -2.90).

5.2.4 Effect of stimulation on running style

The speed deficits produced by amplifying and 130 Hz stimulation must be the end result of a more specific motor impairment. To investigate this further, we first looked at how running style varied with stimulation. Rats employed two distinct styles (Figure 5-6A): slow 'walking' where opposite diagonal pairs were placed in succession (e.g. left front followed by right hind), or fast 'bounding' where girdle pairs were placed in sequence (e.g. left hind followed by right hind). Girdle pairs were typically placed in synchrony during bounding to maximise speed and was essential to reach speeds above 60 cm/s. The proportion of fast bounding versus slow walking varied between individual rats, with some only bounding around 25% of the time, while others reached up to 90% (Figure 5-6B). Stimulation produced a significant change in the amount of bounding observed on the *CatWalk*, regardless of running style preference ($p = 0.0002$, one-way repeated measures ANOVA, $F_{3, 18} = 11.02$). On average, amplifying stimulation reduced the amount of bounding by 11.7% ± 7.7 when compared to no stimulation (Figure 5-6C, $p = 0.007$, paired t-test, $t_6 = -4.06$), which was significantly different suppressing stimulation ($p = 0.002$, paired t-test, $t_6 = -5.44$), and 130 Hz stimulation ($p = 0.008$, paired t-test, $t_6 = 3.85$). The latter also reduced bounding (6.4% ± 8.0) relative to suppressing stimulation ($p = 0.02$, paired t-test, $t_6 = -3.03$) but not when compared no stimulation ($p = 0.08$, paired t-test, $t_6 = -2.11$). To determine if the deficits in speed observed during amplifying stimulation were produced by reduced speed during bounding and not just a reduction in the amount of bounding (e.g. Figure 5-6C), we split runs into three categories: walking, bounding, or a mix of both styles (Figure 5-7). As expected, bounding (79.5 cm/s ± 11.2) produced much higher average speeds than both walking (39.3 cm/s ± 10.6) and the mixed running style (47.5 cm/s ± 4.7). Stimulation had no effect on the average speed of runs within each style (walking:

$p = 0.4$, $F_{3, 18} = 1.05$; mixed: $p = 0.38$ $F_{3, 18} = 1.08$; bounding: $p = 0.32$ $F_{3, 18} = 1.27$; repeated measures one-way ANOVA), suggesting that amplifying stimulation does not affect the speed of rats once they enter into a particular running style. In support of the amount of bounding being the main determinant of speed, stimulation dependent reductions in bounding strongly correlated with reductions in overall running speed ($R^2 = 0.55$. Figure 5-8). When taken together, these results suggest that phase-locked amplifying stimulation prevents rats from utilising the bounding running style needed to reach high speeds.

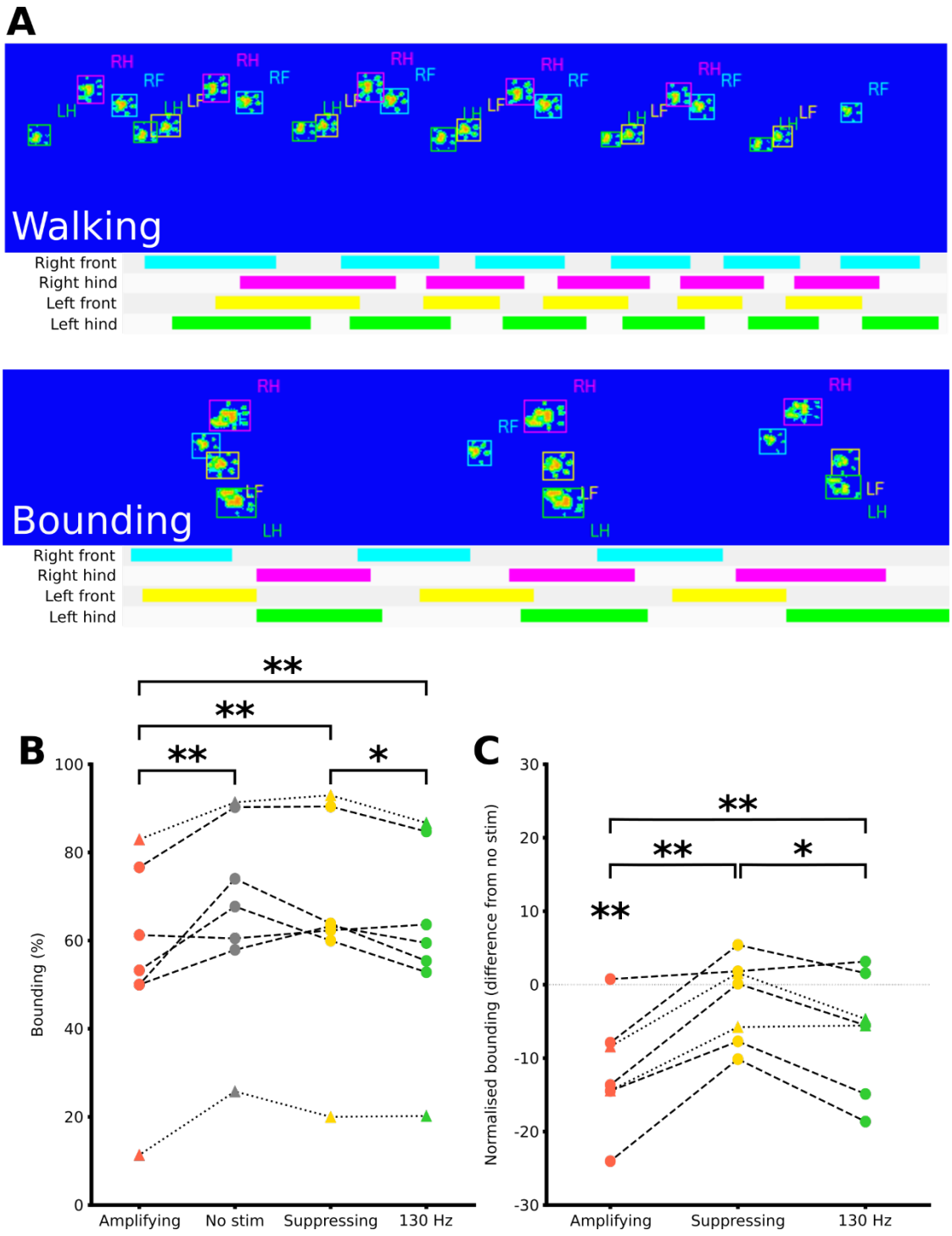


Figure 5-6: Effect of stimulation on running style

(A) Running styles could be split into two distinct categories, fast bounding and slow walking, which were defined by specific gait patterns. (B) The amount of fast bounding behaviour varied greatly between rats during control recordings (grey scatter, 64.9% ± 22.5), and was significantly affected by stimulation (bottom left panel, p = 0.003, one-way repeated measures ANOVA, $F_{3, 18} = 6.75$). (C) Amplifying (p = 0.01, paired t-test, $t_6 = -3.44$) and high frequency stimulation (p = 0.03, paired t-test, $t_6 = -2.72$) significantly reduced the amount of fast bounding when compared to control, which reached -8.7% ± 6.6 and -6.3% ± 6.1 respectively when normalised against control (bottom right panel).

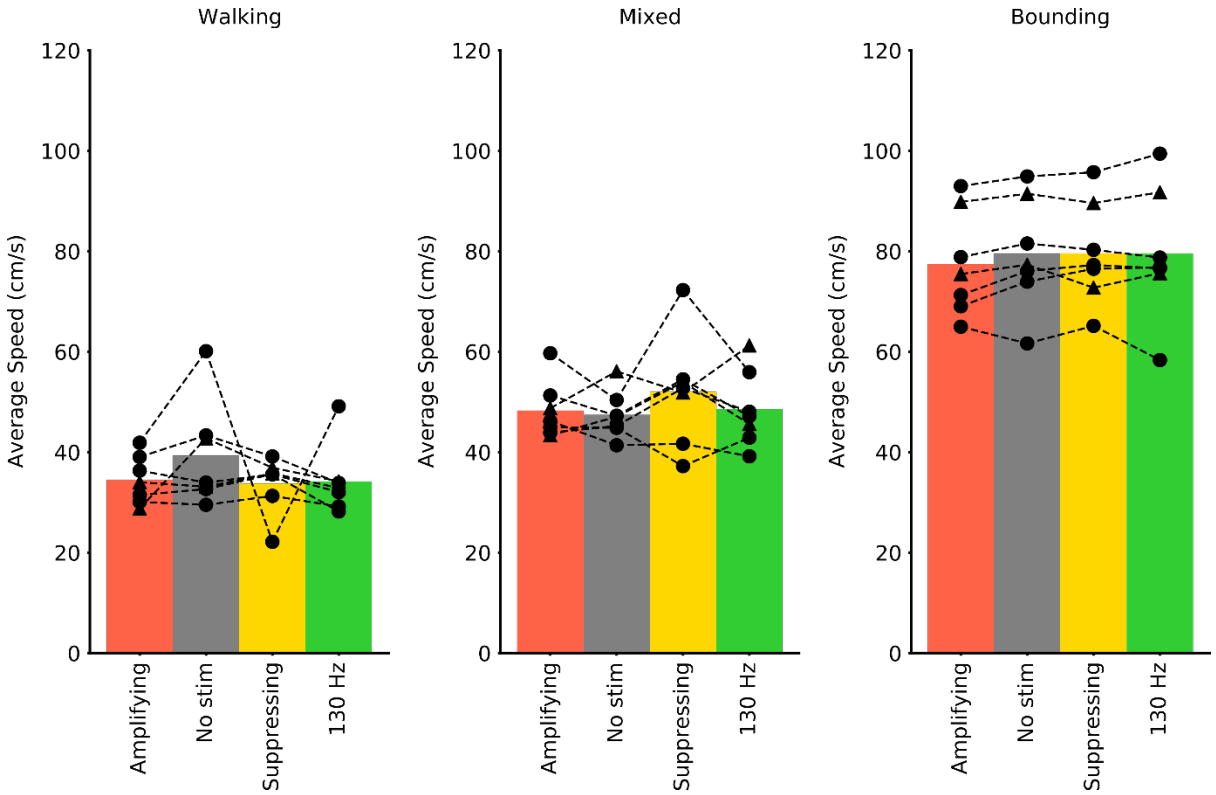


Figure 5-7: Effect of running style on average speed

Rats utilise two running styles when moving across the catwalk that depend upon different footfall patterns. Diagonal walking is produced when one forelimb is followed by the opposite hindlimb or vice-versa (e.g. left front then right hind), while bounding is produced by successive placements of girdle pairs (e.g. left front then right front). The average speed during walking (A), bounding (C), or a mix of both styles (B) are compared during each of the four stimulation conditions. Stimulation had no effect on average speed during each running style (walking: $p = 0.40$, $F_{3, 18} = 1.05$; mixed: $p = 0.38$ $F_{3, 18} = 1.08$; bounding: $p = 0.32$ $F_{3, 18} = 1.27$; repeated measures one-way ANOVA).

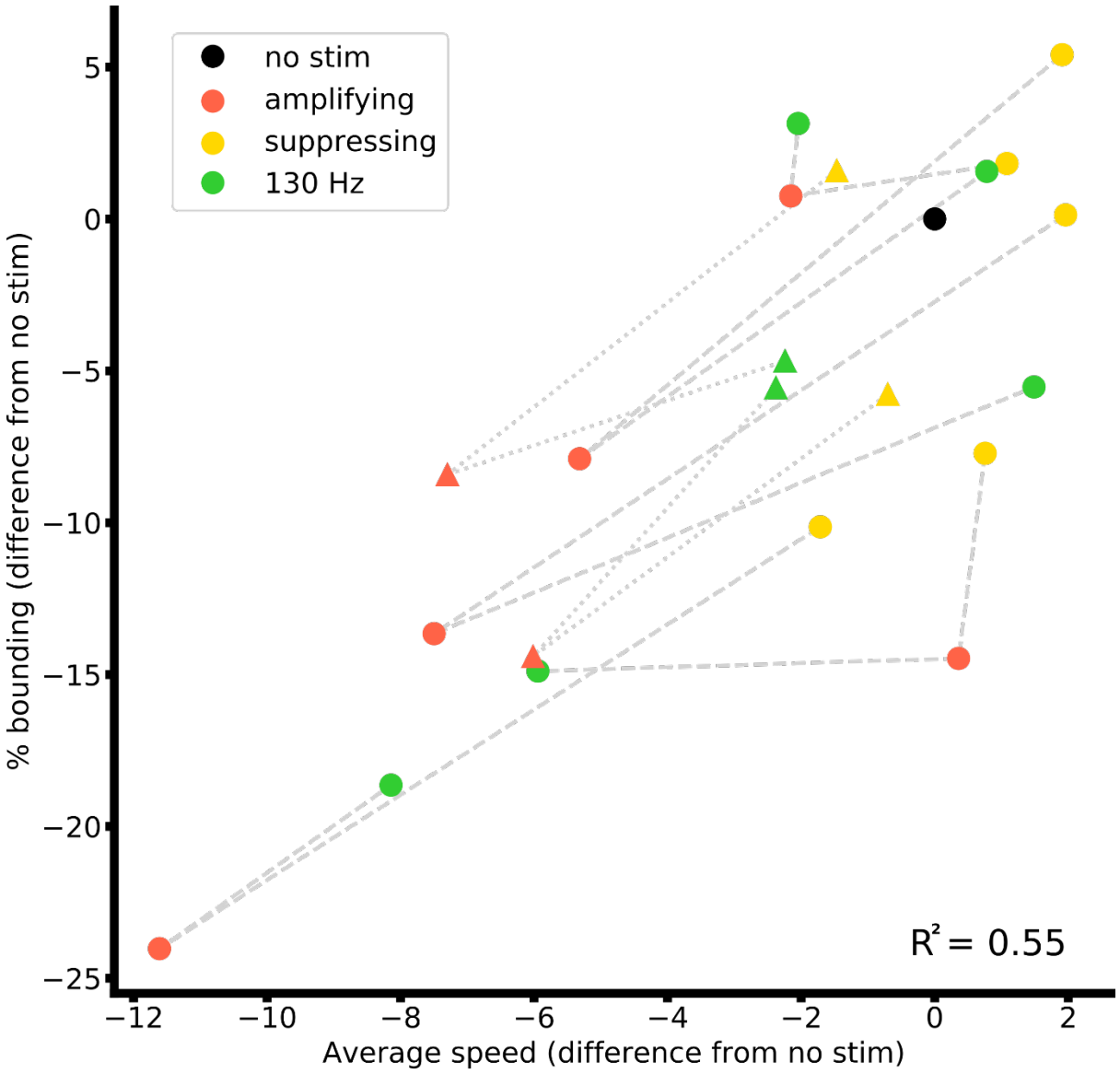


Figure 5-8: Relationship between average speed and bounding

Relative changes in average speed and bounding plotted for amplifying (red), suppressing (gold), and high frequency stimulation (green). A strong correlation between both measures is observed, with amplifying stimulation in particular reducing both measures (R-squared = 0.55). Each rat has one data point per stimulation condition that are connected by grey dashed lines (7 rats, 21 points), with triangles highlighting those receiving STN stimulation. The black circle at zero represents performance during no stimulation.

5.2.5 Effect of stimulation on gait asymmetry

Finally, we examined individual paw parameters on the side contralateral to the lesion to assess the impact of stimulation on fine-scale measures of gait performance. In particular, we looked at parameters that make up a single step cycle: stand time, stride length, and swing speed. These measures are highly correlated with average speed in absolute terms, and therefore mirror the global speed changes described in Figure 5-4 (data not shown). In an attempt to tease apart the contribution each parameter has on locomotor speed, we analysed performance on the affected side (left) relative to the unaffected side (right). Although right performance cannot be viewed as completely independent from left, the normalised measure acts as a critical within subject control that takes into account the speed and style with which the rat is travelling, thus isolating motor deficits on the affected side.

Average stride length on the affected side was significantly increased in both front (+4.6 % ± 2.5, $p = 0.003$, t-test to zero, $t_6 = 4.97$) and hind limbs (+3.6 ± 2.3, $p = 0.006$, t-test to zero, $t_6 = 4.16$) when normalised against the unaffected side, while swing speed (-7.6 % ± 3.6, $p = 0.001$, t-test to zero, $t_6 = -5.56$) and stand time asymmetry (-3.7 % ± 2.1, $p = 0.004$, t-test to zero, $t_6 = -4.63$) was only present in the front limbs (Figure 5-9). These deficits highlight the relatively small (but also consistent) impact of our lesion on step cycle asymmetry, on which stimulation had no significant impact ($p > 0.05$, one-way repeated measures ANOVA). By far the largest asymmetric deficit produced by our lesion was recorded in the left hindlimb, where maximum contact area was significantly increased on average by 22.0% ± 17.7 ($p = 0.02$, no stim vs zero, one-sample t-test, $t_6 = 3.30$). As with the step cycle parameters, stimulation had no effect on maximum contact area asymmetry ($p = 0.68$, one-way repeated measures ANOVA, $F_{3, 18} = 0.50$). In conclusion, the effect of stimulation was

no longer present when normalising affected left performance against unaffected right, despite clear asymmetry in each measure.

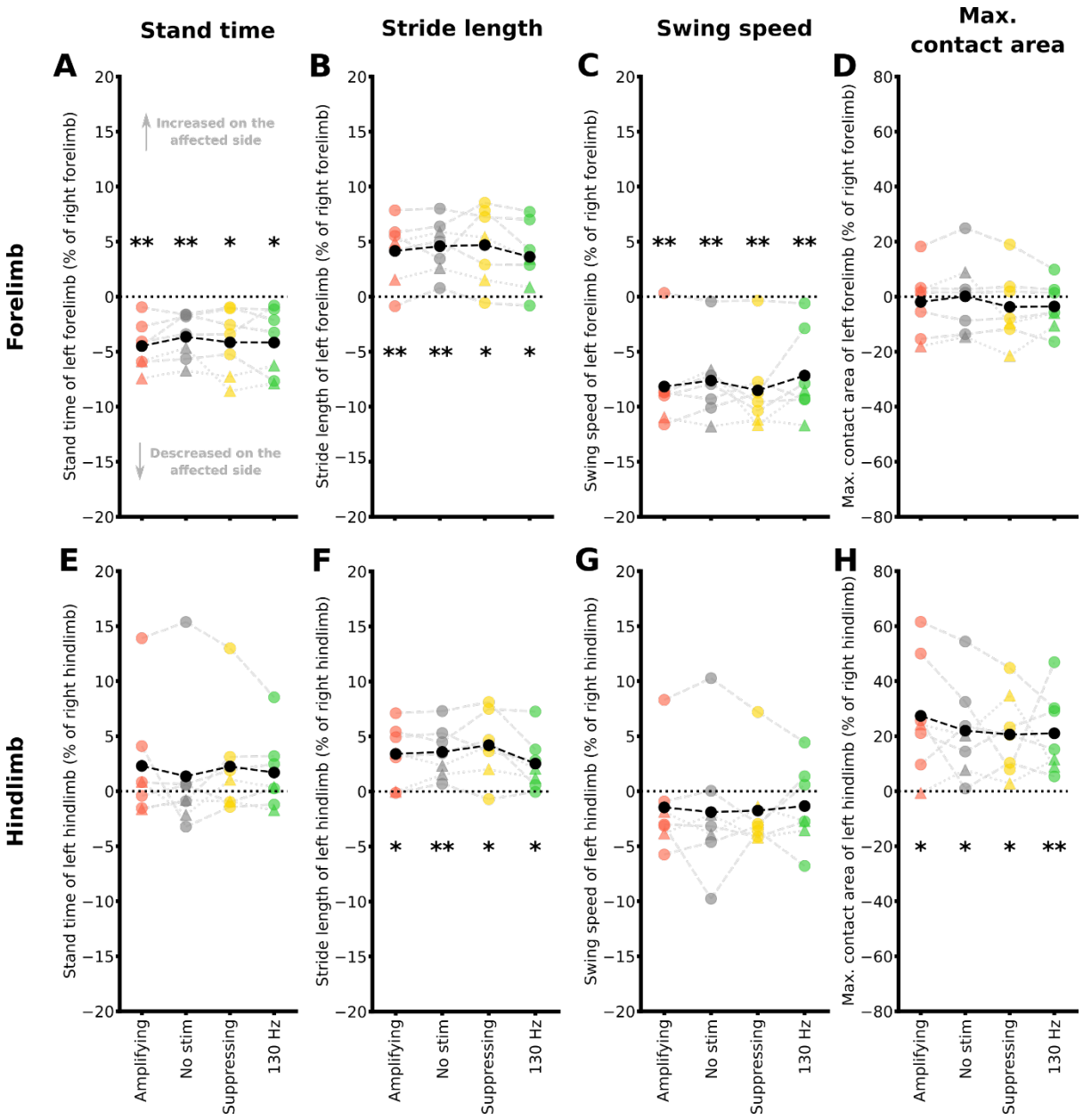


Figure 5-9: Effect of stimulation on gait asymmetry

The effect of stimulation on individual characteristics of the step cycle (columns) were analysed for each paw (rows). Deficits in the stand time (A, E), stride length (B, F), swing speed (C, G), and maximum contact area (D, H) were restricted to the affected left side of the body due to the unilateral 6-OHDA lesion. Performance on the affected side is displayed as a percentage of the unaffected right side for both front- and hindlimbs, thus positive values indicate greater values on the affected left side. Each measure produced consistent asymmetry in the front and/or hindlimbs ($p \leq 0.05$, t-tests to zero) that was not significantly affected by stimulation ($p > 0.05$, one-way repeated measures ANOVA).

5.2.6 Effect of stimulation on within-run variance

It has been reported that gait disturbances in PD patients are driven by increased variation in step cycle measures such as a stride length and stride time (Blin et al., 1990; Hausdorff et al., 2003). To see if comparable changes in gait are observed here, we examined the effect of stimulation on parameter variance during individual runs (e.g. left forelimb s.d. – right forelimb s.d.). Only stand time variance in the front limbs was significantly affected by stimulation (Figure 5-10A, $p = 0.01$, one-way repeated measures ANOVA, $F_{3, 18} = 5.05$). Post-hoc comparisons showed that phase-locked amplifying stimulation significantly reduced stand time variance in the left forelimb when compared to both no stimulation ($p = 0.007$, paired t-test, $t_6 = -4.05$) and 130 Hz stimulation ($p = 0.04$, paired t-test, $t_6 = -2.66$), but just failed to reach significance versus suppressing stimulation ($p = 0.06$, paired t-test, $t_6 = -2.36$). Due to the nature of walking on four limbs, variation in stand times produced in the forelimbs are likely to affect the hindlimbs and it should be noted that a mirrored increase in left hindlimb stand time variance was observed in five of the seven rats (Figure 5-10E). This did not reach significance at a group level however ($p = 0.21$, one-way repeated measures ANOVA, $F_{3, 18} = 1.63$), as one rat with the weakest asymmetry in the front limbs failed to follow this trend. These results suggest that amplifying stimulation disrupts the regulation of stand times during individual runs. When you consider that fast bounding behaviour requires highly synchronous limb activity to reach high speeds, it is entirely possible that amplifying stimulation reduced the amount of bounding in this study by impairing interlimb coordination.

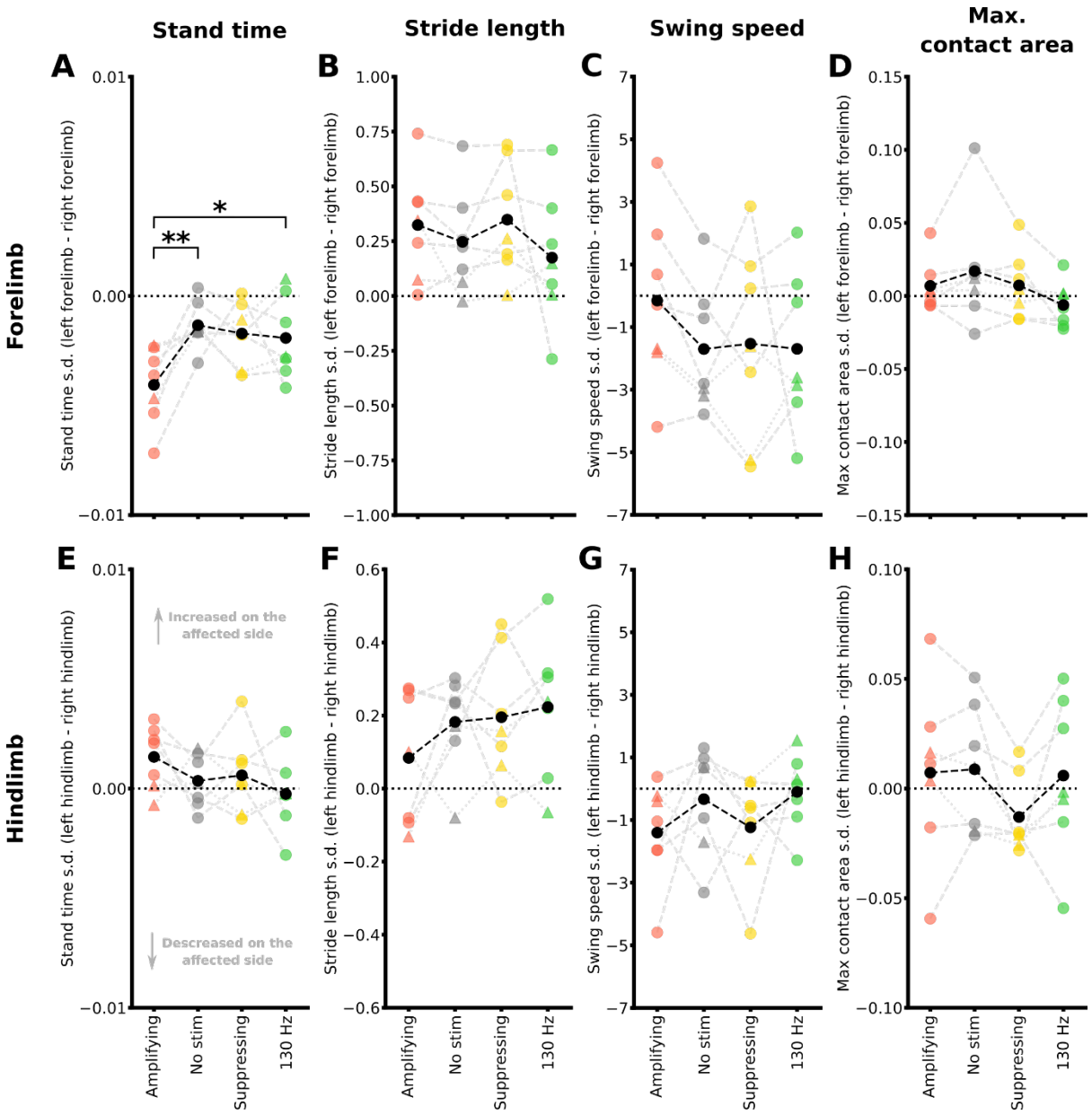


Figure 5-10: Effect of stimulation on within-run variance

The effect of stimulation on within run variance of individual characteristics of the step cycle (columns) were analysed for each paw (rows). Deficits in the stand time (A, E), stride length (B, F), swing speed (C, G), and maximum contact area (D, H) were restricted to the affected left side of the body due to the unilateral 6-OHDA lesion. The difference in standard deviation between the affected and unaffected side were calculated for both front- and hind-limbs, thus positive values indicate greater variance on the affected left side. Only stand time variance was significantly affected by stimulation ($p = 0.01$, one-way repeated measures ANOVA, $F_{3, 18} = 5.05$), with amplifying stimulation reducing variance on the affected left side when compared to no stimulation ($p = 0.007$, paired t-test, $t_6 = -4.05$) and 130 Hz stimulation ($p = 0.04$, paired t-test, $t_6 = -2.66$).

5.3 Discussion

In this chapter, we modulate ongoing cortical beta activity while concurrently assessing motor performance in parkinsonian rats. Unilateral dopamine depletion produced deficits in both spontaneous paw use during the cylinder task and gait asymmetry during the *CatWalk*. The main finding here is that phase-locked stimulation impairs motor performance when delivered at amplifying phases. More specifically, it altered the amount of bounding performed by each rat, which is essential for reaching high speeds on the *CatWalk*. Despite producing similar patterns of activity, stimulation targeting the suppressing phase had no effect on average speed or bounding, confirming that the impairments in gait observed here were phase specific. This result provides new evidence for the functional role of cortical beta oscillations in natural walking, and is in line with previous human data linking increased beta activity with impaired motor performance in humans (Chen et al., 2007; Kühn et al., 2008; Pogosyan et al., 2009; Tinkhauser et al., 2017a; Torrecillos et al., 2019).

The reduction in average speed produced by phase-locked amplifying stimulation was not explained by changes in stand time, swing speed, or stride length when normalised against the unaffected side, but was instead driven by changes in running style whereby fast bounding behaviour was reduced in favour of slow walking. We characterise ‘bounding’ as successive placements of both front paws followed by both hind paws, which when placed in synchrony produced runs of maximal speed. The ‘walking’ style is produced when one front paw is followed by the contralateral hind paw, it generates much slower speeds that require shorter strides and a more stable base of support (i.e. more paws contacting the floor at any one time). The

difference between both styles is highlighted by representative examples in Figure 5-6A, with the walking style (20 steps) requiring a much greater number of steps to cross the walkway in comparison to bounding (12 steps). Walking in this context can therefore be considered as parkinsonian in nature, as it is defined by both smaller and slower stepping. In addition to the impact on running style, we found that amplifying stimulation significantly altered stand time variance on the affected left side relative to the unaffected right, which may represent a disruption in interlimb coordination that is essential for bounding at high-speeds. Changes to stand time variance were not observed during 130 Hz stimulation that also significantly reduced speed when compared to suppressing stimulation, suggesting that this effect was specific to amplifying stimulation and not a secondary effect to changes in speed. There are relatively few rodent studies that have measured gait performance in any detail, but one such study also reported changes in running style after dopamine depletion that were accompanied by specific reductions in stand time (Baldwin et al., 2017). They used a unilateral MFB lesion however, meaning that average speeds were much slower than observed here (40 cm/s) and do not perfectly compare to the fast bounding we have characterised. Nevertheless, it supports our conclusion that changes in running style and stand time characterise the parkinsonian-like deficit produced by this model. Impaired coordination is also been observed in PD, where increased stride-to-stride variability in measures such as stride length and stride time are common, as are impairments in left-right stepping coordination (Plotnik & Hausdorff, 2008). Phase-locked amplifying stimulation therefore induced deficits in gait performance that are consistent with clinical observations in advanced PD.

What is the neural basis for this effect? Cortico-BG circuits are thought to be responsible for modulating central pattern generators in the brainstem that are critical

for locomotion (Roseberry et al., 2016). By amplifying beta activity in the motor cortex using GPe or STN stimulation, we are directly influencing information processing within and between structures thought to be responsible for the planning and scaling of movement (Nachev et al., 2008; Yttri & Dudman, 2016). Without directly recording cell activity from the structures involved, it is difficult to predict how this will manifest itself during locomotion in a quadrupedal rat. In humans, the effect of beta activity on locomotion is typically studied in patients with freezing of gait, where abnormal beta activity has been found during rest (Toledo et al., 2014), walking (Singh et al., 2013), and is predictive of freezing episodes (Chen et al., 2019). Beta burst amplitude and duration are increased in freezers compared to non-freezers, while reductions in both measures were observed in the freezing group during clinically effective DBS (Anidi et al., 2018). They also found that the difference in mean burst duration between the left and right STN correlated with the mean difference in stride times between legs, whereas no such association was observed between either STN and the absolute stride times in the contralateral limb. The authors suggest that bursting activity is critical for synchronising information between hemispheres that is critical for rhythmic walking. They predict that gait impairments in PD are driven by asymmetric beta bursting, which uncouples information routed through frontostriatal circuits. This hypothesis is supported by a wealth of evidence showing that gait asymmetry predicts freezing in PD (Peterson & Horak, 2016; Plotnik et al., 2005; Plotnik & Hausdorff, 2008). While we do not observe freezing behaviour in our study, this data provides a framework by which unilateral amplification of beta bursts in the motor network can produce gait asymmetry and impair performance.

If the deleterious effect of beta bursts on motor function explains reduced bounding during phase-locked amplifying stimulation, then why does beta suppression

not improve performance? It could simply be a matter of system performance, as amplifying stimulation produced larger more consistent beta-band modulation than suppressing stimulation. This was highlighted when quantifying the effect sizes produced during the open-loop playback experiments in chapter 2 (Figure 4-4), where amplifying stimulation over doubled the change produced by suppressing stimulation. While this may have contributed toward the lack of motor improvement, we speculate that suppressing stimulation failed to modulate behaviour due to the mildness of our lesion. The visible deficit observed in the left hindlimb during home cage exploration was a strong contributing factor in choosing the *CatWalk* as a primary output measure. This did not translate into a large deficit during goal-directed behaviour however, with rats averaging speeds of 67 cm/s. It is hard to quantify this lesion-induced deficit without implanted control animals, but one large scale *CatWalk* study using healthy untethered rats reported average speeds between 70 and 80 cm/s (Koopmans et al., 2007). Although not a perfect comparison due to differences in weight and age, we estimate that on average we saw a maximum speed deficit of no more than 15%, while deficits in the two rats that averaged over 80 cm/s were likely to be even smaller. In agreement with this prediction, differences between left and right performance in terms of stand time, swing speed, and stride length only averaged around 5%, while contact area produced the largest deficit at around 20%. A much stronger lesion is produced when injecting 6-OHDA into the MFB, with rats unable to produce the high speed bounding characterised here and only reaching average speeds of 40 cm/s (Boix et al., 2018; Baldwin et al., 2017). Taken together, this data suggests that our model failed to produced advanced parkinsonian like motor deficits and more closely resembled early-stage PD.

It is therefore unsurprising that suppressing stimulation was unable to recover motor deficits that were only mild to begin with. In this regard, it has been shown that behavioural recovery can occur in the weeks or months following a partial dopamine lesion that is potentially driven by compensatory changes in the remaining dopaminergic neurones (Robinson et al., 1994). *CatWalk* data was collected between 30 and 90 days post-lesion and it has been shown that dendritic arborisation, dopamine production, and dopamine hypersensitivity are all increased in mildly lesioned rats during this period (Blanchard et al., 1996; Robinson & Whishaw, 1988). When you consider the variability in cell loss produced by our lesion (as highlighted by example 2 in Figure 3-1), it is possible that compensation accounts for the anecdotal behavioural improvements observed here between lesion surgery and subsequent behavioural testing. It is also possible that our behavioural design aided motor performance through the use of sugar pellets, as reward-seeking behaviour is likely to differ from ambulatory behaviour in the home cage due to engagement of the mesolimbic pathway (Howe & Dombeck, 2016). It stands to reason that phase-locked suppressing stimulation and 130 Hz stimulation may produce behavioural improvement using the MFB injection protocol, which destroys all dopaminergic cells originating in the midbrain and may help to explain potential discrepancies across studies relating to arousal, motivation, and compensation.

From a clinical perspective, the effect of stimulation on motor performance and beta activity in early-stage PD remains unknown, due to the fact that only patients with advanced PD undergo DBS surgery. In this regard, DBS actually impairs performance in the unaffected limbs of patients with lateralised PD (Chen et al., 2006), which could explain why high frequency stimulation reduced speeds on the *CatWalk*. When you consider the detrimental performance of 130 Hz stimulation in this study – and the fact

that open-loop stimulation delivered at beta frequencies consistently produces motor deficits in humans (Chen et al., 2007, Pogosyan et al., 2009) – the fact suppressing stimulation did not impair motor performance is a finding in of itself. Finally, the subtlety of our manipulation in comparison to classic DBS should also be stressed when considering the lack of effect produced on the *CatWalk*. By suppressing beta oscillations in the cortex using subcortical stimulation we are disrupting the synchrony between structures in real time using extremely low-amplitude stimulation over long periods. It has been proposed that sustained bursts of beta activity are pathological in advanced PD (Tinkhauser et la., 2017a) and are responsible for gait impairment (Anidi et al., 2018). It is therefore possible that the efficacy of our system was limited due to interacting mainly with shorter non-pathological bursts due to a mild lesion. In order to capture the effect of this approach in our model, it may be necessary to correlate system performance to specific measures on a run-by-run or even step-by-step basis.

If the effect of suppressing stimulation (and potentially 130 Hz) was limited on the *CatWalk* due to small measurable deficits in gait performance, then the opposite should hold true for the cylinder test, where strong reductions in contralateral paw use were observed following dopamine depletion (approximately one contralateral touch in ten). Several studies report that high frequency stimulation reverses paw use asymmetry during the cylinder task in unilaterally lesion rats (Dorval & Grill, 2014; Mottaghi et al., 2020; Shi et al., 2004). We report no change in contralateral paw use however, which may be unsurprising considering that 130 Hz stimulation failed to suppress beta oscillations in this study, and is in line with the lack of evidence supporting DBS efficacy when targeting the GPe in humans. There are also several methodological reasons that may explain why high frequency stimulation failed to restore forelimb symmetry. Firstly, the cylinder test provides a low resolution measure

of motor impairment when the number of overall touches is extremely low, meaning that small improvements in paw use would fail to be registered. For instance, a 10% improvement may equate to under one paw contact if the total number of touches is below 10. This becomes a significant problem as exploration is reduced by repeat testing. Previous studies that delivered high frequency stimulation during the cylinder test have reported around 20% improvements in paw use, which may only equate to a couple of extra contacts in some animals (Dorval & Grill, 2014; Mottaghi et al., 2020). Secondly, the amplitudes used to obtain these improvements were much greater than those used here. Both of the above studies chose the highest amplitude possible that did not induce dyskinetic side effects, which in some instances meant stimulating as high at 400 μA. Another study that produced a remarkably strong reversal of asymmetry (around 50%), increased stimulation from 50 to 200 μA until an anti-asymmetric deficit was produced (Shi et al., 2004). For comparison, we used between 30 and 70 μA in order to match the charge density applied in humans. Finally, acute unilateral lesions are fundamentally not comparable to the chronic bilateral dopamine depletion seen in PD, and the lack of effect produced by stimulation might simply be due to poor behavioural translatability. One issue with motor deficits produced by unilateral lesions is that they are accompanied by severe sensory neglect, so much so that rats fail to retrieve easily accessible sugar pellets on the contralateral side when completing the corridor task (Dowd et al., 2005). This makes it difficult to tease apart sensory and motor deficits, which could lead to a 'learned' reduction in contralateral paw use that is resistant to stimulation therapy targeting the motor deficit. The fact that strong deficits during the cylinder test did not match the mild deficits produced on the *CatWalk*, could suggest that learned neglect-like deficits drive paw-use asymmetry during the cylinder test. There is also a motivational component to consider, as the

studies described above used an MFB lesion that completely destroys all fibres projecting from the midbrain, including those from the mesolimbic reward pathway. It is possible that some of restorative effect observed in the cylinder test is produced by changes in motivation that are not present when restricting the lesion to the SNc only.

While stimulation amplitude may primarily explain the inefficacy of high frequency stimulation on spontaneous paw use, it does not explain the inefficacy of supressing phase-locked stimulation that was strong enough to reduce beta power in the cortex. One potential reason for this is that simple locomotion is not thought to be under cortical control. For instance, basic patterns of rhythmic locomotion can be generated by the spinal cord alone (Grillner & Zangger, 1979), and locomotor speed is governed by activity in the brainstem (Caggiano et al., 2018; Capelli et al., 2017; Roseberry et al., 2016). Moreover, the cerebellum is thought to be responsible for inter-limb coordination and damage to this structure produces marked locomotor deficits that are not present even when you lesion large areas of cortex (Darmohray et al., 2019; Machado et al., 2015). It is therefore entirely possible for phase-locked stimulation to successfully manipulate information routed through the basal ganglia as intended, but still have little to no effect on locomotion.

Although activity in the cortex predicts network-wide beta synchronisation in rodents and humans (Cagnan et al., 2019b), it is possible that exaggerated beta oscillations in the cortex do not directly contribute toward motor impairment, which has been suggested by a recent optogenetic study that found inhibiting cortical activity did not impact beta oscillations in other parts of the network (Crompe et al., 2020). Despite evidence reporting task-dependent fluctuations in cortical beta-band activity in rodents, power has been shown to increase (Brazhnik et al., 2012), decrease (Polar

et al., 2018), or not change during movement (Leventhal et al., 2012). Nor does it consistently correlate with motor impairment, with one study reporting a strong correlation across several behavioural measures (Mottaghi et al., 2020) and others not (Haumesser et al., 2021). Similarly, changes in absolute cortical power did not predict DBS-induced improvements in gait (Polar et al., 2018), which reflects similar findings in patients (de Hemptinne et al., 2015). The use of cortical beta power as a proxy of stimulation efficacy may therefore not have been optimal, and it may be necessary to utilise alternative network-state measures such as phase amplitude coupling, which has been shown to strongly correlate with motor improvement in PD (de Hemptinne et al., 2013, 2015).

Having said this, the idea that either the cortex or cortical beta do not contribute towards gait deficits in PD does not fit with the clear reductions in average speed produced by amplifying stimulation in this study. Comparable findings to our own have recently been published using closed-loop stimulation to modulate cortical beta activity (Peles et al., 2020). To do so, they trained monkeys to increase beta power in the cortex to initiate reaching trials, the amount of which correlated with reaction time and task success. Interestingly, they report that only suppressing beta activity post-trial initiation modulates behaviour and is therefore the opposite to that achieved here using amplifying stimulation. The self-induced beta activity produced in order to initiate a trial was much larger than under physiological conditions, meaning that phase-locked stimulation was only delivered during periods of extremely high power, which may explain why amplifying stimulation failed to have an effect. When combining this data with our own, it is tempting to conclude that beta activity has both an upper (Peles et al. 2020) and lower limit (our data), at which points the behavioural effect becomes saturated. While further study is needed to address the failure of suppressing

stimulation to improve motor function in this study, the phase-dependent impairments in gait produced by amplifying stimulation provides evidence for the functional role of beta oscillations in PD and supports the development of phase-locked technology in humans.

6 General discussion

Normal brain function is associated with an assortment of oscillations of various frequencies, each reflecting the timing of separate computational processes and levels of synchronisation within and between brain areas (Fries, 2005). The ability to stimulate at a specific phase of a specific oscillation therefore provides an opportunity to interact with a specific functional process in real time. To achieve this, we developed a highly responsive system that provides continuous online phase estimation, which we utilised here in dopamine depleted rats to target the exaggerated beta-band oscillations thought to underlie motor impairment in PD (Brittain et al., 2014). We first performed necessary proof-of-principle studies *in vivo* to characterise our system in terms of accuracy, efficacy, and reliability (Chapters 1 and 2); before using this technology to enhance or disrupt beta-band oscillations in parkinsonian rats undergoing motor assessment (Chapter 3). Our main findings were:

- Dopamine depletion produced a robust spectral beta peak centred at 35 Hz.

- Using our system, sixty percent of stimulation pulses arrived within a quarter cycle of the intended phase (calculated post-hoc) when targeting beta-band oscillations.

- The accuracy of our system was unaffected by artifacts produced using electrical stimulation.

- GPe or STN stimulation phase-locked to ongoing cortical beta oscillations modulated cortical beta power in a bidirectional manner.

- GPe stimulation phase-locked to just after the peak amplified beta activity in most cases, while stimulation locked to just after the trough suppressed it.

- Stimulation output was altered by the modulation in the brain it itself produced. Thus, the combined brain and electronic system entered into a stable state equilibrium determined by target phase.

- Closed-loop activity patterns amplified beta power when delivered open-loop irrespective of target phase, suggesting that consistent phase-locking is essential for suppressing oscillations.

- Phase-locked stimulation failed to significantly improve motor impairments in spontaneous paw use or gait when suppressing beta activity, but did produce reproducible deficits in the speed of locomotion when amplifying it.

The experimental findings detailed above support the development of phase-locked stimulation for academic and clinical uses, providing a powerful demonstration of it's accuracy and specificity in complex *in vivo* experiments. Importantly, phase-locked stimulation was able to strongly modulate the motor network despite using

relatively little current to stimulate well under once per cycle. We also provide evidence for the functional impact of such modulation, as stimulation targeting amplifying phases produced a consistent deficit in average speed that was driven by a change in running style. Since no such behavioural change was seen during suppressing stimulation, we conclude that these deficits were produced as a result of the phase-dependent amplification of endogenous beta activity.

6.1 Implications for academic research

Local field potentials provide a stable signal that represents pre-synaptic input to the target structure (Buzsáki et al., 2012). By modulating this signal as done here, we are able to modulate the information going to and coming from the target structure, which in a wider scientific context should allow for basic-science investigations into adaption, plasticity, and neural state changes. In this regard, one study has already produced robust long-lasting plasticity changes on a vast cortical network using rudimentary phase-locking (Zanos et al., 2018). Importantly, oscillations at different frequencies have been associated with an assortment of functional roles (Buzsáki et al., 2002; Buzsáki & Draguhn, 2004; Buzsáki & Wang, 2012; Engel & Fries, 2010; Fries, 2005) and are often used to segregate independent information arriving into the same node (Colgin et al., 2009). By being both frequency and phase specific, our system provides a unique strategy for targeting a specific functional process in real time without altering ongoing processes occurring in parallel, thus providing truly unrivalled specificity when it comes to manipulating neural networks *in vivo*.

The true potential of phase-locked stimulation may yet be realised in combination with an array of newly developed technologies. The most obvious of which is optogenetics, which uses light stimulation to selectively modulate genetically identifiable cell populations, and has revolutionised modern neuroscience (Grosenick et al., 2015). The current gold standard optogenetic manipulation is guided by behavioural cues, which is particularly useful when studying the deleterious effects produced by silencing an entire population. Being able to enhance oscillatory amplitude is equally important, and is currently achieved by continuously driving the network at specific frequencies based on prior literature. In the context of PD, studies using patterned light stimulation to drive the network at beta frequencies have been able to delineate the contributions of BG nuclei in propagating such activity (Crompe et al., 2020). This approach is likely to alter overall neuronal excitability however, and does not reflect the transient nature of the activity it seeks to recreate (Cagnan et al., 2019b). Combining optogenetic stimulation with phase-tracking technology will allow input to be guided using real-time readouts of network activity, thus modulating specific population of neurones only when they are physiologically active. It would also overcome several limitations produced when using electrical stimulation, which was only used here to match conventional DBS treatment. In particular, light stimulation would have the immediate advantage of not producing off-target modulation in neurones close to the stimulation site; nor would it generate a large stimulus artifact making phase-tracking easier and potentially allowing for a simplified study design that utilises a single input and output channel (Zhang et al., 2009).

Investigations into the role of oscillations in neural computations have been limited by the lack of tools that specifically target network synchrony over other parameters of neural activity. The combination of both optogenetics with real time

phase-tracking is particularly appealing as it provides greater specificity than either technology does on its own, allowing researchers to modulate neural synchrony without affecting firing rate (Kanta et al., 2019; Nicholson et al., 2018). The ability to manipulate specific neural process in real time has obvious wide ranging applications, and has the potential to provide genuine insight and impact across the field of neuroscience in future. In this regard, the data presented here adds to an increasing amount of evidence accumulated using some form of phase-locked stimulation, all of which support the functional significance of oscillations in a wide range of behavioural settings (Kanta et al., 2019; Siegle & Wilson, 2014; Peles et al., 2020).

6.2 Implications for Parkinson's disease

Vast amounts of associative evidence suggests that exaggerated oscillations in the beta-band contribute to motor impairment in PD (Stein & Bar-Gad, 2013). If this does indeed reflect causality, the clinical impact of phase-tracking technology is clear, as we were able to suppress beta activity in real time by stimulating well under once per cycle using very little current. The specificity of this intervention should mean that it improves upon classic high frequency stimulation delivered either continuously (Follet et al., 2010) or when triggered by absolute beta power (Little et al., 2013). Our approach would also have the substantial benefit of hugely limiting electrical input to the brain, thus reducing side effects such as speech intelligibility (Tripoliti et al., 2011) and cognitive impairment (Hershey et al., 2004; Jahanshahi et al., 2000, 2013), which are presumably driven by off-target activation that is unavoidable when continuously delivering large amounts of current. Reducing stimulation input would also lower the

cost and risk associated with multiple surgeries by increasing the battery life of each device.

The results in chapters one and two confirm the efficacy, reliability, and safety of phase-locked stimulation *in vivo.* Our system produced remarkable consistency across all rats when suppressing beta activity, suggesting the effect is resistant to differences in electrode placement, behavioural state, and spectral profile. A recent study showed that similar modulation can be achieved in MPTP monkeys, which used beta activity in the STN to trigger phase-locked stimulation in the GPi (Sanabria et al., 2020). Beta activity in primates is typically lower than that seen in humans (8-15 Hz) and bursts of activity can last up to several seconds (Deffains et al., 2018), which is substantially longer than those recorded in both humans and rodents (Cagnan et al., 2019b). When taken with our own data, this study suggests that phase-locked stimulation can robustly modulate beta frequency oscillations across a wide range of spatial, spectral, and temporal parameters that encompass those described by patients. It is equally important from a clinical perspective that the effects of phase-locked stimulation are reproducible over long periods of time. Although we only report the effects of stimulation over short time periods here (~5 minutes), comparable beta suppression could be achieved across recording sessions separated by several weeks or even months. The time between each recording session varied between rats and in some instances the phase of maximal suppression moved up to $1/8^{th}$ of a cycle, suggesting it may be necessary to allow users to control target phase within a restricted window to maximise treatment benefit over long periods. The importance of reliability cannot be overstated, as amplifying pathological activity could worsen symptoms, and future studies utilising our system in a more systematic way over long periods are needed to address such issues. System reliability may be the deciding

factor in whether or not phase-locked stimulation is applied in several clinical fields. For instance, fluctuations in medications can lead to dyskinesias, postural instability, and falls in PD; the latter of which has particularly high morbidity (Balash et al., 2005; Hely et al., 2005). While the exciting potential of closed-loop stimulation in epilepsy is evident in both humans (Jobst et al., 2017) and rodents (Krook-Magnuson et al., 2014; Paz et al., 2013), but also comes with increased risk of severe side effects if inaccurate phase-tracking produced erroneous amplification of pathological activity. The results produced here are encouraging however, and suggest that our phase-tracking system performs with the required efficacy and reliability to be considered for study in humans.

The results in chapter three provide evidence for the functional importance of beta oscillations in locomotion. In particular, a phase-dependent reduction in average speed was produced on the *CatWalk* when targeting amplifying phases that was not present when targeting suppressing phases. Changes in speed were driven by reduced bounding in favour of a slower walking style, which in this context reflects a parkinsonian motor state with both smaller and slower steps. Phase-locked stimulation failed to recover locomotor deficits however, which most likely reflects the small baseline deficit produced by our dopamine lesion on the *CatWalk*. Performance in the cylinder task was unresponsive to stimulation and questions remain as to which behavioural task best represents a translatable motor deficit in 6-OHDA rats. Considering the efficacy and reliability of our system from an electrophysiological standpoint, and the challenges associated with producing a parkinsonian-like state in rodents, the next logical step is for phase-locked stimulation to be tested in humans. In this regard, implementation of closed-loop strategies is becoming increasingly tractable given the emerging generation of medical devices that can both sense and stimulate (Cagnan et al., 2019a). Our approach offers a number of attractive features

making it ideal for incorporation into future devices. First and foremost, it requires minimal computational resources to provide near instantaneous phase estimation, leaving additional computational resources free. This means it could be used in combination with other potential closed-loop systems that provide complimentary information such as behavioural state. Secondly, it has the potential to be extremely flexible and, while not demonstrated here, can operate at centre frequencies spanning the full range relevant in neuroscience (4 to 250 Hz). In our experience the phase of optimal suppression was broadly similar across subjects but varied enough to warrant individual tuning sessions for each rat. The flexibility to chose a target phase and frequency is unique to our system, providing a significant advantage over competing designs (Kanta et al., 2019), and may be important when optimising therapy in a clinical setting that targets a heterogeneous population. With this point in mind, it would be possible in future iterations of the system to also target multiple frequency peaks or a single moving peak, making it well suited to adapt to the need of individual patients.

While it is clear there is still work to be done before phase-locked stimulation is ready to be implemented on larger scales, not least proving its efficacy in patients, the work here provides proof-of-principle evidence of its efficacy in parkinsonian rats. In summary, we were able to consistently suppress cortical beta-band oscillations in real-time using low amplitude phase-locked subcortical stimulation. The success of this technology in a clinical setting obviously relies on a causal relationship being established between beta oscillations and motor impairment, which we were unable to establish here despite modulating behaviour in a phase-dependent manner. Nevertheless, a wealth of studies over the past two decades have clearly linked exaggerated beta activity with PD symptoms (Stein & Bar-Gad, 2013), and our phase-

tracking system provides a tool with which to finally realise the therapeutic potential of this large body of work.

6.3 Future directions

The inconclusive findings produced when suppressing beta activity highlights the difficulties associated with monitoring network and behavioural changes during phase-locked stimulation. As with the combination of phase-tracking and optogenetics technologies, utilising our system alongside new video analysis tools will help overcome these challenges in future studies. When you consider that oscillations typically fluctuate rapidly in a task dependent manner, it is likely that behavioural output will need to be assessed with high temporal resolution. In terms of PD, beta modulation is typically locked to individual limb movements, meaning that motor performance will need to be assessed on a movement-by-movement basis (Torrecillos et al., 2018). Open-source visual processing software such as *DeepLabCut* has recently been developed, making it both easy and accessible to autonomously track extremely fine-scale movements during concurrent electrophysiology (Mathis et al., 2018). Such technology provides much greater resolution, flexibility, and analytical insight, than either the *CatWalk* or cylinder assessments provided in this study. For example, it is now possible to accurately track reaching dynamics using only a relatively inexpensive camera, meaning that reach or grasp trajectories can now be quantified automatically. This simple task would negate confounding effects such as neglect and motivation, which are typically ignored when studying behaviour in 6-OHDA lesioned rats, while also measuring translatable deficits in reaction time and

fine motor control. Technologies such as *DeepLabCut* provide exciting new opportunities to test translatable motor impairments that were not readily available at the beginning of this project, and could be critical in unlocking the nuanced role of oscillations in coordinating BG activity.

Finally, it is important to recognise the necessity of recording action potential activity from single neurons during phase-locked stimulation in future studies. Action potentials report the ground truth impact of phase-locked stimulation and make it possible to properly assess the scale of synchronisation produced by modulating beta activity. We made a number of predictions in chapter 1 with regards to the underlying mechanism by which phase-locked stimulation reduced cortical beta power. The common denominator in these predictions was the population of prototypic pallidal cells, which form reciprocal connections both upstream to the striatum and downstream to the STN (Mallet et al., 2012). Both of these feedback loops have been implicated in pathological generation of beta oscillations in PD (Corbit et al., 2016, Crompe et al., 2020). By recording spiking activity in each of these structures we can start to tease apart the potential contributions of each population on beta activity in the motor network. But how best to achieve this? Vast technological advancements have been made in recording equipment over the past decade, making it possible to record from over 500 neurones simultaneously in awake rodents using Neuropixel probes (Jun et al., 2017). While technology such as this provides exciting potential for probing network dynamics, it currently has limitations in targeting multiple brain structures in freely moving rodents. To such an end, we developed a 3D-printable drive in-house that can record from up to 32 tetrodes across the motor network, which we used to record extensively from two freely moving rats during phase-locked stimulation. We will use this large data set (in terms of cells if not animals) to determine if spectral

changes in the ECoG are reflected in the oscillatory properties of specific cell populations throughout the motor network. In this regard, one interesting aspect of stimulation when targeting the suppressing phase is that it can produce peaks of spectral activity on either side of the centre frequency where suppression is greatest. Single unit activity will be able to resolve the importance of these peaks and help provide insight into how to best quantify the effects of supressing beta activity, thus helping to optimise stimulation in future experiments.

6.4 Concluding remarks

Here, we developed and validated a novel system for accurately tracking oscillatory phase in real time, which can be used to drive electrical or optogenetic stimulation in a wide range of experimental settings. We utilised this approach to stimulate at specific phases of ongoing beta activity in parkinsonian rats, allowing us to invigorate or disrupt pathological activity as it occurred naturally within the brain, which led to phase-dependent changes in motor performance. More specifically, phase-dependent amplification of cortical beta power consistently reduced fast bounding behaviour in favour of a slower walking style, which reflected a parkinsonian-like motor deficit in this context. Phase-locked suppressing stimulation had no such effect however, suggesting that gait impairments were the result of phase-dependent amplification of endogenous beta activity. These findings support the functional role of beta oscillations in locomotion and provide justification for the development of phased-locked stimulation in PD. In this regard, our system performed with remarkable consistency, producing reliable beta-band modulation in a relatively large cohort of animals that could be replicated across sessions. This is incredibly important from a

clinical perspective where any future treatment must provide long-term benefits to a heterogenous patient group. Considering the efficacy of our system *in vivo* and the complexity of modelling behavioural deficits in rodents, the logical next step is for phase-locked suppressing stimulation to be tested in PD patients, where its therapeutic potential can be assessed more definitively.

In addition to its clear translational utility in PD, implementation of phase-locked stimulation also has wide-ranging implications and applications in fundamental science; where there has been a cultural shift over the past decade toward celebrating tool development, borne from recognition that the greatest advancements in scientific understanding are typically driven by new technologies. This has resulted in the formation of funding bodies such as the BRAIN initiative (*braininitiative.nih.gov*), who are promoting tool development and their dissemination in the wider scientific community. In this regard, phase-tracking technology has the potential to revolutionise how oscillations are studied in neuroscience and is beginning to provide insight into how, or indeed whether, oscillations contribute toward computation (Kanta et al., 2019; Nicholson et al., 2018; Peles et al., 2020; Siegle and Wilson, 2014; Zanos et al., 2018). The system developed here is the most sophisticated design to date, allowing for more accurate phase-tracking that can target phases across the entire cycle of the target oscillation. Furthermore, it maintained this accuracy across successive cycles of an oscillation that waxes and wanes naturally over time while also delivering stimulation. The ability of our system to utilise phase and frequency input signals from one area to control the timing of stimulation or inhibition to another part of the network over a range of timescales presents an unprecedented opportunity to define the role of neuronal oscillations across different systems.

7 References

Abdi, A., Mallet, N., Mohamed, F.Y., Sharott, A., Dodson, P.D., Nakamura, K.C., Suri, S., Avery, S. v., Larvin, J.T., Garas, F.N., Garas, S.N., Vinciati, F., Morin, S., Bezard, E., Baufreton, J., Magill, P.J., 2015. Prototypic and arkypallidal neurons in the dopamine-intact external globus pallidus. Journal of Neuroscience 35, 6667–6688.

Albin, R.L., Young, A.B., Penney, J.B., 1989. The functional anatomy of basal ganglia disorders. Trends in Neurosciences 12, 366–375.

Alexander, G.E., DeLong, M.R., Strick, P.L., 1986. Parallel Organization of Functionally Segregated Circuits Linking Basal Ganglia and Cortex. Annual Review of Neuroscience 9, 357–381.

Andy, O.J., 1983. Thalamic stimulation for control of movement disorders. Applied Neurophysiology 46, 107–111.

Anidi, C., O'Day, J.J., Anderson, R.W., Afzal, M.F., Syrkin-Nikolau, J., Velisar, A., Bronte-Stewart, H.M., 2018. Neuromodulation targets pathological not physiological beta bursts during gait in Parkinson's disease. Neurobiology of Disease 120, 107–117.

Appleby, B.S., Duggan, P.S., Regenberg, A., Rabins, P. v., 2007. Psychiatric and neuropsychiatric adverse events associated with deep brain stimulation: A meta-analysis of ten years' experience. Movement Disorders 22, 1722–1728.

Arbuthnott, G.W., Wickens, J., 2007. Space, time and dopamine. Trends in Neurosciences 30(2), pp.62-69.

Avila, I., Parr-Brownlie, L.C., Brazhnik, E., Castañeda, E., Bergstrom, D.A., Walters, J.R., 2010. Beta frequency synchronization in basal ganglia output during rest and walk in a hemiparkinsonian rat. Experimental Neurology 221, 307–319.

Baaske, M., Kormann, E., Holt, A., Gulberti, A., McNamara, C., Poetter-Nerger, M., Westphal, M., Engel, A., Hamel, W., Brown, P., Moll, C., Sharott, A., 2019. Parkinson's disease uncovers an underlying sensitivity of subthalamic nucleus neurons to beta-frequency cortical input. bioRxiv 513234.

Baker, K.B., Zhang, J., Vitek, J.L., 2011. Pallidal stimulation: Effect of pattern and rate on bradykinesia in the non-human primate model of Parkinson's disease. Experimental Neurology 231, 309–313.

Baker, S.N., Olivier, E., Lemon, R.N., 1997. Coherent oscillations in monkey motor cortex and hand muscle EMG show task-dependent modulation. Journal of Physiology 501, 225–241.

Baker, S.N., Pinches, E.M., Lemon, R.N., 2003. Synchronization in monkey motor cortex during a precision grip task. II. Effect of oscillatory activity on corticospinal output. Journal of Neurophysiology 89, 1941–1953.

Balash, Y., Peretz, C., Leibovich, G., Herman, T., Hausdorff, J.M., Giladi, N., 2005. Falls in outpatients with Parkinson's disease: Frequency, impact and identifying factors. Journal of Neurology 252, 1310–1315.

Baldwin, H.A., Koivula, P.P., Necarsulmer, J.C., Whitaker, K.W., Harvey, B.K., 2017. Step sequence is a critical gait parameter of unilateral 6-OHDA Parkinson's rat models. Cell Transplantation 26, 659–667.

Barbera, G., Liang, B., Zhang, L., Gerfen, C.R., Culurciello, E., Chen, R., Li, Y., Lin, D.T., 2016. Spatially Compact Neural Clusters in the Dorsal Striatum Encode Locomotion Relevant Information. Neuron 92, 202–213.

Baron, M.S., Vitek, J.L., Bakay, R.A.E., Green, J., Kaneoke, Y., Hashimoto, T., Turner, R.S., Woodard, J.L., Cole, S.A., McDonald, W.M., DeLong, M.R., 1996. Treatment of advanced Parkinson's disease by posterior GPi pallidotomy: 1-Year results of a pilot study. Annals of Neurology 40, 355–366.

Benabid, A.L., Koudsié, A., Benazzouz, A., Vercueil, L., Fraix, V., Chabardes, S., LeBas, J.F., Pollak, P., 2001. Deep brain stimulation of the corpus luysi (subthalamic nucleus) and other targets in Parkinson's disease. Extension to new indications such as dystonia and epilepsy. In: Journal of Neurology, Supplement. D. Steinkopff-Verlag, pp. 37–47.

Benazzouz, A., Gross, C., Féger, J., Boraud, T., Bioulac, B., 1993. Reversal of Rigidity and Improvement in Motor Performance by Subthalamic High-frequency Stimulation in MPTP-treated Monkeys. European Journal of Neuroscience 5, 382–389.

Bergman, H., Feingold, A., Nini, A., Raz, A., Slovin, H., Abeles, M., Vaadia, E., 1998. Physiological aspects of information processing in the basal ganglia of normal and parkinsonian primates. Trends in Neurosciences 21, 32–38.

Bergman, H., Wichmann, T., DeLong, M.R., 1990. Reversal of experimental parkinsonism by lesions of the subthalamic nucleus. Science 249, 1436–1438.

Bergman, H., Wichmann, T., Karmon, B., DeLong, M.R., 1994. The primate subthalamic nucleus. II. Neuronal activity in the MPTP model of parkinsonism. Journal of Neurophysiology 72, 507–520.

Bertler, Å., Rosengren, E., 1959. Occurrence and distribution of dopamine in brain and other tissues. Experientia 15, 10–11.

Bertran-Gonzalez, J., Bosch, C., Maroteaux, M., Matamales, M., Hervé, D., Valjent, E., Girault, J.A., 2008. Opposing patterns of signaling activation in dopamine D1 and D2 receptor-expressing striatal neurons in response to cocaine and haloperidol. Journal of Neuroscience 28, 5671–5685.

Bevan, M.D., 1998. Selective innervation of neostriatal interneurons by a subclass of neuron in the globus pallidus of the rat. Journal of Neuroscience 18, 9438–9452.

Blanchard, V., Anglade, P., Dziewczapolski, G., Savasta, M., Agid, Y., Raisman-Vozari, R., 1996. Dopaminergic sprouting in the rat striatum after partial lesion of the substantia nigra. Brain Research 709, 319–325.

Blin, O., Ferrandez, A.M., Serratrice, G., 1990. Quantitative analysis of gait in Parkinson patients: increased variability of stride length. Journal of the Neurological Sciences 98, 91–97.

Boix, J., von Hieber, D., Connor, B., 2018. Gait Analysis for Early Detection of Motor Symptoms in the 6-OHDA Rat Model of Parkinson's Disease. Frontiers in Behavioral Neuroscience 12, 39.

Boraud, T., Bezard, E., Guehl, D., Bioulac, B., Gross, C., 1998. Effects of L-DOPA on neuronal activity of the globus pallidus externalis (GPe) and globus pallidus internalis (GPi) in the MPTP-treated monkey. Brain Research 787, 157–160.

Boyden, E.S., Zhang, F., Bamberg, E., Nagel, G., Deisseroth, K., 2005. Millisecond-timescale, genetically targeted optical control of neural activity. Nature Neuroscience 8, 1263–1268.

Brazhnik, E., Cruz, A. v., Avila, I., Wahba, M.I., Novikov, N., Ilieva, N.M., McCoy, A.J., Gerber, C., Walters, J.R., 2012. State-dependent spike and local field synchronization between motor cortex and substantia nigra in hemiparkinsonian rats. Journal of Neuroscience 32, 7869–7880.

Brittain, J.S., Probert-Smith, P., Aziz, T.Z., Brown, P., 2013. Tremor suppression by rhythmic transcranial current stimulation. Current Biology 23, 436–440.

Brittain, J.-S., Sharott, A., Brown, P., 2014. The highs and lows of beta activity in cortico-basal ganglia loops. European Journal of Neuroscience 39, 1951–1959.

Brown, P., 2003. Oscillatory nature of human basal ganglia activity: Relationship to the pathophysiology of parkinson's disease. Movement Disorders 18(4), pp.357-363.

Brown, P., Oliviero, A., Mazzone, P., Insola, A., Tonali, P., di Lazzaro, V., 2001. Dopamine dependency of oscillations between subthalamic nucleus and pallidum in Parkinson's disease. Journal of Neuroscience 21, 1033–1038.

Bunney, B.S., Aghajanian, G.K., 1976. The precise localization of nigral afferents in the rat as determined by a retrograde tracing technique. Brain Research 117, 423–435.

Buonamici, M., Maj, R., Pagani, F., Rossi, A.C., Khazan, N., 1986. Tremor at rest episodes in unilaterally 6-OHDA-induced substantia nigra lesioned rats: EEG-EMG and behavior. Neuropharmacology 25, 323–325.

Burns, R.S., Chiueh, C.C., Markey, S.P., Ebert, M.H., Jacobowitz, D.M., Kopin, I.J., 1983. A primate model of parkinsonism: Selective destruction of dopaminergic neurons in the pars compacta of the substantia nigra by N-methyl-4-phenyl-1,2,3,6-tetrahydropyridine. Proceedings of the National Academy of Sciences of the United States of America 80, 4546–4550.

Buzsáki, G., 2002. Theta oscillations in the hippocampus. Neuron 33(3), pp.325-340.

Buzsáki, G., Anastassiou, C.A., Koch, C., 2012. The origin of extracellular fields and currents-EEG, ECoG, LFP and spikes. Nature Reviews Neuroscience 13(6), pp.407-420.

Buzsáki, G., Draguhn, A., 2004. Neuronal olscillations in cortical networks. Science 304(5679), pp.1926-1929.

Buzsáki, G., Wang, X.-J., 2012. Mechanisms of Gamma Oscillations. Annual Review of Neuroscience 35, 203–225.

Caggiano, V., Leiras, R., Goñi-Erro, H., Masini, D., Bellardita, C., Bouvier, J., Caldeira, V., Fisone, G., Kiehn, O., 2018. Midbrain circuits that set locomotor speed and gait selection. Nature 553, 455–460.

Cagnan, H., Brittain, J.S., Little, S., Foltynie, T., Limousin, P., Zrinzo, L., Hariz, M., Joint, C., Fitzgerald, J., Green, A.L., Aziz, T., Brown, P., 2013. Phase dependent modulation of tremor amplitude in essential tremor through thalamic stimulation. Brain 136, 3062–3075.

Cagnan, H., Denison, T., McIntyre, C., Brown, P., 2019a. Emerging technologies for improved deep brain stimulation. Nature Biotechnology 37(9), pp.1024-1033.

Cagnan, H., Duff, E.P., Brown, P., 2015. The relative phases of basal ganglia activities dynamically shape effective connectivity in Parkinson's disease. Brain 138, 1667–1678.

Cagnan, H., Mallet, N., Moll, C.K.E., Gulberti, A., Holt, A.B., Westphal, M., Gerloff, C., Engel, A.K., Hamel, W., Magill, P.J., Brown, P., Sharott, A., 2019b. Temporal evolution of beta bursts in the parkinsonian cortical and basal ganglia network. Proceedings of the National Academy of Sciences of the United States of America 116, 16095–16104.

Cagnan, H., Pedrosa, D., Little, S., Pogosyan, A., Cheeran, B., Aziz, T., Green, A., Fitzgerald, J., Foltynie, T., Limousin, P., Zrinzo, L., Hariz, M., Friston, K.J., Denison, T., Brown, P., 2017. Stimulating at the right time: Phase-specific deep brain stimulation. Brain 140, 132–145.

Capelli, P., Pivetta, C., Esposito, M.S., Arber, S., 2017. Locomotor speed control circuits in the caudal brainstem. Nature 551, 373–377.

Cassidy, M., Mazzone, P., Oliviero, A., Insola, A., Tonali, P., di Lazzaro, V., Brown, P., 2002. Movement-related changes in synchronization in the human basal ganglia. Brain 125, 1235–1246.

Chan, V., Starr, P.A., Turner, R.S., 2011. Bursts and oscillations as independent properties of neural activity in the parkinsonian globus pallidus internus. Neurobiology of Disease 41, 2–10.

Chen, C.C., Brücke, C., Kempf, F., Kupsch, A., Lu, C.S., Lee, S.T., Tisch, S., Limousin, P., Hariz, M., Brown, P., 2006. Deep brain stimulation of the subthalamic nucleus: A two-edged sword. Current Biology 16(22), pp.R952-R953.

Chen, C.C., Litvak, V., Gilbertson, T., Kühn, A., Lu, C.S., Lee, S.T., Tsai, C.H., Tisch, S., Limousin, P., Hariz, M., Brown, P., 2007. Excessive synchronization of basal ganglia neurons at 20 Hz slows movement in Parkinson's disease. Experimental Neurology 205, 214–221.

Chen, C.C., Yeh, Chien Hung, Chan, H.L., Chang, Y.J., Tu, P.H., Yeh, Chih Hua, Lu, C.S., Fischer, P., Tinkhauser, G., Tan, H., Brown, P., 2019. Subthalamic nucleus oscillations correlate with vulnerability to freezing of gait in patients with Parkinson's disease. Neurobiology of Disease 132, 104605.

Chuang, C. sen, Su, H.L., Cheng, F.C., Hsu, S.H., Chuang, C.F., Liu, C.S., 2010. Quantitative evaluation of motor function before and after engraftment of dopaminergic neurons in a rat model of Parkinson's disease. Journal of Biomedical Science 17, 9.

Clarke, C.E., Sambrook, M.A., Mitchell, I.J., Crossman, A.R., 1987. Levodopa-induced dyskinesia and response fluctuations in primates rendered parkinsonian with 1-methyl-4-phenyl-1,2,3,6-tetrahydropyridine (MPTP). Journal of the Neurological Sciences 78, 273–280.

Cole, S.R., van der Meij, R., Peterson, E.J., de Hemptinne, C., Starr, P.A., Voytek, B., 2017. Nonsinusoidal beta oscillations reflect cortical pathophysiology in parkinson's disease. Journal of Neuroscience 37, 4830–4840.

Colgin, L.L., Denninger, T., Fyhn, M., Hafting, T., Bonnevie, T., Jensen, O., Moser, M.B., Moser, E.I., 2009. Frequency of gamma oscillations routes flow of information in the hippocampus. Nature 462, 353–357.

Connolly, A.T., Jensen, A.L., Bello, E.M., Netoff, T.I., Baker, K.B., Johnson, M.D., Vitek, J.L., 2015. Modulations in oscillatory frequency and coupling in globus pallidus with increasing Parkinsonian severity. Journal of Neuroscience 35, 6231–6240.

Constantoyannis, C., Kumar, A., Stoessl, A.J., Honey, C.R., 2004. Tremor induced by thalamic deep brain stimulation in patients with complex regional facial pain. Movement Disorders 19, 933–936.

Corbit, V.L., Whalen, T.C., Zitelli, K.T., Crilly, S.Y., Rubin, J.E., Gittis, A.H., 2016. Pallidostriatal projections promote β oscillations in a dopamine-depleted biophysical network model. Journal of Neuroscience 36, 5556–5571.

Courtemanche, R., Fujii, N., Graybiel, A.M., 2003. Synchronous, Focally Modulated β-Band Oscillations Characterize Local Field Potential Activity in the Striatum of Awake Behaving Monkeys. Journal of Neuroscience 23, 11741–11752.

Crompe, B. de la, Aristieta, A., Leblois, A., Elsherbiny, S., Boraud, T., Mallet, N.P., 2020. The globus pallidus orchestrates abnormal network dynamics in a model of Parkinsonism. Nature Communications 11, 1–14.

Cruz, A. v., Mallet, N., Magill, P.J., Brown, P., Averbeck, B.B., 2011. Effects of dopamine depletion on information flow between the subthalamic nucleus and external globus pallidus. Journal of Neurophysiology 106, 2012–2023.

Cui, G., Jun, S.B., Jin, X., Pham, M.D., Vogel, S.S., Lovinger, D.M., Costa, R.M., 2013. Concurrent activation of striatal direct and indirect pathways during action initiation. Nature 494, 238–242.

Darmohray, D.M., Jacobs, J.R., Marques, H.G., Carey, M.R., 2019. Spatial and Temporal Locomotor Learning in Mouse Cerebellum. Neuron 102, 217-231.e4.

Day, M., Wang, Z., Ding, J., An, X., Ingham, C.A., Shering, A.F., Wokosin, D., Ilijic, E., Sun, Z., Sampson, A.R., Mugnaini, E., Deutcch, A.Y., Sesack, S.R., Arbuthnott, G.W., Surmeier, D.J., 2006. Selective elimination of glutamatergic synapses on striatopallidal neurons in Parkinson disease models. Nature Neuroscience 9, 251–259.

de Hemptinne, C., Ryapolova-Webb, E.S., Air, E.L., Garcia, P.A., Miller, K.J., Ojemann, J.G., Ostrem, J.L., Galifianakis, N.B., Starr, P.A., 2013. Exaggerated phase-amplitude coupling in the primary motor cortex in Parkinson disease. Proceedings of the National Academy of Sciences of the United States of America 110, 4780–4785.

de Hemptinne, C., Swann, N.C., Ostrem, J.L., Ryapolova-Webb, E.S., San Luciano, M., Galifianakis, N.B., Starr, P.A., 2015. Therapeutic deep brain stimulation reduces cortical phase-amplitude coupling in Parkinson's disease. Nature Neuroscience 18, 779–786.

Deffains, M., Bergman, H., 2019. Parkinsonism-related β oscillations in the primate basal ganglia networks – Recent advances and clinical implications. Parkinsonism and Related Disorders 59, 2–8.

Deffains, M., Iskhakova, L., Katabi, S., Haber, S.N., Israel, Z., Bergman, H., 2016. Subthalamic, not striatal, activity correlates with basal ganglia downstream activity in normal and parkinsonian monkeys. eLife 5.

Deffains, M., Iskhakova, L., Katabi, S., Israel, Z., Bergman, H., 2018. Longer β oscillatory episodes reliably identify pathological subthalamic activity in Parkinsonism. Movement Disorders 33, 1609–1618.

Dejean, C., Hyland, B., Arbuthnott, G., 2009. Cortical effects of subthalamic stimulation correlate with behavioral recovery from dopamine antagonist induced akinesia. Cerebral Cortex 19, 1055–1063.

Delaville, C., McCoy, A.J., Gerber, C.M., Cruz, A. v., Walters, J.R., 2015. Subthalamic nucleus activity in the awake hemiparkinsonian rat: Relationships with motor and cognitive networks. Journal of Neuroscience 35, 6918–6930.

DeLong, M.R., 1971. Activity of pallidal neurons during movement. Journal of neurophysiology 34, 414–427.

DeLong, M.R., 1990. Primate models of movement disorders of basal ganglia origin. Trends in Neurosciences 13(7), pp.281-285.

Deumens, R., Blokland, A., Prickaerts, J., 2002. Modeling Parkinson's disease in rats: An evaluation of 6-OHDA lesions of the nigrostriatal pathway. Experimental Neurology 175(2), pp.303-317.

Devergnas, A., Caiola, M., Pittard, D., Wichmann, T., 2019. Cortical Phase-Amplitude Coupling in a Progressive Model of Parkinsonism in Nonhuman Primates. Cerebral Cortex 29, 167–177.

DiFiglia, M., Pasik, P., Pasik, T., 1976. A Golgi study of neuronal types in the neostriatum of monkeys. Brain Research 114, 245–256.

Dorsey, R.E., Elbaz, A., Nichols, E., Abd-Allah, F., Abdelalim, A., Adsuar, J.C., Ansha, M.G., Brayne, C., Choi, J.Y.J., Collado-Mateo, D., Dahodwala, N., Do, H.P., Edessa, D., Endres, M., Fereshtehnejad, S.M., Foreman, K.J., Gankpe, F.G., Gupta, R., Hankey, G.J., Hay, S.I., Hegazy, M.I., Hibstu, D.T., Kasaeian, A., Khader, Y., Khalil, I., Khang, Y.H., Kim, Y.J., Kokubo, Y., Logroscino, G., Massano, J., Ibrahim, N.M., Mohammed, M.A., Mohammadi, A., Moradi-Lakeh, M., Naghavi, M., Nguyen, B.T., Nirayo, Y.L., Ogbo, F.A., Owolabi, M.O., Pereira, D.M., Postma, M.J., Qorbani, M., Rahman, M.A., Roba, K.T., Safari, H., Safiri, S., Satpathy, M., Sawhney, M., Shafieesabet, A., Shiferaw, M.S., Smith, M., Szoeke, C.E.I., Tabarés-Seisdedos, R., Truong, N.T., Ukwaja, K.N., Venketasubramanian, N., Villafaina, S., Weldegwergs, K.G., Westerman, R., Wijeratne, T., Winkler, A.S., Xuan, B.T., Yonemoto, N., Feigin, V.L., Vos, T., Murray, C.J.L., 2018. Global, regional, and national burden of Parkinson's disease, 1990–2016: a systematic analysis for the Global Burden of Disease Study 2016. The Lancet Neurology 17, 939–953.

Dorval, A.D., Grill, W.M., 2014. Deep brain stimulation of the subthalamic nucleus reestablishes neuronal information transmission in the 6-OHDA rat model of parkinsonism. Journal of Neurophysiology 111, 1949–1959.

Dorval, A.D., Russo, G.S., Hashimoto, T., Xu, W., Grill, W.M., Vitek, J.L., 2008. Deep brain stimulation reduces neuronal entropy in the MPTP-primate model of Parkinson's disease. Journal of Neurophysiology 100, 2807–2818.

Dowd, E., Monville, C., Torres, E.M., Dunnett, S.B., 2005. The Corridor Task: A simple test of lateralised response selection sensitive to unilateral dopamine deafferentation and graft-derived dopamine replacement in the striatum. Brain Research Bulletin 68, 24–30.

Dupre, K.B., Cruz, A. v., McCoy, A.J., Delaville, C., Gerber, C.M., Eyring, K.W., Walters, J.R., 2016. Effects of L-dopa priming on cortical high beta and high gamma oscillatory activity in a rodent model of Parkinson's disease. Neurobiology of Disease 86, 1–15.

Durieux, P.F., Schiffmann, S.N., de Kerchove d'Exaerde, A., 2012. Differential regulation of motor control and response to dopaminergic drugs by D1R and D2R neurons in distinct dorsal striatum subregions. The EMBO Journal 31, 640–653.

Engel, A.K., Fries, P., 2010. Beta-band oscillations-signalling the status quo? Current Opinion in Neurobiology 20(2), pp.156-165.

Ermentrout, B., Pascal, M., Gutkin, B., 2001. The effects of spike frequency adaptation and negative feedback on the synchronization of neural oscillators. Neural Computation 13, 1285–1310.

Feingold, J., Gibson, D.J., Depasquale, B., Graybiel, A.M., 2015. Bursts of beta oscillation differentiate postperformance activity in the striatum and motor cortex of monkeys performing movement tasks. Proceedings of the National Academy of Sciences of the United States of America 112, 13687–13692.

Feldman, D.E., 2012. The Spike-Timing Dependence of Plasticity. Neuron. 75(4), pp.556-571.

Filali, M., Hutchison, W.D., Palter, V.N., Lozano, A.M., Dostrovsky, J.O., 2004. Stimulation-induced inhibition of neuronal firing in human subthalamic nucleus. Experimental Brain Research 156, 274–281.

Filion, M., Tremblay, L., 1991. Abnormal spontaneous activity of globus pallidus neurons in monkeys with MPTP-induced parkinsonism. Brain Research 547, 140–144.

Filion, M., Tremblay, L., Bédard, P.J., 1991. Effects of dopamine agonists on the spontaneous activity of globus pallidus neurons in monkeys with MPTP-induced parkinsonism. Brain Research 547, 145–149.

Follett, K.A., Weaver, F.M., Stern, M., Hur, K., Harris, C.L., Luo, P., Marks, W.J., Rothlind, J., Sagher, O., Moy, C., Pahwa, R., Burchiel, K., Hogarth, P., Lai, E.C., Duda, J.E., Holloway, K., Samii, A., Horn, S., Bronstein, J.M., Stoner, G., Starr, P.A., Simpson, R., Baltuch, G., de Salles, A., Huang, G.D., Reda, D.J., 2010. Pallidal versus Subthalamic Deep-Brain Stimulation for Parkinson's Disease. New England Journal of Medicine 362, 2077–2091.

Fox, C.A., Andrade, A.N., Hillman, D.E., Schwyn, R.C., 1971. The spiny neurons in the primate striatum: a Golgi and electron microscopic study. Journal fur Hirnforschung 13, 181–201.

Fraix, V., Pollak, P., Vercueil, L., Benabid, A.L., Mauguière, F., 2008. Effects of subthalamic nucleus stimulation on motor cortex excitability in Parkinson's disease. Clinical Neurophysiology 119, 2513–2518.

Frenkel-Toledo, S., Giladi, N., Peretz, C., Herman, T., Gruendlinger, L., Hausdorff, J.M., 2005. Treadmill walking as an external pacemaker to improve gait rhythm and stability in Parkinson's disease. Movement Disorders 20, 1109–1114.

Fries, P., 2005. A mechanism for cognitive dynamics: Neuronal communication through neuronal coherence. Trends in Cognitive Sciences 9, 474–480.

Fujiyama, F., Sohn, J., Nakano, T., Furuta, T., Nakamura, K.C., Matsuda, W., Kaneko, T., 2011a. Exclusive and common targets of neostriatofugal projections of rat striosome neurons: A single neuron-tracing study using a viral vector. European Journal of Neuroscience 33, 668–677.

Gardner, J., 2013. A history of deep brain stimulation: Technological innovation and the role of clinical assessment tools. Social Studies of Science 43, 707–728.

Ge, S., Yang, C., Li, M., Li, J., Chang, X., Fu, J., Chen, L., Chang, C., Wang, X., Zhu, J., Gao, G., 2012. Dopamine depletion increases the power and coherence of high-voltage spindles in the globus pallidus and motor cortex of freely moving rats. Brain Research 1465, 66–79.

Gerfen, C.R., 1992. The neostriatal mosaic: Multiple levels of compartmental organization in the basal ganglia. Annual Review of Neuroscience 15(1), pp.285-320.

Gerfen, C.R., Engber, T.M., Mahan, L.C., Susel, Z., Chase, T.N., Monsma, F.J., Sibley, D.R., 1990. D1 and D2 dopamine receptor-regulated gene expression of striatonigral and striatopallidal neurons. Science 250, 1429–1432.

Gerfen, C.R., Surmeier, D.J., 2011. Modulation of striatal projection systems by dopamine. Annual Review of Neuroscience 34, 441–466.

German, D.C., Manaye, K., Smith, W.K., Woodward, D.J., Saper, C.B., 1989. Midbrain dopaminergic cell loss in parkinson's disease: Computer visualization. Annals of Neurology 26, 507–514.

Gilbertson, T., Lalo, E., Doyle, L., di Lazzaro, V., Cioni, B., Brown, P., 2005. Existing motor state is favored at the expense of new movement during 13-35 Hz oscillatory synchrony in the human corticospinal system. Journal of Neuroscience 25, 7771–7779.

Girasole, A.E., Lum, M.Y., Nathaniel, D., Bair-Marshall, C.J., Guenthner, C.J., Luo, L., Kreitzer, A.C., Nelson, A.B., 2018. A Subpopulation of Striatal Neurons Mediates Levodopa-Induced Dyskinesia. Neuron 97, 787-795.e6.

Gittis, A.H., Hang, G.B., LaDow, E.S., Shoenfeld, L.R., Atallah, B. v., Finkbeiner, S., Kreitzer, A.C., 2011. Rapid target-specific remodeling of fast-spiking inhibitory circuits after loss of dopamine. Neuron 71, 858–868.

Gittis, A.H., Nelson, A.B., Thwin, M.T., Palop, J.J., Kreitzer, A.C., 2010. Distinct roles of GABAergic interneurons in the regulation of striatal output pathways. Journal of Neuroscience 30, 2223–2234.

Goldberg, J.A., Rokni, U., Boraud, T., Vaadia, E., Bergman, H., 2004. Spike synchronization in the cortex-basal ganglia networks of parkinsonian primates reflects global dynamics of the local field potentials. Journal of Neuroscience 24, 6003–6010.

Goldberg, J.H., Farries, M.A., Fee, M.S., 2012. Integration of cortical and pallidal inputs in the basal ganglia-recipient thalamus of singing birds. Journal of Neurophysiology 108, 1403–1429.

Goto, S., Hirano, A., Matsumoto, S., 1989. Subdivisional involvement of nigrostriatal loop in idiopathic parkinson's disease and striatonigral degeneration. Annals of Neurology 26, 766–770.

Grillner, S., Zangger, P., 1979. On the central generation of locomotion in the low spinal cat. Experimental Brain Research 34, 241–261.

Grosenick, L., Marshel, J.H., Deisseroth, K., 2015. Closed-loop and activity-guided optogenetic control. Neuron 86(1), pp.106-139.

Hammond, C., Bergman, H., Brown, P., 2007. Pathological synchronization in Parkinson's disease: networks, models and treatments. Trends in Neurosciences 30(7), pp.357-364.

Hariz, M.I., Rehncrona, S., Quinn, N.P., Speelman, J.D., Wensing, C., 2008. Multicenter study on deep brain stimulation in Parkinson's disease: An independent assessment of reported adverse events at 4 years. Movement Disorders 23, 416–421.

Hashimoto, T., Elder, C.M., Okun, M.S., Patrick, S.K., Vitek, J.L., 2003. Stimulation of the subthalamic nucleus changes the firing pattern of pallidal neurons. Journal of Neuroscience 23, 1916–1923.

Hasselmo, M.E., 2005. What is the function of hippocampal theta rhythm? - Linking bahavioral data to phasic properties of field potential and unit recording data. Hippocampus 15(7), pp.936-949.

Hasselmo, M.E., Bodelón, C., Wyble, B.P., 2002. A proposed function for hippocampal theta rhythm: Separate phases of encoding and retrieval enhance reversal of prior learning. Neural Computation 14, 793–817.

Hausdorff, J.M., Schaafsma, · J D, Balash, Y., Bartels, · A L, Gurevich, · T, Giladi, · N, 2003. Impaired regulation of stride variability in Parkinsons disease subjects with freezing of gait. Exp Brain Res 149, 187–194.

Heimer, G., Bar-Gad, I., Goldberg, J.A., Bergman, H., 2002. Dopamine replacement therapy reverses abnormal synchronization of pallidal neurons in the 1-methyl-4-phenyll-1,2,3,6-tetrahydropyridine primate model of parkinsonism. Journal of Neuroscience 22, 7850–7855.

Heimer, G., Rivlin-Etzion, M., Bar-Gad, I., Goldberg, J.A., Haber, S.N., Bergman, H., 2006. Dopamine replacement therapy does not restore the full spectrum of normal pallidal activity in the 1-methyl-4-phenyl-1,2,3,6-tetra-hydropyridine primate model of Parkinsonism. Journal of Neuroscience 26, 8101–8114.

Helmstaedter, C., 2007. Cognitive outcome of status epilepticus in adults. Epilepsia 48, 85–90.

Hely, M.A., Morris, J.G.L., Reid, W.G.J., Trafficante, R., 2005. Sydney Multicenter Study of Parkinson's disease: Non-L-dopa-responsive problems dominate at 15 years. Movement Disorders 20, 190–199.

Hershey, T., Revilla, F.J., Wernle, A., Gibson, P.S., Dowling, J.L., Perlmutter, J.S., 2004. Stimulation of STN impairs aspects of cognitive control in PD. Neurology 62, 1110–1114.

Holt, A.B., Kormann, E., Gulberti, A., Pötter-Nerger, M., McNamara, C.G., Cagnan, H., Baaske, M.K., Little, S., Köppen, J.A., Buhmann, C., Westphal, M., Gerloff, C., Engel, A.K., Brown, P., Hamel, W., Moll, C.K.E., Sharott, A., 2019. Phase-dependent suppression of beta oscillations in parkinson's disease patients. Journal of Neuroscience 39, 1119–1134.

Howe, M.W., Dombeck, D.A., 2016. Rapid signalling in distinct dopaminergic axons during locomotion and reward. Nature 535, 505–510.

Jahanshahi, M., 2013. Effects of deep brain stimulation of the subthalamic nucleus on inhibitory and executive control over prepotent responses in parkinson's disease. Frontiers in Systems Neuroscience 7.

Jahanshahi, M., Ardouin, C.M.A., Brown, R.G., Rothwell, J.C., Obeso, J., Albanese, A., Rodriguez-Oroz, M.C., Moro, E., Benabid, A.L., Pollak, P., Limousin-Dowsey, P., 2000. The impact of deep brain stimulation on executive function in Parkinson's disease. Brain 123, 1142–1154.

Jankovic, J., 2005. Motor fluctuations and dyskinesias in Parkinson's disease: Clinical manifestations. Movement Disorders 20, S11–S16.

Jobst, B.C., Kapur, R., Barkley, G.L., Bazil, C.W., Berg, M.J., Bergey, G.K., Boggs, J.G., Cash, S.S., Cole, A.J., Duchowny, M.S., Duckrow, R.B., Edwards, J.C., Eisenschenk, S., Fessler, A.J., Fountain, N.B., Geller, E.B., Goldman, A.M., Goodman, R.R., Gross, R.E., Gwinn, R.P., Heck, C., Herekar, A.A., Hirsch, L.J., King-Stephens, D., Labar, D.R., Marsh, W.R., Meador, K.J., Miller, I., Mizrahi, E.M., Murro, A.M., Nair, D.R., Noe, K.H., Olejniczak, P.W., Park, Y.D., Rutecki, P., Salanova, V., Sheth, R.D., Skidmore, C., Smith, M.C., Spencer, D.C., Srinivasan, S., Tatum, W., van Ness, P., Vossler, D.G., Wharen, R.E., Worrell, G.A., Yoshor, D., Zimmerman, R.S., Skarpaas, T.L., Morrell, M.J., 2017. Brain-responsive neurostimulation in patients with medically intractable seizures arising from eloquent and other neocortical areas. Epilepsia 58, 1005–1014.

Jun, J.J., Steinmetz, N.A., Siegle, J.H., Denman, D.J., Bauza, M., Barbarits, B., Lee, A.K., Anastassiou, C.A., Andrei, A., Aydin, Ç., Barbic, M., Blanche, T.J., Bonin, V., Couto, J., Dutta, B., Gratiy, S.L., Gutnisky, D.A., Häusser, M., Karsh, B., Ledochowitsch, P., Lopez, C.M., Mitelut, C., Musa, S., Okun, M., Pachitariu, M., Putzeys, J., Rich, P.D., Rossant, C., Sun, W.L., Svoboda, K., Carandini, M., Harris, K.D., Koch, C., O'Keefe, J., Harris, T.D., 2017. Fully integrated silicon probes for high-density recording of neural activity. Nature 551, 232–236.

Kanta, V., Pare, D., Headley, D.B., 2019. Closed-loop control of gamma oscillations in the amygdala demonstrates their role in spatial memory consolidation. Nature Communications 10, 1–14.

Kestenbaum, M., Ford, B., Louis, E.D., 2015. Estimating the Proportion of Essential Tremor and Parkinson's Disease Patients Undergoing Deep Brain Stimulation Surgery: Five-Year Data From Columbia University Medical Center (2009–2014). Movement Disorders Clinical Practice 2, 384–387.

Kilpatrick, M., Church, E., Danish, S., Stiefel, M., Jaggi, J., Halpern, C., Kerr, M., Maloney, E., Robinson, M., Lucki, I., Krizman-Grenda, E., Baltuch, G., 2010. Intracerebral microdialysis during deep brain stimulation surgery. Journal of Neuroscience Methods 190, 106–111.

Kitai, S.T., Kocsis, J.D., Preston, R.J., Sugimori, M., 1976. Monosynaptic inputs to caudate neurons identified by intracellular injection of horseradish peroxidase. Brain Research 109, 601–606.

Klaus, A., Martins, G.J., Paixao, V.B., Zhou, P., Paninski, L., Costa, R.M., 2017. The Spatiotemporal Organization of the Striatum Encodes Action Space. Neuron 95, 1171-1180.e7.

Kondabolu, K., Roberts, E.A., Bucklin, M., McCarthy, M.M., Kopell, N., Han, X., 2016. Striatal cholinergic interneurons generate beta and gamma oscillations in the corticostriatal circuit and produce motor deficits. Proceedings of the National Academy of Sciences of the United States of America 113, 3159–3168.

Koopmans, G.C., Deumens, R., Brook, G., Gerver, J., Honig, W.M.M., Hamers, F.P.T., Joosten, E.A.J., 2007. Strain and locomotor speed affect over-ground locomotion in intact rats. Physiology and Behavior 92, 993–1001.

Koshimizu, Y., Fujiyama, F., Nakamura, K.C., Furuta, T., Kaneko, T., 2013. Quantitative analysis of axon bouton distribution of subthalamic nucleus neurons in the rat by single neuron visualization with a viral vector. Journal of Comparative Neurology 521, 2125–2146.

Krack, P., Batir, A., van Blercom, N., Chabardes, S., Fraix, V., Ardouin, C., Koudsie, A., Limousin, P.D., Benazzouz, A., LeBas, J.F., Benabid, A.-L., Pollak, P., 2003. Five-Year Follow-up of Bilateral Stimulation of the Subthalamic Nucleus in Advanced Parkinson's Disease. New England Journal of Medicine 349, 1925–1934.

Kravitz, A. v., Freeze, B.S., Parker, P.R.L., Kay, K., Thwin, M.T., Deisseroth, K., Kreitzer, A.C., 2010. Regulation of parkinsonian motor behaviours by optogenetic control of basal ganglia circuitry. Nature 466, 622–626.

Krook-Magnuson, E., Szabo, G.G., Armstrong, C., Oijala, M., Soltesz, I., 2014. Cerebellar directed optogenetic intervention inhibits spontaneous hippocampal seizures in a mouse model of temporal lobe epilepsy. eNeuro 1.

Kühn, A.A., Kempf, F., Brücke, C., Doyle, L.G., Martinez-Torres, I., Pogosyan, A., Trottenberg, T., Kupsch, A., Schneider, G.H., Hariz, M.I., Vandenberghe, W., Nuttin, B., Brown, P., 2008. High-frequency stimulation of the subthalamic nucleus suppresses oscillatory β activity in patients with Parkinson's disease in parallel with improvement in motor performance. Journal of Neuroscience 28, 6165–6173.

Kühn, A.A., Williams, D., Kupsch, A., Limousin, P., Hariz, M., Schneider, G.H., Yarrow, K., Brown, P., 2004. Event-related beta desynchronization in human subthalamic nucleus correlates with motor performance. Brain 127, 735–746.

Kuriakose, R., Saha, U., Castillo, G., Udupa, K., Ni, Z., Gunraj, C., Mazzella, F., Hamani, C., Lang, A.E., Moro, E., Lozano, A.M., Hodaie, M., Chen, R., 2010. The nature and time course of cortical activation following subthalamic stimulation in parkinson's disease. Cerebral Cortex 20, 1926–1936.

Labyt, E., Cassim, F., Devos, D., Bourriez, J.L., Destée, A., Guieu, J.D., Defebvre, L., Derambure, P., 2005. Abnormal cortical mechanisms in voluntary muscle relaxation in de novo parkinsonian patients. Journal of Clinical Neurophysiology 22, 192–203.

Laitinen, L. v., Bergenheim, A.T., Hariz, M.I., 1992. Leksell's posteroventral pallidotomy in the treatment of Parkinson's disease. Journal of Neurosurgery 76, 53–61.

Leblois, A., Meissner, W., Bioulac, B., Gross, C.E., Hansel, D., Boraud, T., 2007. Late emergence of synchronized oscillatory activity in the pallidum during progressive parkinsonism. European Journal of Neuroscience 26, 1701–1713.

Lemaire, N., Hernandez, L.F., Hu, D., Kubota, Y., Howe, M.W., Graybiel, A.M., 2012. Effects of dopamine depletion on LFP oscillations in striatum are task- and learning-dependent and selectively reversed by L-DOPA. Proceedings of the National Academy of Sciences of the United States of America 109, 18126–18131.

Leventhal, D.K., Gage, G.J., Schmidt, R., Pettibone, J.R., Case, A.C., Berke, J.D., 2012. Basal ganglia beta oscillations accompany cue utilization. Neuron 73, 523–536.

Levy, R., Hutchison, W.D., Lozano, A.M., Dostrovsky, J.O., 2000. High-frequency Synchronization of Neuronal Activity in the Subthalamic Nucleus of Parkinsonian Patients with Limb Tremor.

Li, Q., Ke, Y., Chan, D.C.W., Qian, Z.M., Yung, K.K.L., Ko, H., Arbuthnott, G.W., Yung, W.H., 2012. Therapeutic Deep Brain Stimulation in Parkinsonian Rats Directly Influences Motor Cortex. Neuron 76, 1030–1041.

Little, S., Pogosyan, A., Kuhn, A.A., Brown, P., 2012. Beta band stability over time correlates with Parkinsonian rigidity and bradykinesia. Experimental Neurology 236, 383–388.

Little, S., Pogosyan, A., Neal, S., Zavala, B., Zrinzo, L., Hariz, M., Foltynie, T., Limousin, P., Ashkan, K., FitzGerald, J., Green, A.L., Aziz, T.Z., Brown, P., 2013. Adaptive deep brain stimulation in advanced Parkinson disease. Annals of neurology 74, 449–457.

Little, S., Tripoliti, E., Beudel, M., Pogosyan, A., Cagnan, H., Herz, D., Bestmann, S., Aziz, T., Cheeran, B., Zrinzo, L., Hariz, M., Hyam, J., Limousin, P., Foltynie, T., Brown, P., 2016. Adaptive deep brain stimulation for Parkinson's disease demonstrates reduced speech side effects compared to conventional stimulation in the acute setting. Journal of Neurology, Neurosurgery and Psychiatry 87(12), pp.1388-1389.

Lobb, C.J., Jaeger, D., 2015. Bursting activity of substantia nigra pars reticulata neurons in mouse parkinsonism in awake and anesthetized states. Neurobiology of Disease 75, 177–185.

Lundblad, M., Andersson, M., Winkler, C., Kirik, D., Wierup, N., Cenci, M.A., 2002. Pharmacological validation of behavioural measures of akinesia and dyskinesia in a rat model of Parkinson's disease. European Journal of Neuroscience 15, 120–132.

Machado, A.S., Darmohray, D.M., Fayad, J., Marques, H.G., Carey, M.R., 2015. A quantitative framework for whole-body coordination reveals specific deficits in freely walking ataxic mice. eLife 4.

Magno, L.A.V., Tenza-Ferrer, H., Collodetti, M., Aguiar, M.F.G., Rodrigues, A.P.C., da Silva, R.S., do Prado Silva, J., Nicolau, N.F., Rosa, D.V.F., Birbrair, A., Miranda, D.M., Romano-Silva, M.A., 2019. Optogenetic stimulation of the M2 cortex reverts motor dysfunction in a mouse model of Parkinson's disease. Journal of Neuroscience 39, 3234–3248.

Mallet, N., Ballion, B., le Moine, C., Gonon, F., 2006. Cortical inputs and GABA interneurons imbalance projection neurons in the striatum of parkinsonian rats. Journal of Neuroscience 26, 3875–3884.

Mallet, N., Micklem, B.R., Henny, P., Brown, M.T., Williams, C., Bolam, J.P., Nakamura, K.C., Magill, P.J., 2012. Dichotomous Organization of the External Globus Pallidus. Neuron 74, 1075–1086.

Mallet, N., Pogosyan, A., Márton, L.F., Bolam, J.P., Brown, P., Magill, P.J., 2008a. Parkinsonian beta oscillations in the external globus pallidus and their relationship with subthalamic nucleus activity. Journal of Neuroscience 28, 14245–14258.

Mallet, N., Pogosyan, A., Sharott, A., Csicsvari, J., Bolam, J.P., Brown, P., Magill, P.J., 2008b. Disrupted dopamine transmission and the emergence of exaggerated beta oscillations in subthalamic nucleus and cerebral cortex. Journal of Neuroscience 28, 4795–4806.

Mallet, N., Schmidt, R., Leventhal, D., Chen, F., Amer, N., Boraud, T., Berke, J.D., 2016. Arkypallidal Cells Send a Stop Signal to Striatum. Neuron 89, 308–316.

Manning, J.R., Jacobs, J., Fried, I., Kahana, M.J., 2009. Broadband shifts in local field potential power spectra are correlated with single-neuron spiking in humans. Journal of Neuroscience 29, 13613–13620.

Masilamoni, G.J., Smith, Y., 2018. Chronic MPTP administration regimen in monkeys: a model of dopaminergic and non-dopaminergic cell loss in Parkinson's disease. Journal of Neural Transmission 125(3), pp.337-363.

Matamales, M., Bertran-Gonzalez, J., Salomon, L., Degos, B., Deniau, J.M., Valjent, E., Hervé, D., Girault, J.A., 2009. Striatal medium-sized spiny neurons: Identification by nuclear staining and study of neuronal subpopulations in BAC transgenic mice. PLoS ONE 4.

Mathis, A., Mamidanna, P., Cury, K.M., Abe, T., Murthy, V.N., Mathis, M.W., Bethge, M., 2018. DeepLabCut: markerless pose estimation of user-defined body parts with deep learning. Nature Neuroscience 21, 1281–1289.

McCarthy, M.M., Moore-Kochlacs, C., Gu, X., Boyden, E.S., Han, X., Kopell, N., 2011. Striatal origin of the pathologic beta oscillations in Parkinson's disease. Proceedings of the National Academy of Sciences of the United States of America 108, 11620–11625.

McConnell, G.C., Grill, W.M., 2013. Stimulation location within the substantia nigra pars reticulata differentially modulates gait in hemiparkinsonian rats. In: International IEEE/EMBS Conference on Neural Engineering, NER. pp. 1210–1213.

McConnell, G.C., So, R.Q., Hilliard, J.D., Lopomo, P., Grill, W.M., 2012. Effective deep brain stimulation suppresses low-frequency network oscillations in the basal ganglia by regularizing neural firing patterns. Journal of Neuroscience 32, 15657–15668.

McGeorge, A.J., Faull, R.L.M., 1989. The organization of the projection from the cerebral cortex to the striatum in the rat. Neuroscience 29, 503–537.

McRitchie, D.A., Cartwright, H.R., Halliday, G.M., 1997. Specific A10 dopaminergic nuclei in the midbrain degenerate in Parkinson's disease. Experimental Neurology 144, 202–213.

Meldrum, B.S., Brierley, J.B., 1973. Prolonged Epileptic Seizures in Primates: Ischemic Cell Change and Its Relation to Ictal Physiological Events. Archives of Neurology 28, 10–17.

Melgari, J.-M., 2014. Alpha and beta EEG power reflects L-dopa acute administration in parkinsonian patients. Frontiers in Aging Neuroscience 6, 302.

Miller, K.J., Hermes, D., Honey, C.J., Hebb, A.O., Ramsey, N.F., Knight, R.T., Ojemann, J.G., Fetz, E.E., 2012. Human Motor Cortical Activity Is Selectively Phase-Entrained on Underlying Rhythms. PLoS Computational Biology 8, 1002655.

Mink, J.W., 1996. The basal ganglia: Focused selection and inhibition of competing motor programs. Progress in Neurobiology 50, 381–425.

Moran, A., Bergman, H., Israel, Z., Bar-Gad, I., 2008. Subthalamic nucleus functional organization revealed by parkinsonian neuronal oscillations and synchrony. Brain 131, 3395–3409.

Morrell, M.J., 2011. Responsive cortical stimulation for the treatment of medically intractable partial epilepsy. Neurology 77, 1295–1304.

Mottaghi, S., Kohl, S., Biemann, D., Liebana, S., Montano, R., Buchholz, O., Wilson, M., Klaus, C., Uchenik, M., Münkel, C., Schmidt, R., Hofmann, U.G., 2020. Bilateral Intracranial Beta Activity during Forced and Spontaneous Movements in a Hemi-PD Rat Model. bioRxiv 2020.08.16.252957.

Mundinger, F., 1977. New stereotactic treatment of spasmodic torticollis with a brain stimulation system (author's transl). Medizinische Klinik, 72(46), pp.1982-1986.

Munro-Davies, L.E., Gregory, R., Squires, W., Radatz, M., Silburn, P., Scott, R., Aziz, T., Stein, J.F., 1999. Lateral pallidotomy exacerbates akinesia in the Parkinsonian patient. Journal of Clinical Neuroscience 6, 474–476.

Muralidharan, A., Jensen, A.L., Connolly, A., Hendrix, C.M., Johnson, M.D., Baker, K.B., Vitek, J.L., 2016. Physiological changes in the pallidum in a progressive model of Parkinson’s disease: Are oscillations enough? Experimental Neurology 279, 187–196.

Murthy, V.N., Fetz, E.E., 1996. Synchronization of neurons during local field potential oscillations in sensorimotor cortex of awake monkeys. Journal of Neurophysiology 76, 3968–3982.

Nachev, P., Kennard, C., Husain, M., 2008. Functional role of the supplementary and pre-supplementary motor areas. Nature Reviews Neuroscience 9(11), pp.856-869.

Nevado-Holgado, A.J., Mallet, N., Magill, P.J., Bogacz, R., 2014. Effective connectivity of the subthalamic nucleus-globus pallidus network during Parkinsonian oscillations. Journal of Physiology 592, 1429–1455.

Nicholson, E., Kuzmin, D.A., Leite, M., Akam, T.E., Kullmann, D.M., 2018. Analogue closed-loop optogenetic modulation of hippocampal pyramidal cells dissociates gamma frequency and amplitude. eLife 7.

Nini, A., Feingold, A., Slovin, H., Bergman, H., 1995. Neurons in the globus pallidus do not show correlated activity in the normal monkey, but phase-locked oscillations appear in the MPTP model of Parkinsonism. Journal of Neurophysiology 74, 1800–1805.

Nonomura, S., Nishizawa, K., Sakai, Y., Kawaguchi, Y., Kato, S., Uchigashima, M., Watanabe, M., Yamanaka, K., Enomoto, K., Chiken, S., Sano, H., Soma, S., Yoshida, J., Samejima, K., Ogawa, M., Kobayashi, K., Nambu, A., Isomura, Y., Kimura, M., 2018. Monitoring and Updating of Action Selection for Goal-Directed Behavior through the Striatal Direct and Indirect Pathways. Neuron 99, 1302-1314.e5.

Oorschot, D.E., 1996. Total number of neurons in the neostriatal, pallidal, subthalamic, and substantia nigral nuclei of the rat basal ganglia: A stereological study using the cavalieri and optical disector methods. Journal of Comparative Neurology 366, 580–599.

Özkurt, T.E., Butz, M., Homburger, M., Elben, S., Vesper, J., Wojtecki, L., Schnitzler, A., 2011. High frequency oscillations in the subthalamic nucleus: A neurophysiological marker of the motor state in Parkinson's disease. Experimental Neurology 229, 324–331.

Paillé, V., Henry, V., Lescaudron, L., Brachet, P., Damier, P., 2007. Rat model of Parkinson's disease with bilateral motor abnormalities, reversible with levodopa, and dyskinesias. Movement Disorders 22, 533–539.

Papa, S.M., Desimone, R., Fiorani, M., Oldfield, E.H., 1999. Internal globus pallidus discharge is nearly suppressed during levodopa- induced dyskinesias. Annals of Neurology 46, 732–738.

Parker, J.G., Marshall, J.D., Ahanonu, B., Wu, Y.W., Kim, T.H., Grewe, B.F., Zhang, Y., Li, J.Z., Ding, J.B., Ehlers, M.D., Schnitzer, M.J., 2018. Diametric neural ensemble dynamics in parkinsonian and dyskinetic states. Nature 557, 177–182.

Parkinson, J., 2002. An essay on the shaking palsy. 1817. The Journal of neuropsychiatry and clinical neurosciences 14(2), pp.223-236.

Paxinos, G., Watson, C., 2006. The Rat Brain in Stereotaxic Coordinates, 6th Edn. Vol. 70.

Paz, J.T., Davidson, T.J., Frechette, E.S., Delord, B., Parada, I., Peng, K., Deisseroth, K., Huguenard, J.R., 2013. Closed-loop optogenetic control of thalamus as a tool for interrupting seizures after cortical injury. Nature Neuroscience 16, 64–70.

Peles, O., Werner-Reiss, U., Bergman, H., Israel, Z., Vaadia, E., 2020. Phase-Specific Microstimulation Differentially Modulates Beta Oscillations and Affects Behavior. Cell Reports 30, 2555-2566.e3.

Peterson, D.S., Horak, F.B., 2016. Neural Control of Walking in People with Parkinsonism. Physiology 31, 95–107.

Plenz, D., Kital, S.T., 1999. A basal ganglia pacemaker formed by the subthalamic nucleus and external globus pallidus. Nature 400, 677–682.

Plotnik, M., Giladi, N., Balash, Y., Peretz, C., Hausdorff, J.M., 2005. Is Freezing of Gait in Parkinson's Disease Related to Asymmetric Motor Function? 57(5), pp.656-663.

Plotnik, M., Hausdorff, J.M., 2008. The role of gait rhythmicity and bilateral coordination of stepping in the pathophysiology of freezing of gait in Parkinson's disease. Movement Disorders pp.S444-S450 .

Pogosyan, A., Gaynor, L.D., Eusebio, A., Brown, P., 2009. Boosting Cortical Activity at Beta-Band Frequencies Slows Movement in Humans. Current Biology 19, 1637–1641.

Polar, C.A., Gupta, R., Lehmkuhle, M.J., Dorval, A.D., 2018. Correlation between cortical beta power and gait speed is suppressed in a parkinsonian model, but restored by therapeutic deep brain stimulation. Neurobiology of Disease 117, 137–148.

Priori, A., Foffani, G., Pesenti, A., Bianchi, A., Chiesa, V., Baselli, G., Caputo, E., Tamma, F., Rampini, P., Egidi, M., Locatelli, M., Barbieri, S., Scarlato, G., 2002. Movement-related modulation of neural activity in human basal ganglia and its L-DOPA dependency: Recordings from deep brain stimulation electrodes in patients with Parkinson's disease. Neurological Sciences 23, 101–102.

Quinn, E.J., Blumenfeld, Z., Velisar, A., Koop, M.M., Shreve, L.A., Trager, M.H., Hill, B.C., Kilbane, C., Henderson, J.M., Brontë-Stewart, H., 2015. Beta oscillations in freely moving Parkinson's subjects are attenuated during deep brain stimulation. Movement Disorders 30, 1750–1758.

Rattka, M., Fluri, F., Krstić, M., Asan, E., Volkmann, J., 2016. A novel approach to assess motor outcome of deep brain stimulation effects in the hemiparkinsonian rat: Staircase and cylinder test. Journal of Visualized Experiments 2016, 53951.

Rice, M.E., Cragg, S.J., 2008. Dopamine spillover after quantal release: Rethinking dopamine transmission in the nigrostriatal pathway. Brain Research Reviews 58(2), pp.303-313.

Robinson, T.E., Mocsary, Z., Camp, D.M., Whishaw, I.Q., 1994. Time course of recovery of extracellular dopamine following partial damage to the nigrostriatal dopamine system. Journal of Neuroscience 14, 2687–2696.

Robinson, T.E., Whishaw, I.Q., 1988. Normalization of extracellular dopamine in striatum following recovery from a partial unilateral 6-OHDA lesion of the substantia nigra: a microdialysis study in freely moving rats. Brain Research 450, 209–224.

Rodriguez-Pallares, J., Parga, J.A., Muñoz, A., Rey, P., Guerra, M.J., Labandeira-Garcia, J.L., 2007. Mechanism of 6-hydroxydopamine neurotoxicity: The role of NADPH oxidase and microglial activation in 6-hydroxydopamine-induced degeneration of dopaminergic neurons. Journal of Neurochemistry 103, 145–156.

Roemmich, R.T., Field, A.M., Elrod, J.M., Stegemöller, E.L., Okun, M.S., Hass, C.J., 2013. Interlimb coordination is impaired during walking in persons with Parkinson's disease. Clinical Biomechanics 28, 93–97.

Rosa, M., Giannicola, G., Servello, D., Marceglia, S., Pacchetti, C., Porta, M., Sassi, M., Scelzo, E., Barbieri, S., Priori, A., 2011. Subthalamic local field beta oscillations during ongoing deep brain stimulation in Parkinson's disease in hyperacute and chronic phases. NeuroSignals 19, 151–162.

Roseberry, T.K., Lee, A.M., Lalive, A.L., Wilbrecht, L., Bonci, A., Kreitzer, A.C., 2016. Cell-Type-Specific Control of Brainstem Locomotor Circuits by Basal Ganglia. Cell 164, 526–537.

Rosin, B., Slovik, M., Mitelman, R., Rivlin-Etzion, M., Haber, S.N., Israel, Z., Vaadia, E., Bergman, H., 2011. Closed-loop deep brain stimulation is superior in ameliorating parkinsonism. Neuron 72, 370–384.

Sanabria, D., Johnson, L.A., Yu, Y., Busby, Z., Nebeck, S., Zhang, J., Harel, N., Johnson, M.D., Molnar, G.F., Vitek, J.L., 2020. Real-time suppression and amplification of frequency-specific neural activity using stimulation evoked oscillations. Brain Stimulation 13, 1732–1742.

Sanders, T.H., Jaeger, D., 2016. Optogenetic stimulation of cortico-subthalamic projections is sufficient to ameliorate bradykinesia in 6-ohda lesioned mice. Neurobiology of Disease 95, 225–237.

Scheeringa, R., Fries, P., Petersson, K.M., Oostenveld, R., Grothe, I., Norris, D.G., Hagoort, P., Bastiaansen, M.C.M., 2011. Neuronal Dynamics Underlying High- and Low-Frequency EEG Oscillations Contribute Independently to the Human BOLD Signal. Neuron 69, 572–583.

Schrag, A., Quinn, N., 2000. Dyskinesias and motor fluctuations in Parkinson's disease: A community-based study. Brain 123, 2297–2305.

Sharott, A., Doig, N.M., Mallet, N., Magill, P.J., 2012. Relationships between the firing of identified striatal interneurons and spontaneous and driven cortical activities in vivo. Journal of Neuroscience 32, 13221–13236.

Sharott, A., Gulberti, A., Zittel, S., Tudor Jones, A.A., Fickel, U., Münchau, A., Köppen, J.A., Gerloff, C., Westphal, M., Buhmann, C., Hamel, W., Engel, A.K., Moll, C.K.E., 2014. Activity parameters of subthalamic nucleus neurons selectively predict motor symptom severity in Parkinson's disease. Journal of Neuroscience 34, 6273–6285.

Sharott, A., Magill, P.J., Harnack, D., Kupsch, A., Meissner, W., Brown, P., 2005. Dopamine depletion increases the power and coherence of β-oscillations in the cerebral cortex and subthalamic nucleus of the awake rat. European Journal of Neuroscience 21, 1413–1422.

Sharott, A., Moll, C.K.E., Engler, G., Denker, M., Grün, S., Engel, A.K., 2009. Different Subtypes of Striatal Neurons Are Selectively Modulated by Cortical Oscillations. Journal of Neuroscience 29, 4571–4585.

Sharott, A., Vinciati, F., Nakamura, K.C., Magill, P.J., 2017. A population of indirect pathway striatal projection neurons is selectively entrained to parkinsonian beta oscillations. Journal of Neuroscience 37, 9977–9998.

Sherman, M.A., Lee, S., Law, R., Haegens, S., Thorn, C.A., Hämäläinen, M.S., Moore, C.I., Jones, S.R., 2016. Neural mechanisms of transient neocortical beta rhythms: Converging evidence from humans, computational modeling, monkeys, and mice. Proceedings of the National Academy of Sciences of the United States of America 113, E4885–E4894.

Shi, L.-H., Luo, F., Woodward, D.J., Chang, J.-Y., 2006. Basal ganglia neural responses during behaviorally effective deep brain stimulation of the subthalamic nucleus in rats performing a treadmill locomotion test. Synapse 59, 445–457.

Shi, L.H., Woodward, D.J., Luo, F., Anstrom, K., Schallert, T., Chang, J.Y., 2004. High-frequency stimulation of the subthalamic nucleus reverses limb-use asymmetry in rats with unilateral 6-hydroxydopamine lesions. Brain Research 1013, 98–106.

Shimamoto, S.A., Ryapolova-Webb, E.S., Ostrem, J.L., Galifianakis, N.B., Miller, K.J., Starr, P.A., 2013. Subthalamic nucleus neurons are synchronized to primary motor cortex local field potentials in Parkinson's disease. Journal of Neuroscience 33, 7220–7233.

Siegle, J.H., Wilson, M.A., 2014. Enhancement of encoding and retrieval functions through theta phase-specific manipulation of hippocampus. eLife 2014.

Silberstein, P., Kühn, A.A., Kupsch, A., Trottenberg, T., Krauss, J.K., Wöhrle, J.C., Mazzone, P., Insola, A., di Lazzaro, V., Oliviero, A., Aziz, T., Brown, P., 2003. Patterning of globus pallidus local field potentials differs between Parkinson's disease and dystonia. Brain 126, 2597–2608.

Singh, A., Plate, A., Kammermeier, S., Mehrkens, J.H., Ilmberger, J., Bötzel, K., 2013. Freezing of gait-related oscillatory activity in the human subthalamic nucleus. Basal Ganglia 3, 25–32.

Soares, J., Kliem, M.A., Betarbet, R., Greenamyre, J.T., Yamamoto, B., Wichmann, T., 2004. Role of external pallidal segment in primate parkinsonism: Comparison of the effects of 1-methyl-4-phenyl-1,2,3,6-tetrahydropyridine-induced parkinsionism and lesions of the external pallidal segment. Journal of Neuroscience 24, 6417–6426.

Spinks, R.L., Kraskov, A., Brochier, T., Umilta, M.A., Lemon, R.N., 2008. Selectivity for grasp in local field potential and single neuron activity recorded simultaneously from M1 and F5 in the awake macaque monkey. Journal of Neuroscience 28, 10961–10971.

Stein, E., Bar-Gad, I., 2013a. Beta oscillations in the cortico-basal ganglia loop during parkinsonism. Experimental Neurology 245, pp.52-59.

Stoffers, D., Bosboom, J.L.W., Deijen, J.B., Wolters, E.C., Berendse, H.W., Stam, C.J., 2007. Slowing of oscillatory brain activity is a stable characteristic of Parkinson's disease without dementia. Brain 130, 1847–1860.

Surmeier, D.J., Ding, J., Day, M., Wang, Z., Shen, W., 2007. D1 and D2 dopamine-receptor modulation of striatal glutamatergic signaling in striatal medium spiny neurons. Trends in Neurosciences 30(5), pp.228-235.

Surmeier, D.J., Song, W.J., Yan, Z., 1996. Coordinated expression of dopamine receptors in neostriatal medium spiny neurons. Journal of Neuroscience 16, 6579–6591.

Sutton, A.C., Yu, W., Calos, M.E., Smith, A.B., Ramirez-Zamora, A., Molho, E.S., Pilitsis, J.G., Brotchie, J.M., Shin, D.S., 2013. Deep brain stimulation of the substantia nigra pars reticulata improves forelimb akinesia in the hemiparkinsonian rat. Journal of Neurophysiology 109, 363–374.

Sutton, R., Fisher, J.D., Linde, C., Benditt, D.G., 2007. History of electrical therapy for the heart. European Heart Journal, Supplement 9, I3–I10.

Svennilson, E., Torvik, A., Lowe, R., Leksell, L., 1960. TREATMENT OF PARKINSONISM BY STEREOTACTIC THERMOLESIONS IN THE PALLIDAL REGION. A clinical evaluation of 81 cases. Acta Psychiatrica Scandinavica 35, 358–377.

Swan, C.B., Schulte, D.J., Brocker, D.T., Grill, W.M., 2019. Beta frequency oscillations in the subthalamic nucleus are not sufficient for the development of symptoms of parkinsonian bradykinesia/akinesia in rats. eNeuro 6.

Tachibana, Y., Iwamuro, H., Kita, H., Takada, M., Nambu, A., 2011. Subthalamo-pallidal interactions underlying parkinsonian neuronal oscillations in the primate basal ganglia. European Journal of Neuroscience 34, 1470–1484.

Tan, H., Pogosyan, A., Anzak, A., Ashkan, K., Bogdanovic, M., Green, A.L., Aziz, T., Foltynie, T., Limousin, P., Zrinzo, L., Brown, P., 2013. Complementary roles of different oscillatory activities in the subthalamic nucleus in coding motor effort in Parkinsonism. Experimental Neurology 248, 187–195.

Tecuapetla, F., Jin, X., Lima, S.Q., Costa, R.M., 2016. Complementary Contributions of Striatal Projection Pathways to Action Initiation and Execution. Cell 166, 703–715.

Tinkhauser, G., Pogosyan, A., Little, S., Beudel, M., Herz, D.M., Tan, H., Brown, P., 2017a. The modulatory effect of adaptive deep brain stimulation on beta bursts in Parkinson's disease. Brain 140, 1053–1067.

Tinkhauser, G., Pogosyan, A., Tan, H., Herz, D.M., Kühn, A.A., Brown, P., 2017b. Beta burst dynamics in Parkinson's disease off and on dopaminergic medication. Brain 140, 2968–2981.

Toledo, J.B., López-Azcárate, J., Garcia-Garcia, D., Guridi, J., Valencia, M., Artieda, J., Obeso, J., Alegre, M., Rodriguez-Oroz, M., 2014. High beta activity in the subthalamic nucleus and freezing of gait in Parkinson's disease. Neurobiology of Disease 64, 60–65.

Torrecillos, F., Tinkhauser, G., Fischer, P., Green, A.L., Aziz, T.Z., Foltynie, T., Limousin, P., Zrinzo, L., Ashkan, K., Brown, P., Tan, H., 2018. Modulation of beta bursts in the subthalamic nucleus predicts motor performance. Journal of Neuroscience 38, 8905–8917.

Treiman, D.M., Walker, M.C., 2006. Treatment of seizure emergencies: Convulsive and non-convulsive status epilepticus. In: Epilepsy Research. Elsevier, pp. 77–82.

Tripoliti, E., Zrinzo, L., Martinez-Torres, I., Frost, E., Pinto, S., Foltynie, T., Holl, E., Petersen, E., Roughton, M., Hariz, M.I., Limousin, P., 2011. Effects of subthalamic stimulation on speech of consecutive patients with Parkinson disease. Neurology 76, 80–86.

Udupa, K., Chen, R., 2013. Motor cortical plasticity in Parkinson's disease. Frontiers in Neurology.

Ungerstedt, U., 1971. Adipsia and Aphagia after 6-Hydroxydopamine Induced Degeneration of the Nigro-striatal Dopamine System. Acta Physiologica Scandinavica 82, 95–122.

Vitek, J.L., Chockkan, V., Zhang, J.Y., Kaneoke, Y., Evatt, M., DeLong, M.R., Triche, S., Mewes, K., Hashimoto, T., Bakay, R.A.E., 1999. Neuronal activity in the basal ganglia in patients with generalized dystonia and hemiballismus. Annals of Neurology 46, 22–35.

Vitek, J.L., Hashimoto, T., Peoples, J., DeLong, M.R., Bakay, R.A.E., 2004. Acute stimulation in the external segment of the globus pallidus improves parkinsonian motor signs. Movement Disorders 19, 907–915.

Vitek, J.L., Zhang, J., Hashimoto, T., Russo, G.S., Baker, K.B., 2012. External pallidal stimulation improves parkinsonian motor signs and modulates neuronal activity throughout the basal ganglia thalamic network. Experimental Neurology 233, 581–586.

Vlamings, R., Visser-Vandewalle, V., Koopmans, G., Joosten, E.A.J., Kozan, R., Kaplan, S., Steinbusch, H.W.M., Temel, Y., 2007. High frequency stimulation of the subthalamic nucleus improves speed of locomotion but impairs forelimb movement in Parkinsonian rats. Neuroscience 148, 815–823.

Volder, J., 1959, March. The CORDIC computing technique. In Papers presented at the March 3-5, 1959, western joint computer conference, pp. 257-261.

Volkmann, J., Albanese, A., Kulisevsky, J., Tornqvist, A.L., Houeto, J.L., Pidoux, B., Bonnet, A.M., Mendes, A., Benabid, A.L., Fraix, V., van Blercom, N., Xie, J., Obeso, J., Rodriguez-Oroz, M.C., Guridi, J., Schnitzler, A., Timmermann, L., Gironell, A.A., Molet, J., Pascual-Sedano, B., Rehncrona, S., Moro, E., Lang, A.C., Lozano, A.M., Bentivoglio, A.R., Scerrati, M., Contarino, M.F., Romito, L., Janssens, M., Agid, Y., 2009. Long-term effects of pallidal or subthalamic deep brain stimulation on quality of life in Parkinson's disease. Movement Disorders 24, 1154–1161.

Voon, V., Fox, S.H., 2007. Medication-related impulse control and repetitive behaviors in Parkinson disease. Archives of Neurology 64(8), pp.1089-1096.

W Langston, J., Ballard, P., Tetrud, J.W., Irwin, I., 1983. Chronic parkinsonism in humans due to a product of meperidine-analog synthesis. Science 219, 979–980.

Wang, D.D., de Hemptinne, C., Miocinovic, S., Ostrem, J.L., Galifianakis, N.B., Luciano, M.S., Starr, P.A., 2018. Pallidal deep-brain stimulation disrupts pallidal beta oscillations and coherence with primary motor cortex in Parkinson's disease. Journal of Neuroscience 38, 4556–4568.

Weerasinghe, G., Duchet, B., Cagnan, H., Brown, P., Bick, C., Bogacz, R., 2019. Predicting the effects of deep brain stimulation using a reduced coupled oscillator model. PLoS Computational Biology 15, e1006575.

Weinberger, M., Hutchison, W.D., Alavi, M., Hodaie, M., Lozano, A.M., Moro, E., Dostrovsky, J.O., 2012. Oscillatory activity in the globus pallidus internus: Comparison between Parkinson's disease and dystonia. Clinical Neurophysiology 123, 358–368.

Weinberger, M., Mahant, N., Hutchison, W.D., Lozano, A.M., Moro, E., Hodaie, M., Lang, A.E., Dostrovsky, J.O., 2006. Beta oscillatory activity in the subthalamic nucleus and its relation to dopaminergic response in Parkinson's disease. Journal of Neurophysiology 96, 3248–3256.

Welch, P.D., 1967. The Use of Fast Fourier Transform for the Estimation of Power Spectra: A Method Based on Time Averaging Over Short, Modified Periodograms. IEEE Transactions on Audio and Electroacoustics 15, 70–73.

Westin, J.E., Janssen, M.L.F., Sager, T.N., Temel, Y., 2012. Automated gait analysis in bilateral Parkinsonian rats and the role of l-DOPA therapy. Behavioural Brain Research 226, 519–528.

Whitmer, D., de Solages, C., Hill, B., Yu, H., Henderson, J.M., Bronte-Stewart, H., 2012. High frequency deep brain stimulation attenuates subthalamic and cortical rhythms in Parkinson's disease. Frontiers in Human Neuroscience 6.

Whittier, J.R., 1947. Ballism and the subthalamic nucleus (nucleus hypothalamicus; corpus luysi): Review of the Literature and Study of Thirty Cases. Archives of Neurology And Psychiatry 58, 672–692.

Williams, A., Gill, S., Varma, T., Jenkinson, C., Quinn, N., Mitchell, R., Scott, R., Ives, N., Rick, C., Daniels, J., Patel, S., Wheatley, K., 2010. Deep brain stimulation plus best medical therapy versus best medical therapy alone for advanced Parkinson's disease (PD SURG trial): a randomised, open-label trial. The Lancet Neurology 9, 581–591.

Williams, D., Kühn, A., Kupsch, A., Tijssen, M., van Bruggen, G., Speelman, H., Hotton, G., Loukas, C., Brown, P., 2005. The relationship between oscillatory activity and motor reaction time in the parkinsonian subthalamic nucleus. European Journal of Neuroscience 21, 249–258.

Wilson, C.J., Groves, P.M., 1981. Spontaneous firing patterns of identified spiny neurons in the rat neostriatum. Brain Research 220, 67–80.

Yang, A.I., Vanegas, N., Lungu, C., Zaghloul, K.A., 2014. Beta-coupled high-frequency activity and beta-locked neuronal spiking in the subthalamic nucleus of parkinson's disease. Journal of Neuroscience 34, 12816–12827.

Yttri, E.A., Dudman, J.T., 2016. Opponent and bidirectional control of movement velocity in the basal ganglia. Nature 533, 402–406.

Zanos, S., Rembado, I., Chen, D., Fetz, E.E., 2018. Phase-Locked Stimulation during Cortical Beta Oscillations Produces Bidirectional Synaptic Plasticity in Awake Monkeys. Current Biology 28, 2515-2526.e4.

Zariwala, H.A., Borghuis, B.G., Hoogland, T.M., Madisen, L., Tian, L., de Zeeuw, C.I., Zeng, H., Looger, L.L., Svoboda, K., Chen, T.W., 2012. A Cre-dependent GCaMP3 reporter mouse for neuronal imaging in vivo. Journal of Neuroscience 32, 3131–3141.

Zhang, J., Laiwalla, F., Kim, J.A., Urabe, H., van Wagenen, R., Song, Y.K., Connors, B.W., Zhang, F., Deisseroth, K., Nurmikko, A. v., 2009. Integrated device for optical stimulation and spatiotemporal electrical recording of neural activity in light-sensitized brain tissue. Journal of Neural Engineering 6.

Zhang, J., Russo, G.S., Mewes, K., Rye, D.B., Vitek, J.L., 2006. Lesions in monkey globus pallidus externus exacerbate parkinsonian symptoms. Experimental Neurology 199, 446–453.

Zhang, S., Song, Y., Wang, M., Xiao, G., Gao, F., Li, Z., Tao, G., Zhuang, P., Yue, F., Chan, P., Cai, X., 2018. Real-time simultaneous recording of electrophysiological activities and dopamine overflow in the deep brain nuclei of a non-human primate with Parkinson's disease using nano-based microelectrode arrays. Microsystems & Nanoengineering 4, 1–9.

Zhang, S., Song, Y., Wang, M., Zhang, Z., Fan, X., Song, X., Zhuang, P., Yue, F., Chan, P., Cai, X., 2016. A silicon based implantable microelectrode array for electrophysiological and dopamine recording from cortex to striatum in the non-human primate brain. Biosensors and Bioelectronics 85, 53–61.

Zhang, Y., Wang, X., Bressler, S.L., Chen, Y., Ding, M., 2008. Prestimulus cortical activity is correlated with speed of visuomotor processing. Journal of Cognitive Neuroscience 20, 1915–1925.